UNCLASSIFIED

AD NUMBER
AD353599

CLASSIFICATION CHANGES	
TO:	**UNCLASSIFIED**
FROM:	**CONFIDENTIAL**

LIMITATION CHANGES	
TO: Approved for public release; distribution is unlimited.	
FROM: Distribution authorized to U.S. Gov't. agencies and their contractors; Administrative/Operational Use; 28 AUG 1964. Other requests shall be referred to Defense Atomic Support Agency, Washington, DC.	

AUTHORITY
DNA ltr 9 Oct 1984; DNA ltr 9 Oct 1984

THIS PAGE IS UNCLASSIFIED

AD NUMBER
AD353599
CLASSIFICATION CHANGES

TO:

CONFIDENTIAL

FROM:

SECRET

AUTHORITY

31 Aug 1976, DoDD 5200.10

UNCLASSIFIED

AD _353599_

UNCLASSIFIED

AD- 353599

SECURITY REMARKING REQUIREMENTS

DOD 5200.1-R, DEC 78

REVIEW ON 28 AUG 84

UNCLASSIFIED

AD_____

DEFENSE DOCUMENTATION CENTER

FOR

SCIENTIFIC AND TECHNICAL INFORMATION

CAMERON STATION ALEXANDRIA, VIRGINIA

UNCLASSIFIED

SECRET

AD 353599

DEFENSE DOCUMENTATION CENTER

FOR
SCIENTIFIC AND TECHNICAL INFORMATION
CAMERON STATION. ALEXANDRIA. VIRGINIA

SECRET

POR-2022
(WT-2022)

Operation
DOMINIC

FISH BOWL SERIES

PROJECT OFFICERS REPORT—PROJECT 6.5c

VERTICAL IONOSPHERIC SOUNDING MEASUREMENTS (U)

W. F. Utlaut, Project Officer

T. N. Gautier

National Bureau of Standards
Central Radio Propagation Laboratory
Boulder, Colorado

DDC

SEP 30 1964

QUALIFIED REQUESTERS MAY OBTAIN
COPIES OF THIS REPORT FROM DDC.

SECRET

Inquiries relative to this report may be made to

Chief, Defense Atomic Support Agency
Washington, D. C. 20301

When no longer required, this document may be
destroyed in accordance with applicable security
regulations.

DO NOT RETURN THIS DOCUMENT

SECRET

OPERATION DOMINIC

FISH BOWL SERIES

PROJECT OFFICERS REPORT— PROJECT 6.5c

VERTICAL IONOSPHERIC SOUNDING MEASUREMENTS (U)

W. F. Utlaut, Project Officer
T. N. Gautier

National Bureau of Standards
Central Radio Propagation Laboratory
Boulder, Colorado

SECRET

ABSTRACT

This report presents data on the ionospheric perturbations resulting from the five 1962 high-altitude nuclear detonations, Star Fish, Check Mate, Blue Gill, King Fish, and Tight Rope, as obtained with sweep-frequency vertical-incidence ionosondes operated at the islands of Maui, Tern (French Frigate Shoals), Midway, Wake (Star Fish only), Canton, Tutuila (American Samoa), and Tongatapu. The ionosondes at Midway and Tongatapu had a frequency range of 1 to 25 Mc. At the other stations the range was 0.25 to 20 Mc.

The objective was to obtain information on the immediate and delayed effects on the ionosphere, including radio wave absorption and changes in electron density, at various distances and directions from the detonations. Beginning a few minutes before detonation, each ionosonde was operated continuously until about H + 2 hours, when the interval between ionograms was increased to five minutes for several more hours. Otherwise, ionograms were made at 15-minute intervals.

The results are presented in the form of

a. selected ionograms,

b. plots of F-layer critical frequencies and minimum observable reflected frequencies (f-min) versus time from H - 10 minutes to H + 3 hours,

c. plots of F-layer virtual heights at several frequencies as a function of time from H - 10 minutes to H + 3 hours,

d. f-plots for a four-day period encompassing each detonation.

The greatest effects were produced by Star Fish and the least by Tight Rope. A prompt increase in absorption was observed at all stations for all events except Tight Rope. It was

SECRET

especially great for Star Fish, and obliterated all echoes
(blackout) at most stations for periods ranging from a few
seconds at Tutuila to an hour and a half at Tern. Substantial
atmospheric acoustic-type waves were generated by Star Fish and
King Fish, and waves of somewhat less amplitude were generated
by Check Mate and Blue Gill. No positively identified effects
from Tight Rope were observed at any of the stations.

Effects associated with its proximity to the magnetic con-
jugate area were observed at Tutuila. Thus, whereas substantial
decreases in F-layer ionization density occurred after Star Fish
at the northern hemisphere stations, a large (25-fold) and al-
most simultaneous increase was observed at Tutuila, and later,
apparently in association with the atmospheric wave acoustic-
type disturbance, there was another (6-fold) increase. A
similar (4-fold) increase in association with the passage of
an atmospheric acoustic-type wave was observed at Tutuila
following King Fish.

6

CONTENTS

SECRET

FIGURES

9

SECRET

10

SECRET

INTRODUCTION

When a nuclear weapon is exploded in the high atmosphere, drastic effects occur in the ionosphere. Because of the effects on radio communication, it is necessary to gain all possible information on the nature of the phenomena.

The effects of nuclear detonations are felt on all layers from about 70 or 80 kilometers on up through the F-region and into the exosphere. Increased ionization at the lower height (D-region) causes absorption of HF radio waves and seriously disrupts radio communication in this part of the spectrum. On VLF circuits serious perturbations in the phase of the signal can be caused by D-region effects. Sporadic-E-like increases in the E-region have been observed following earlier high-altitude nuclear bursts. Changes in F-region electron density are observed in association with high-altitude bursts, and large distortions are often present.

The full theory of the effect of nuclear blasts on the ionosphere has not yet been formulated, although a number of theoretical treatments have been made and are summarized in various classified documents. Because of the complexity of these theories, they will not be discussed here, but details may be found in References 1 through 4 provided at the end of this report.

The ionospheric vertical soundings technique provides a vast amount of information on these various effects. By taking these kinds of observations at both primary and conjugate areas, the relative importance of direct photon and particle effect versus trapped particle effect can be assessed.

The objectives of this project (DASA Project 6.5C) were to obtain information on the immediate and delayed effects of the Fish Bowl detonations on the ionosphere, including radio wave absorption and changes in electron density, at various distances and directions from the detonations, using vertical-incidence ionosondes.

Ionosondes were operated at seven locations: the islands of Maui, Tern (French Frigate Shoals), Midway, Wake (for Star Fish only), Canton, Tutuila (American Samoa), and Tonga (Tongatapu). Their locations and distances from Johnston Island are shown in Figure 1. Other ionosondes were operated at Palmyra by Project 6.5A, at Johnston and Kwajalein by 6.5D, and at Viti Levu and an aircraft by Project 3.10.

Preliminary 6.5C results for Star Fish were reported in Fish Bowl POIR 2022 and in the proceedings of the August 31 - September 1, 1962, DASA Symposium (page 131, DASA Data Center Special Report 3). Preliminary results for the fall series were reported in POIR 2022-1 and in NBS Rept. No. 1QB109, to be included in the proceedings of the February 26-28, 1963 DASA Symposium. (POR-2022 supersedes POIR's 2022 and 2022-1.)

The ionosonde is a radar-type instrument which transmits short pulses (typically 50 microseconds long at a rate of 60 per second) as the radio frequency is changed continuously or in short steps over a range which may begin at about a megacycle per second, or lower, and go to 20 Mc or higher. The round-trip travel time to the ionosphere and back, recorded as a function of radio frequency, is called an ionogram. The travel time is usually expressed as the range in kilometers to the point of reflection, or rather what the range would

12

SECRET

have been had the entire trip been made at the free-space velocity. This apparent range, or _virtual height_ (h') as it is called on the ionogram is always greater than the actual height, because the velocity of pulse propagation in an ionized medium is less than in free space.

The wave is reflected at the height where the refractive index becomes zero. The refractive index is a complicated function of the wave frequency, the electron density, the strength of the earth's magnetic field, and the frequency of collisions of the electrons with other objects, but may be thought of as tending toward zero with increasing electron density and tending toward unity (the free-space value) with increasing wave frequency. Thus, as the wave progresses upward into the ionosphere, the refractive index and the pulse velocity decrease, and if a level is reached at which the refractive index becomes zero, the pulse velocity also becomes zero, and the wave is reflected. The higher the frequency, the higher the wave must go to be reflected. Eventually, the height of maximum density is reached. The frequency which can just reach this height is called the _critical frequency_. At higher frequencies the wave penetrates the ionosphere and is not reflected. Small-scale irregularities in the ionosphere (on the order of a wave-length in size) may, however, produce scatter echoes at fre-quencies extending beyond the critical frequency.

The presence of the earth's magnetic field causes the ionosphere to have two values of refractive index for a given wave frequency, depending upon the polarization of the wave. There are normally, then, two echoes for each wave frequency, having different virtual heights and different reflection levels.

SECRET

One is called the ordinary wave echo and the other the extra-
ordinary wave echo, by analogy with the ordinary and extra-
ordinary waves of birefringent crystal optics. There is a dif-
ferent critical frequency for each of the two waves. The ordinary
wave critical frequency is the same as it would be in the absence
of the magnetic field. At frequencies well above the frequency
of gyration of free electrons in the magnetic field ('n the
ionosphere this varies from about 0.7 Mc near the equator to
about 1.6 Mc near the magnetic poles), the extraordinary wave
critical frequency is greater than the ordinary wave critical
frequency by about one-half the electron gyrofrequency.

At night the ionosphere consists principally of a single
layer, the F-layer, with a minimum height near 200 to 250 km,
and a height of maximum electron density in the vicinity of
300 to 400 km. In the daytime, however, the sun's rays produce
ionization at lower heights, and the result is an E-layer, with
maximum density near 120 km, and often an intermediate layer
near 200 km. If the latter is present, it is called the F1-layer,
and the remainder of the F-layer is called the F2-layer. The
maximum densities, and therefore the critical frequencies, of
the E-and F1-layers are usually less than that of the F2-layer.
The night F-layer is considered to be, at least in part, a
remnant of the daytime F2-layer. The night layer is therefore
sometimes referred to as the F2-layer even though the F1-F2
bifurcation is not apparent. Likewise, an unresolved daytime
F-layer is usually referred to as the F2-layer. The critical
frequencies associated with the various layers are designated
by the symbols foE, foF1, foF2 for the ordinary wave, and fxE,
fxF1, fxF2 for the extraordinary wave.

14

SECRET

The exact expression for the refractive index in the presence of collisions and a magnetic field is quite complicated and will not be discussed here. However, in the absence of collisions and magnetic field, the refractive index n is given by the simple expression

$$n^2 = 1 - 81 \times 10^6 \, N_e \, f^{-2} \tag{1}$$

where N_e is the electron density per cm^3 and f is the wave frequency in cycles per second. In the presence of collisions and magnetic field, it is still a good approximation if the collision frequency and the gyrofrequency are both much less than the wave frequency. Since, at reflection, the ordinary wave is unaffected by the magnetic field, and in the F2-layer the collision frequency is quite small, the maximum electron density N_{max} of the F2-layer is given exactly by N_e in Equation 1 if the ordinary wave critical frequency foF2 is substituted for f and n is equated to zero. Thus:

$$0 = 1 - 81 \times 10^6 \, N_{max} \, (foF2)^{-2}$$

or

$$N_{max} = 1.24 \times 10^{-8} \, (foF2)^2 \tag{2}$$

15

SECRET

Under conditions in which Equation 1 is valid, the velocity U of a pulse of waves (the group velocity) is given by

$$U = cn \qquad (3)$$

where c is the free-space velocity (velocity of light), and n is the refractive index given by Equation 1. This relationship is a good approximation in the ionosphere for waves well above the gyrofrequency. Thus, U is always less than or equal to c, because n is always less than or equal to unity. The virtual height, which is equal to the integral of c/U over the path from the ground to the level of reflection, is thus always greater than or equal to the real height.

In addition to the critical frequencies and the virtual heights of the echoes, an important readily observed indicator of conditions in the ionosphere, and in particular of disturbances caused by nuclear detonations, is the minimum echoing frequency on the ionogram which is designated by the symbol f-min. Because ionospheric absorption tends to be inversely related to the wave frequency, and even in the absence of absorption the echo strength tends to decrease with decreasing frequency, especially at the lower frequencies, as a result of decreasing efficiency of the antennas, an increase in absorption tends to increase f-min.

Since absorption takes place mainly in and below the E-layer (the D-region) where the electron collision frequency is greatest, an increase in f-min is usually indicative of an

16

SECRET

increase in electron density in the D-region. As the ionosonde is not readily calibrated to give absolute values of absorption in terms of f-min, only relative values of the changes in absorption are given by the changes in f-min.

Frequent reference will be made to bomb-generated traveling disturbances, which bring about certain changes in F2-layer critical frequencies and virtual heights and may cause stratification of the layer. Naturally occurring large-scale traveling disturbances and their effects on the F-region have been known for years (Reference 5). They travel with velocities of 5 to 15 km/minute, and are thought to be gravity waves (Reference 6) involving transverse (vertical) displacements like ocean waves. The bomb-generated disturbances travel much faster, (50 km/minute and faster), although the speed decreases systematically with distance from the source (Reference 7). These speeds are more like acoustic speeds, so these disturbances may have more the character of acoustic shock waves than of gravity waves. Their nature is not yet well understood.

17

SECRET

PROCEDURE

Operation of the ionosondes was begun several weeks prior to Star Fish, and again in the fall several weeks before Check Mate. A copy of the ionograms for the periods indicated below was deposited in the DASA Data Center. The beginning and ending times and dates (GMT) were 0001 July 4 to 2359 July 14 for all stations, and 0001 October 15 to 2359 Nov 10 for Maui

"	"	to 2030 Nov	5	for Tern
"	"	to 0815 Nov	5	for Midway
"	"	to 1810 Nov	6	for Canton
"	"	to 2359 Nov	6	for Tutuila
"	"	to 2359 Nov	6	for Tonga

Note, however, that times and dates printed on the Maui film are in 150° W time.

Except for a period of hours beginning just before each shot, ionograms were made at 15-minute intervals around the clock. The time required for each ionogram was 15 seconds, except at Maui where the time was 30 seconds during the fall series. Beginning 10 minutes prior to each of the detonations, the ionosondes were programmed to run continuously, sweeping through the full frequency range in a period of 15 seconds (except at Maui where the period was 30 seconds during the fall series). This mode of operation was continued for several hours, at which time the frequency of observation was reduced to five-minute intervals followed at a later time by observations at the usual 15-minute intervals.

Virtual height calibration markers, generated from time division circuits synchronized with the transmitted pulse, are photographed along with the echo returns and show on the photo-

18

SECRET

graphic records as horizontal lines at 100-km virtual range intervals. Frequency markers, which are generated by circuits tuned at one megacycle intervals, are produced on the ionogram records as the transmitted frequency sweeps through each integral megacycle. The ionospheric parameters f-min, virtual height h', and the critical frequencies are scaled from projected enlargements of the film record and are usually accurate to within a few percent.

For reference, the types of ionosondes and the general characteristics of the group are given below.

Type C-2 ionospheric sounder at Midway and Tonga

Type C-3 ionospheric sounder at Canton Island

Type C-4 ionospheric sounders at Maui, Tern (French Frigate Shoals), Wake, and Tutuila

Pulse characteristics:

About 15-kw peak pulse power; pulse length approximately 50 microseconds; pulse repetition frequency normally 60 per second; recording range nominally 0 to 700, 0 to 1,000, or 0 to 1,400 km.

Nominal frequency coverage:

0.25 to 20 Mc at Maui and Tern (French Frigate Shoals), Wake, Canton, and Tutuila; 1.0 to 25 Mc at Midway and Tonga. Records are linear in time, logarithmic in frequency.

Antenna:

Delta-type antenna directed vertically; beamwidth varies from approximately 30° to 60° at ½-power point as frequency is varied.

Sweep time:

15 seconds, except at Maui where it was 30 seconds in the full series.

SECRET

Equipment accuracy:

The accuracy of the frequency markers for the C-2, C-3, and C-4 ionosondes is equal to or better than 0.1%. It is based on a 1-Mc crystal oscillator. The oscillators for Fish Bowl were checked in the laboratory prior to setting up the stations. Checks were made in the field against WWVH, the National Bureau of Standards Time and Frequency station located on Maui, Hawaii.

The height marker oscillator in the C-4 ionosondes has an accuracy equal to or better than 0.02%. It is based on a 3000-cps temperature-controlled crystal oscillator. The height marker oscillator in the C-2 and C-3 ionosondes is not crystal controlled but is compared with a crystal oscillator at regular intervals. The accuracy of the crystal controlled test equipment was equal to or better than 0.1%.

On C-2, C-3, and C-4 ionosondes the proper adjustment of the ground pulse on the zero-km height marker is set manually and checked photographically on the ionograms through the use of a built-in ground pulse interrupter.

20

SECRET

RESULTS

The results presented are:

(a) a group of selected ionograms for each station and event for which significant effects were observed, each group characteristically consisting of the ionograms made just prior to, at the time of, and at one or more significant times following the detonation.

(b) plots of F-layer critical frequencies and f-min versus time from H - 10 minutes to H + 3 hours,

(c) plots of F-layer virtual heights at several frequencies as a function of time from H - 10 minutes to H + 3 hours,

(d) f-plots for a four-day period beginning the day before each event.

In addition there are two figures showing the time variation of the virtual range of new echoes on the Tutuila and Tonga ionograms resulting from Star Fish.

The narrative description of the results is organized by event in chronological order, and by station for each event in the order Maui, Tern, Midway, Wake, Canton, Tutuila, Tonga. With a few exceptions, the graphical results are presented in the same order (see list of figures in the table of contents). All dates and times in the text and on the figures, other than times referred to detonation (H) time, are in GMT. An exception is the 150°W date and time that appears along the right-hand edge of each Maui ionogram, which was placed on the original film at the time the ionogram was made.

The f-plot needs special explanation. It is a graph

SECRET

showing the diurnal variation of certain characteristic fre-
quencies on the ionogram, including the critical frequencies
and f-min, according to internationally adopted conventions.
It is a very useful technique for showing the hour-to-hour
variations of some important ionospheric characteristics. A
description of f-plot conventions and symbols is given in the
Appendix.

The remainder of this section will be devoted to a de-
scription of the effects at each station of each shot.

Star Fish, Maui.

The detonation occurred at 11 PM local time at the Maui
location. At this time the F-region was experiencing its nor-
mal late-evening decline in maximum electron density. Typical
values for this time of day are between 5 and 6 Mc for foF2,
while f-min is normally about 0.4 Mc and quite frequently
sporadic-E is also observed. The sounder was sweeping through
about 5 Mc at the time of the detonation. Figure 2A shows the
last normal sounding taken just prior to detonation. Multiple
reflections from the E-and F-regions are clearly observed, and
this along with the low value of f-min indicate that low night-
time absorption conditions in the ionosphere prevailed. Figure
2B shows the ionogram made at the time of detonation, and it may
be seen that echoes immediately cease at 9 seconds after the
hour (indicated by the white timing dot at top edge of the iono-
gram) and complete blackout sets in. In the right-hand portion
of this ionogram it may be seen that noise and interference as
well as vertical incidence echoes are completely eliminated.
The term "blackout" is used to indicate the absence of echo return
on the ionogram. Figure 2C shows the ionogram made $2\frac{1}{4}$ minutes
later. Faint echoes are visible just below 5 Mc, but at greater

22

SECRET

virtual heights than the pre-shot echoes at the same frequencies. This is believed to be additional retardation caused by new ionization formed in the E-region. Figure 2D is an ionogram made 24 minutes after the detonation. Absorption is still considerable, and the critical frequency has decreased to a value less than 4 Mc. Figure 2E is an ionogram made one and a half hours after detonation and, except for lower than normal critical frequencies, represents a rather normal ionosphere.

Figure 3 shows the changes in f-min, foF2 and fxF2 at Maui. Total blackout lasted for a period of about 105 seconds; i.e., f-min exceeded 5.5 Mc for this length of time. Following blackout, the value of f-min decreased approximately exponentially with a decrement coefficient of about 15 minutes. As shown in Figure 4, it continued to decrease, with fluctuations for several hours. Also in Figure 3 it may be seen that the F-layer critical frequencies decreased rapidly starting at approximately H + 10 min. The value of foF2 decreased from a pre-shot value of 5 Mc to 2.5 Mc within 35 minutes of the explosion, which corresponds to a reduction in electron density by a factor of 4. The normal rate of decrease in ionization density at this time of day is much slower. The F-region critical frequency remained near this low value until sunrise (see Figure 4).

The upper part of Figure 25 shows for Maui the variation of virtual height at selected frequencies on the same time scale as the frequency plot in Figure 3. The variations following the shot are mainly the result of changes in f-min and in the electron density of the layer and attendant changes in

23

SECRET

height of reflection and retardation. Thus, the gap of 10
minutes following the shot resulted because f-min exceeded the
highest frequency plotted (3 Mc) during this interval. Sub-
sequent breaks in the 3-Mc curve resulted from the decrease of
foF2 below 3 Mc, and the variations of the 2-Mc curve are pri-
marily the result of foF2 variations with attendant changes in
virtual height as well as height of reflection at 2 Mc.

In Figure 4 are f-plots covering the four-day period
beginning the day before the Star Fish shot. It is note-
worthy that f-min rose to exceptionally high values, 5 Mc,
near local noon following the shot. The usual noon value
is more like 2 Mc. Higher than normal values also occurred
near noon on July 10. F-region critical frequencies appear
to have been normal after sunrise on July 9. The "C" in the
f-plot for July 8 refers to equipment outage.

Star Fish, Tern.

Figure 5A shows the last sounding taken at Tern just
prior to detonation. Strong multiple reflections from the
E-and F-regions were recorded as a consequence of the low
ionospheric absorption at this time of night. Figure 5B
shows the ionogram which was being made at the time of detona-
tion. Complete blackout occurred promptly. Total blackout
was observed for approximately 85 minutes. Weak spread echoes
then followed as shown in ionograms 5C and D made at H + 94
minutes and H + 160 minutes, respectively. Considerable spread-F
was recorded during the remainder of the night as exemplified
in ionogram 5E made about 5 hours after the detonation.

Figure 6 shows the changes in the ionospheric character-
istics for the three-hour period following the detonation,

SECRET

while Figure 7 shows a four-day sequence of f-plots. After recovery from the blackout, f-min slowly decreased, returning nearly to normal by about H + 5 hours. At sunrise, the combination of low critical frequencies and increasing f-min resulted in another period of blackout. High values of f-min persisted throughout the daylight hours of July 9, but daylight values on July 10 and 11 were only slightly above normal values. After sunrise on July 9, F2 critical frequencies were normal.

Because of the long blackout, no virtual height variations are presented for this station.

Star Fish, Midway.

At Midway, prior to the detonation, f-min was below the lower limit of the recorder (1 Mc) which was normal for the hour; foF2 was varying in about the same manner as on the preceding day, decreasing slowly.

Sample ionograms for Midway for the period of interest are shown in Figure 8. Ionogram A in Figure 8 shows the last full sweep before H = 0. In the following ionogram, B, H = 0 occurred just as the frequency reached 3 Mc. The resulting blackout occurred instantly and lasted $8\frac{1}{2}$ minutes followed by a gradual recovery. Ionogram C at 0909 GMT shows an early stage of the recovery. By 0917 the critical frequencies were clearly seen, as shown in Figure 8D.

Shortly after recovery began, foF2 was about the same as the pre-shot value (Figure 9). Thereafter, there was a small increase from about 4.9 Mc to 5.6 Mc by about 0916 GMT, followed by a steady decrease to an abnormally low value of about 2.5 Mc just before 0935 when a second blackout of $2\frac{1}{2}$ minutes duration occurred.

SECRET

Following the second blackout, foF2 gradually increased over the next 60 minutes or so to about 4.0 Mc which is about normal for the hour.

Sporadic-E (Es) of a non-blanketing type was prominent by 1020 GMT as seen in Figure 8H, and by 1110 GMT this became blanketing and obscured the F-layer as shown in ionogram 8I. A considerable amount of spread-F was evident throughout the remainder of the night as exemplified in ionogram 8J.

Virtual height variations for Midway at 2 and 3 Mc are shown in the middle part of Figure 25. As in the case of the curves for Maui in the upper part of the figure, the virtual height variations are primarily the result of variations in foF2 with attendant variations in virtual height and height of reflection.

The f-plots of Figure 10 show the longer term behavior of the ionosphere from the pre-shot day of 8 July to 11 July. Beginning about 1½ hours after sunrise, from about 1830 to 2130 GMT on July 9, and again from 0000 to 0300 GMT on 10 July, blackout prevailed. This possibly indicates the arrival of debris at Midway.

Following the initial blackout, f-min decreased steadily but never reached normal values that night (Fig. 9), and was abnormally high throughout the following daylight period. Thereafter, it behaved normally.

Star Fish, Wake.

Critical frequencies and absorption in the ionosphere were normal for the time of day at Wake preceding the shot. The critical frequencies were decreasing slowly, although occasional increases were not unusual at this hour.

The ionograms of Figure 11 show the effects of the shot.

Figure 11A is the last full ionogram before the shot. The detonation occurred just at the end of ionogram A. Ionogram B shows a considerable diminution of interfering signals from distant stations as well as marked absorption of the echoes. A local marker beacon and its harmonics remain at the low frequency end of the sweep. Ionogram C, made one minute after the shot, shows a marked retardation in the F2-layer echoes at the lower frequencies and the appearance of an F1-layer of the daylight type with foF1 of 2.5 Mc. An E-layer is also visible.

A well-defined daytime type of E-layer, with critical frequencies foE and fxE of 2.2 and 2.7 Mc, respectively, is clearly shown in ionogram D made at H + 3 minutes.

Ionogram E, made at H + 9 minutes, still shows F2-layer retardation at the lower frequencies, although echoes from the lower layers were no longer recorded.

Figure 12 shows a post-shot increase in the critical frequencies of about 0.3 Mc. A small increase in foF2 was underway just before the shot, and a rise of the amount observed could have been a normal rise rather than an event connected change. This, however, was followed by a relatively rapid decrease, then successively smaller increases and decreases like a damped oscillation.

Prior to the shot, f-min was normal. At shot time, there was a sharp increase in f-min, but complete blackout was not recorded. This possibly may have been because the detonation occurred during the period of about one second between the end of one ionogram and the beginning of the next. If a complete blackout had occurred, it would have been of a duration shorter than 9 seconds. In the second ionogram

27

SECRET

following the shot, f-min had already dropped to about 1.5 Mc, after which it decreased very slowly, reaching pre-shot values just before sunrise.

Since at Wake f-min did not exceed the critical frequency, and returned to below 2 Mc almost immediately, there is an almost complete record of the changes in the virtual heights at all frequencies from 2 Mc to the critical frequency. Thus, the lower part of Figure 25 shows the immediate increase in retardation caused by the formation of ionization below the F2-layer. Except at 2 Mc, return to pre-shot virtual heights took place quickly, in about 7 minutes at 3 Mc, and in less time at the higher frequencies. The remaining variations are primarily the result of critical frequency variations and attendant changes in reflection height and retardation.

The f-plots for 9 July in Figure 13 shows the slow decrease of f-min, and a rise to abnormally high values following sunrise. Absorption was only slightly above normal during the sunlight period on the following two days. These plots also show that F-region critical frequencies were lower than usual during the remainder of the night after the explosion.

Star Fish, Canton.

The ionosphere at Canton appeared to be undisturbed prior to the detonation. The critical frequencies and f-min were about normal when compared with the medians for the preceding 22 days. Slow variations in critical frequency of about 1 Mc were not unusual at this hour. At 0900 GMT, foF2 was nearly constant or decreasing slowly on normal days.

Figure 14A is the last complete ionogram before the shot. The shot took place halfway through the next ionogram.

SECRET

Blackout onset was instantaneous and lasted over a minute. Interference from distant stations also vanished instantaneously. Figure 14C is the first ionogram showing an echo after the blackout.

Shortly after the blackout, the ionograms took on the appearance of daylight ionograms (e.g. 14D). Ionogram E in Figure 14, made at H + 30 minutes, shows an early stage of the formation of spread echoes which obliterated normal echoes later on. It should be pointed out, however, that spread echoes normally occur at this time of night at Canton.

As shown in Figure 15, the critical frequency (only foF2 was scaled) following blackout remained at the pre-shot value for about 7 minutes. It then increased rapidly to values higher than normal daytime values, corresponding to an increase in electron density in excess of 2 times. Following this increase, foF2 fell off steadily until about H + 60 minutes and thereafter could not be scaled accurately because the echo was diffuse and spread. Maximum observed frequencies of echo return are plotted thereafter. The spread echoes were abnormal in that there was considerable horizontal stratification without any indication of turn-up at the maximum frequency of echo return. This spread condition persisted until sunrise after which time echoes appeared normal.

The value of f-min decreased rapidly following the blackout, but leveled off after about H + 15 minutes at values well above the pre-shot values. Normal values were reached at about H + 80 minutes. In the following two nights (Figure 16) f-min was higher than normal. The values of f-min for 8 July are very near the median level for the 22 days preceding the detonation (not shown in figures).

Perhaps because Canton is near the magnetic dip equator, the virtual height variations shown in the upper part of Figure 26 cannot be attributed mainly to variations in the critical frequency, as in the case of Maui, Midway, and Wake in Figure 25. The initial jump at all frequencies, following the brief blackout, is the result of fresh ionization formed almost instantaneously below the pre-shot F2 layer. The new F1-layer thus formed seemed to lift up and merge with the old layer while both continued to increase in height for a couple of hours.

Star Fish, Tutuila.

Normal quiet ionospheric conditions prevailed at Tutuila prior to the shot. At 0900 GMT, foF2 was normally constant or slowly fluctuating. The minimum frequency at which echoes were observed was 0.25 Mc, the lower frequency limit of the ionosonde.

The last complete ionogram prior to detonation is shown in Figure 17A. The next ionogram, B, shows a sudden interruption of echoes at H = 0. In the next ionogram, C, echoes appear in the vicinity of 12 to 14 Mc at virtual heights less than 200 km.

Ionograms D and E show the further development of the shot-induced layer. The echoes appear at an unusually low virtual height and at first seem to have some of the appearance of oblique sporadic-E echoes. However, as the echoes develop, the character changes to that of a normal F-layer and shows in ionogram E made at H + 3.75 minutes a second order reflection. The fact that the second order echo occurs at almost exactly twice the time delay of the main echo indicates

30

SECRET

that the echo is a vertical rather than an oblique reflection.

The variation in the value of the maximum observed frequency is shown in Figure 18. This plot shows a sudden rise in the value of the maximum frequency at H = 0 followed by a decrease to near normal values at H + 20 minutes. This was followed by an increase to a maximum around 14 Mc at H + 65 minutes and a second decrease to a minimum by about H + 110 minutes. Thereafter, as seen in the f-plots of Figure 19, the echo becomes very diffuse. At sunrise, there is a general return toward normal with somewhat lower than normal critical frequencies in the morning.

The value of f-min increased sharply at H = 0, then dropped rapidly for about 10 minutes, after which there was a slow decrease for about two hours, leveling off at about 1.2 Mc compared to a value of less than 0.25 Mc through the hours of darkness prior to detonation. The f-min was also somewhat above normal throughout the daylight hours of July 10 and 11.

The virtual heights of various layers show some interesting aspects and are shown in Figure 20. These heights were scaled in the usual manner as minimum virtual heights without regard to frequency. F-layer virtual heights at fixed frequencies are shown in the lower part of Figure 26. Referring first to Figure 20, prior to H = 0 the sporadic-E and F2-layer heights at about 90 and 260 km, respectively, were constant. At H = 0, the two layers were momentarily blacked out by the high absorption, after which a new layer appeared with a virtual height of 135 km. The virtual height increased from 135 to 320 km in 20 minutes. The virtual height decreased to 200 km by H + 80 minutes and varied only slowly for some time thereafter. This layer remained well defined.

31

SECRET

At H + 20 minutes a diffuse layer appeared at a virtual height of 600 km which decreased rapidly to 420 km in 40 minutes. It was not seen thereafter. An additional weak layer appeared at H + 32 minutes and returned echoes for more than 20 seconds. Occasional transient layers were observed from time to time. Sporadic-E layers were intermittently seen after H + 46 minutes but were weak and not persistent.

Figure 26 (lower part) shows the sudden appearance of echoes at frequencies well above those before the shot, at substantially lower virtual heights. The highest frequency scaled for this figure was 14 Mc, but echoes appeared at frequencies well above this in the first two or three minutes (Figures 17 and 18). Here again, as in the case of Canton, the variations of the virtual height curves cannot be wholly explained in terms of critical frequency variation. There was, in addition, substantial variations of the height of the layer as a whole.

The new layer was formed almost instantaneously at abnormally low heights. Then, as the ionizing source strength decreased rapidly, or vanished, recombination quickly ate away the lower part of the layer, causing the rapid increases in virtual heights until about H + 20 minutes. Some retardation contributed to the increases after about H + 10 minutes as the critical frequency was then down to 10 Mc and lower, reaching approximately pre-shot values by about H + 18 minutes.

Thereafter, the critical frequency increased, and virtual heights decreased as a traveling disturbance began to arrive. The heights continued to decrease after the maximum critical frequency associated with the disturbance had passed.

SECRET

Star Fish, Tonga.

Equipment difficulty at Tonga, beginning about 5 minutes
before the detonation, prevented observation of any prompt ef-
fects associated with the shot. The ionogram shown in Figure
21A was made 9 minutes before the explosion and indicates that
ionospheric conditions were near normal. Figure 21B is an
ionogram made at H + 1 minute in which the absence of all echoes
may be noted. Ionograms made thirty minutes after the blast
still showed no echo returns. When continuous operation of the
ionosonde was resumed at H + 48 minutes, nearly total blackout
was still in existence. Very weak echoes which developed into
a new layer were beginning to appear at a virtual height in
excess of 400 km at a frequency of 13 to 14 Mc. The virtual
height of this layer decreased slowly at a rate of about 2
km/min, and the frequency range of echo returns grew, maintain-
ing approximately a constant upper frequency limit but extending
to lower frequencies with time. At H + 57 minutes, a second
layer began to form at about the same virtual height where the
first observed layer had originated, and it also decreased in
height with time. The virtual height of various echo returns
for a period of more than two hours is shown in Figure 24.

The ionograms in Figure 21 show, in addition to the two
layers mentioned above, the development of a third and fourth
layer at virtual heights of 140 and 180 km. The appearance of
echoes without retardation at the upper-frequency end suggests
that all of these layers were thin, or that the echoes were from
an oblique irregularity. In ionogram H, the upper echo region had
developed retardation at the upper frequency end, seen in spite
of the spread echoes. Considerable spread-F was observed
through-out the remainder of the night. Figure 22 shows the
variation of f-min and the frequency ranges over which the echoes

33

SECRET

from the layers discussed above were observed.

Virtual heights at fixed frequencies are not presented for Tonga.

Figure 23 shows the Tonga f-plots. At sunrise following the shot, f-min increased to and remained at higher than normal values throughout the daylight hours of 9 July. Only slightly higher absorption occurred during the daytime on 10 July. Following sunrise on 9 July, the F-region critical frequency behaved normally.

Check Mate, Maui.

Figure 27A shows the pre-shot ionogram. The explosion took place as the ionosonde passed 0.5 Mc on the next (0830 GMT) ionogram, Figure 27B. There was an instantaneous though barely perceptible decrease in noise and interference in the next 100 kc or so (compare Figure 27B with Figure 27A), and the decrease was very noticeable below 0.5 Mc in the following sweep ½ minute later (compare Figure 27C with 27B and 27A).

A faint sporadic-E echo at 100 km between about 0.5 and 0.6 Mc in Figure 27A does not show in Figure 27B and did not reappear until about H + 14 minutes. It seems likely that the disappearance was caused by increased absorption, but because of the variability of sporadic-E itself, the return of the echo indicates only the upper limit of the duration of the absorption.

Near noon the next day (Figure 29), the absorption was somewhat higher than usual, but a similar thing occurred near the noon preceding the shot. An unusual fuzziness of the F-region echoes also occurred near the following noon.

A slight increase in the F2 critical frequencies lasting about five minutes started about H + 24 minutes (Figure 28), suggesting the passage of a shot-generated traveling disturbance.

34

SECRET

Passage of the disturbance is also indicated by the slight decrease in virtual height at 3 Mc between H + 20 minutes and H + 30 minutes in the October 20 section of Figure 87. Otherwise, there was little to suggest any effect of the explosion.

Check Mate, Tern.

At the time of Shot Check Mate, ionospheric conditions appeared to be near normal with multiple F-layer echoes and an E-layer echo as shown in Figure 30A. The shot occurred at about 10 Mc on this ionogram. Figure 30B made immediately after the detonation indicates that a modest increase in absorption occurred which caused a loss of multiple returns, a reduction in the strength of the E-layer echo return, and a diminished amount of interference. The increased retardation at the lower frequency end of the F-region echo indicates an increase of ionization at heights below the reflection level. The variation of f-min in Figure 31 shows that the absorption diminished to pre-shot values within 10 minutes.

The extended range ionogram of Figure 30C made at H + 8 minutes shows that low absorption exists, as evidenced by the multiple-echo returns. There is also indication of an oblique echo extending in frequency to about 6 Mc at a range of about 650 km. The ionogram of Figure 30D, made at H + 10 minutes, shows a continuation of this oblique echo between 5 and 6 Mc at a range greater than 500 km as well as a spread-F condition. At this time, a rapid change in critical frequency begins to occur, with F2 critical frequencies increasing by 2 Mc in an interval of about 7 minutes. This change in critical frequency, (see Figure 31) corresponds to an increase in electron density of 2.5 times. Following the steep increase, in foF2, the

35

SECRET

critical frequencies decreased 1 Mc by about H + 28 minutes. This bump on the critical frequency curves was undoubtedly the effect of the passage of a shot-generated traveling disturbance.

The passage of the traveling disturbance is also well marked in the October 20 section of Figure 88. Note also in this figure the sudden increase in the 2 Mc curve at H = O, caused by the additional retardation resulting from new ionization formed instantaneously in the E- or lower F-region over Tern.

In the f-plots of Figure 32 at 1300 GMT on 20 October (H + 4.5 hours), f-min increased to near its daytime value, although this was some 4 hours before sunrise. Echoes indicating stratification of the F-region was also observed at times during this period of high f-min, and a representative ionogram, made at H + 5 hours, is shown in Figure 30E. The increase in absorption observed at this time may have resulted from debris which arrived over Tern. If this is the case, the average drift velocity from the detonation was approximately 180 km/hr. The absorption which occurred during the daytime hours following Shot Check Mate was no greater than that on normal days. This differs from the effects observed after other shots when significantly greater absorption than normal was produced in the daylight hours.

Attention is called, in Figure 32, to the extraordinarily strong blanketing sporadic-E echoes which occurred for several hours beginning at H + 29 hours (1300 GMT on 21 October). This was possibly caused by bomb debris drifting cver Tern at this time. Similar effects were observed between H + 17 hours and H + 28 hours following King Fish (Figure 66, 0500 to 1600 GMT, 2 November).

Check Mate, Midway.

The last pre-event ionogram is shown in Figure 33A. The

foF2 and f-min were about normal for the hour.

Following the shot, there were no observable prompt changes, but, beginning about H + 20 minutes, a traveling disturbance began to increase the critical frequency (Figure 34) and decrease the virtual heights (Figure 89, October 20 section). Another, much weaker, disturbance seems to have arrived at about H + 105 minutes. It produced a barely perceptible increase in critical frequency and decrease in virtual height. A more marked indication of its arrival is the oblique echo which appears in the ionogram made at H + 100 minutes (Figure 33B). It may, however, have had a natural origin.

Multiple traces, such as those in Figure 33C, continued to appear until about H + 3.5 hours, but are not necessarily bomb-associated.

Interference prevented accurate determinations of f-min, but within the available indications, there was no abnormal local absorption caused by the shot. Both f-min and the critical frequency were normal in the two days following the shot (Figure 35). Check Mate, Canton.

At the time of detonation, f-min was 0.5 Mc, and foF2 was 9.0 Mc and decreasing slowly. For the period 19-31 October, at this hour, foF2 was normally 6.5 to 9.0 Mc, and there was a tendency for spread-F to develop. Immediately prior to the detonation, there was some spreading of the F-trace near 3 Mc and also a faint trace of Es at a virtual height of 160 km. Figure 36A shows the pre-shot ionogram. The shot took place at about 10 Mc on this ionogram. The next ionogram (Figure 36B) shows a moderate increase in f-min to about 1 Mc. There was no discernible effect on the F-layer. Along with the increase in

37

SECRET

f-min, there was a decrease in interference particularly in the broadcast band. Interfering signals are still missing in the ionogram made at H + 30 minutes (Figure 36C).

There was a gradual build-up of oblique echoes faintly seen at 0900 above the regular F-layer trace. By 0923, Figure 36D, echoes at several ranges had appeared. Thereafter, the additional echoes diminished, and by 1000, Figure 36E, the record was not greatly different from the pre-event record, except that f-min was still moderately above normal.

The effect of a traveling disturbance may be discerned in the oscillation of foF2 in the interval between about H + 30 minutes and H + 60 minutes in Figure 37.

The spread-F shown in the f-plots (Figure 38) was moderately diffuse, extending from the lowest observed F-layer frequency up to foF2. An example of this type of spread-F may be seen in Figure 36.

There were no abnormal height variations of the F-layer following the shot.

Check.Mate, Tutuila.

A prompt increase in absorption is indicated by the prompt decrease in noise and interference at the lower frequencies, the increase in f-min, and the disappearance of sporadic-E multiples at the lower frequencies. In the frequency range between about 3 and 6 Mc on the pre-shot ionogram (Figure 39A), there are traces of echoes from the previous pulse (1/60-second additonal delay)--the fuzzy traces sloping upward at about 45^c angle. These had all but disappeared in Figure 39B, indicating a small amount of absorption. By approximately H + 1.5 minutes, however, they were back at nearly full strength. Also, f-min had recovered substantially, although the sporadic-E multiples near

0.5 Mc had not reappeared. A new sporadic-E echo had appeared
at about 80 km between approximately 0.4   and 1.1 Mc. This
echo is still evident at H - 40 minutes in Figure 39D between
0.4 and 0.5 Mc at about H - 40 minutes, although it is not
visible in the extended range ionogram, Figure 39C, made at
H + 9.5 minutes.

In the F-region there was a travelling disturbance which
first appeared at H + 6.5 minutes as a faint trace at a range
of about 460 km. The range decreased and the echo developed
structure, appearing at H - 9.5 minutes as shown in Figure 39C,
at H + 40 minutes as in Figure 39D, and at H + 1.5 hours as
shown in Figure 39E, where its range is substantially less
than that of the first hop of the regular F-echo. In ten
more minutes the regular F-echoes were obscured, and 2-hop
and higher order echoes tended to disappear altogether. The
new echoes then increased in range as though the disturbance
had passed by. By H + 3 hours, the regular F-echoes had reappeared
clearly, and the minimum range of the new echoes was greater than
that of the first hop regular echo. By about H + 4 hours, the
new echoes had completely disappeared.

As is apparent in the ionograms of Figure 39, equipment
difficulty and/or interference above 9 Mc prevented recording
good echoes from the regular F2-layer (although the oblique
echoes show up above 9 Mc in 39C and 39E). Thus, the trend of
the regular F2-layer critical frequencies is not shown beyond
about H + 30 minutes in Figure 40. However, the virtual height
changes associated with the disturbance mentioned above are re-
flected in the curves in the upper section of Figure 90. The
abnormally high f-min values after about H + 90 minutes, shown

39

SECRET

in Figures 40 and 41 may have been associated with the disturbance. The origin and nature of the disturbance is not clear at this writing.

Check Mate, Tonga.

Two ionograms, A and B, of Figure 42 illustrate effects of Shot Check Mate.

Ionogram A, 0829 (3/4) GMT, was the last made prior to the shot, which occurred at its end. On this ionogram, f-min is less than 1 Mc.

Ionogram B, which started about H + 30 seconds, shows an increase of f-min to 1.2 Mc and the loss of a few interfering signals. All other characteristics remained at pre-event values. The increase in f-min may well have been fortuitous, as moderately enhanced f-min continued for about an hour (Figure 43).

The f-plots in Figure 44 show no recognizable effects of the event.

Blue Gill, Maui.

This shot occurred at about 0.7 Mc on the 1000 GMT sweep (Figure 45B). Some slight decrease in interfering signals in the next 100 kc or so is possible but not marked (compare Figure 45B with Figure 45A). In the next ionogram taken 30 seconds later (not shown), the decrease in noise and interference below about 0.6 Mc is very marked. An increase in local absorption was indicated by the disappearance of the sporadic-E echo which appears at 100 km in the vicinity of 0.6 Mc in Figures 45A and 45B. This echo reappeared at about H + 14 minutes. The time of reappearance of the echo coincided with a decrease in local absorption as indicated by the drop in f-min at H + 14 minutes

SECRET

in Figure 46. There were no further indications of abnormal absorption until about 1300. At about this time, the F-region echoes disappeared for a short period (Figure 45G). But this may not have been simply an increase in absorption; it may have been the result of a drop in critical frequency below the occulting frequency (fbEs) of sporadic-E. At about H + 12.5 hours, just after local noon, there was an unusual increase in f-min for about an hour (Figure 47), possibly indicative of debris passing by.

There were several well-marked traveling disturbances in the F-region. One is illustrated in Figures 45C and 45D, another in 45E, and a third in 45F. The passage of the disturbances produced marked stratification. Associated with these three disturbances are the two humps at H + 100 minutes and H + 130 minutes, and the uptilt at H + 165 minutes on the 2-Mc curve for 26 October in Figure 87, and the two jogs in critical frequency at H + 95 minutes and H + 135 minutes in Fig. 46. A jog for the third disturbance did not show up this figure. The disappearance of the 3-Mc curve at H + 5 minutes is the result of the decrease in foF2 which was in progress before the shot. The reappearance at H + 35 minutes may be the result of a disturbance generated by the shot.

Figure 45H illustrated the appearance of the F-region echoes after the period of weak echoes illustrated by Figure 45G.

Blue Gill, Tern.

F-layer critical frequencies and f-min were near normal values prior to the Blue Gill shot. Figures 48A and B show the ionograms made just prior to, and immediately following,

41

SECRET

the shot, which took place at about 8 Mc in 48A. Prompt absorption of considerable strength is denoted by the increase in f-min and loss of the multiple F-layer and E-layer echoes recorded in A. High absorption existed for only a few minutes, however, as indicated by the f-min plot in Figure 49. Pre-shot values were reached again after about 30 minutes.

No prompt F-region effects were observed, but critical frequencies began to be disturbed at about H + 10 minutes (Figure 49). A fairly rapid decrease began at about H + 25 minutes, and the greatest effect (traveling disturbance) took place near H + 40 minutes. See tangled traces in Figure 48C, and rapid development illustrated in Figures 48C through E. Also note the virtual height curves for 26 October in Figure 63.

Taking 25 minutes, the time of beginning of the decline in critical frequency, as the time of the arrival of the disturbance, and 900 km as the approximate distance to the shot, the average velocity was 0.6 km/sec. Additional traveling disturbances moved over Tern beginning at approximately H + 60 and at H + 80 minutes. The ionogram record made at H + 69 minutes, Figure 48F, shows an example of stratification and oblique echoes resulting from these disturbances.

A large increase in absorption near the time of sunrise on the morning after Blue Gill caused near, or total, blackout of echoes for more than an hour. This blackout effect, which may be observed in the f-plots shown in Figure 50, resulted from the fact that f-min increased, due to D-region absorption, more rapidly and to higher values from the solar excitation than did the F-region critical frequencies. Absorption con-

42

SECRET

tinued to remain significantly higher than normal for at least
30 hours following the detonation and included the period of
darkness on 27 October. F-region critical frequencies were
near normal values when observable after the sunrise blackout
on 26 October, and no further anomalous F-region effects were
noted.

Blue Gill, Midway.

The pre-shot ionogram is shown in Figure 33D, which was
cut off at 6 Mc as a result of equipment malfunctioning. All
of the important information is, however, shown in the portion
below 6 Mc. Note that f-min was less than 1 Mc, and sporadic-E
echoes went to 2.6 Mc.

Shot time was at the beginning of the next ionogram,
Figure 33E, at about 1 Mc on this ionogram. The sporadic-
E echoes disappeared resulting in an increase of f-min to about
1.7 Mc. The sporadic-E echoes again appeared faintly in the
next ionogram made 15 seconds later (not shown), and f-min was
again below 1 Mc by H + 10 minutes.

There was no striking evidence of shot-generated travel-
ing disturbances, though some of the fluctuations in critical
frequency in Figure 51 and in the 26 October virtual height
curves of Figure 89 may have been shot-generated. Figure 33F
shows disturbed traces which occurred more than 2.5 hours after
the shot.

By 1425 (Figure 33G) blanketing sporadic-E obliterated
F2-layer echoes to a large extent. The ionograms for the
period from 1430 to 1610 showed complete blanketing by sporadic-
E, perhaps indicative of debris. This period is indicated in
the f-plots of Figure 52. Sporadic-E was also stronger than
usual during the following daylight period.

43

SECRET

Blue Gill, Canton.

At the time of detonation, the F-layer showed considerable spread-F. The maximum echo frequency was about 11 Mc. Sporadic-E was moderately strong, and f-min was about 0.5 Mc. This is seen in Figure 53A. The shot occurred at about 2 Mc on this ionogram. The immediate effect is a marked decrease in the broadcast band interference (500 to 1,500 kc) in Figure 53B, with a diminution of interference up to about 4 Mc. The vertical incidence echoes remained virtually unchanged, although there was a slight increase in f-min.

Following the shot, there was a gradual increase of f-min starting about 10 minutes after the shot. But, this may well have been a normal fluctuation (compare with other nights in Figure 55). Figures 53C and D show the situation at H + 27 minutes and H + 90 minutes, respectively.

Following sunrise, however, f-min increased to somewhat higher than normal values. Figure 53E shows the ionogram for H + 12 hours.

Blue Gill, Tutuila.

The shot occurred at about 13 Mc on Figure 56A. Absorption increased suddenly, as indicated by the increase in f-min (Figures 56 and 57) and the disappearance of sporadic-E echoes (Figure 56B), but recovered substantially in 2 minutes (Figure 56C). Maximum f-min was 2 Mc. Absorption increased again beginning about H + 1 hour and 40 minutes (Figures 57 and 58), f-min reaching 1.5 Mc by about H + 2 hours and 40 minutes, but subsiding to normal by about H + 4 hours. Absorption again became abnormally high at sunrise, lasting about four hours (Figure 58). There were apparently no effects in the F-

44

region. Virtual heights showed no unusual variations following
this shot (Figure 90).

Blue Gill, Tonga.

Three ionograms, C, D, and E of Figure 42, illustrate
effects of the Blue Gill shot.

Ionogram C, 0959 GMT, shows the situation just prior
to the explosion. Multiple echoes from both E-and F-regions
are clearly visible. The shot took place at about 6 Mc on
this ionogram.

Ionogram D, H + 15 seconds, shows very little change in
the F-region, but absorption has obliterated echoes from the E-
region. The result is a sudden increase of f-min from less
than 1 to 2.3 Mc. There is also a marked reduction in the
number of interfering signals. A vestige of the first multiple
echo from the F-layer survived; critical frequencies remained
unchanged.

Ionogram E, H + 25 minutes, begins to look like the pre-
event ionogram. A lack of multiple echoes from the E-region,
however, shows that absorption at the lower frequencies is
still somewhat enhanced.

The behavior of f-min is shown in Figure 59. There was
no appreciable disturbance of the F-region. There were no
unusual fluctuations of the critical frequencies.

The f-plots for October 25, 26, 27, and 28 appear in
Figure 60. These are typical of undisturbed days at this
latitude. The only indication of the event of October 26
is the high f-min value of 2.3 Mc at 1000 GMT.

King Fish, Maui.

The shot took place at about 0.5 Mc in Figure 61B.

Absorption increased abruptly, though moderately, increasing f-min from about 0.5 to about 1.2 Mc (Figures 61 and 62). There was partial recovery in about two minutes, but f-min remained abnormally high for the next several hours (Figures 62 and 63). The increase at sunrise was less than normal (Figure 63), so that daytime values were approximately normal until a little after noon when abnormally high values occurred for a little more than an hour (Figure 63).

At about H + 15 minutes, a traveling disturbance arrived, and the F-region critical frequencies started to increase. By about H + 30 minutes (Figure 62), the increase amounted to about 1 Mc. The critical frequencies then returned to near normal by H + 50 minutes. Figure 61E is an ionogram near the start of this period. From about H + 46 minutes to H + 69 minutes, absorption was high, with an oblique echo and some stratification indicated by a kink appearing about H + 54 minutes which developed into a ledge that moved upward off the record at about E + 74 minutes. Another ledge developed at about H + 81 minutes during another but slighter increase in critical frequencies which took place between about H + 60 minutes and H + 90 minutes. This ledge moved in and took over the trace at about H + 92 minutes. The extraordinary trace became quite weak again about this time and disappeared shortly after, indicating another period of increased absorption (Figure 61F).

At about H + 96 minutes, a cloudy ledge appeared high up on the ordinary trace and developed into a well-defined ledge at about H + 100 minutes. A faint extraordinary trace was also visible. This ledge moved in and took over at about

SECRET

H + 112 minutes. The extraordinary trace remained very weak until about H + 135 minutes.

Note the time relationship of the transients in critical frequency and virtual height in Figures 62 and 87 (1 November) during the passage of the traveling disturbance which arrived about H + 15 minutes.

King Fish, Tern.

Ionospheric conditions which were producing nearly normal ionosonde echo returns just prior to Shot King Fish were changed promptly, and dramatically, for hours following the explosion. Figure 64 shows selected ionograms for a period up to H + 4 hours. Ionogram A shows the echoes just prior to the shot which took place at about 7 Mc on this ionogram. Prompt, high absorption obliterated all echoes in the next two ionograms (not shown). In the ionogram for H + 45 seconds, a weak echo from the F-region appeared over the limited frequency range from 2 to 2.4 Mc, as shown in ionogram B of Figure 64. The initial absorption decreased rapidly as indicated by the variation in f-min in Figure 65.

Ionogram C in Figure 64, made at H + 8 minutes, shows two new echo traces at a range of about 500 km. That the upper trace is a ledge high up in the F2-layer is indicated by the retardation (increased virtual height) near foF2. Note that the extraordinary wave echo is very weak. The newly created ledge continued to decrease in height and merged with the existing layer to produce a thin-layer-type echo within two minutes, H + 10 minutes, as shown in Figure 64D. As time proceeded, the new echo moved overhead and developed typical retardation at the critical frequencies, and multiple echoes (see Figure 64E made at H + 24 minutes). In addition, a new series of echoes

47

may be seen between the first and second overhead multiple echoes, and also a diffuse echo in the vicinity of 14 Mc at a range of between 400 and 500 km. The oblique echo which appears at a virtual height of about 250 km in Figure 64E gradually decreased in range and merged with that echo which had been overhead, (ionogram F in the vicinity 1.5 to 2.5 Mc). At the same time, the diffuse oblique echo, observed in E around 14 Mc, decreased in range and expanded to cover the frequency range from 2.5 Mc to a frequency in excess of the upper limit of the ionosonde. This echo may be seen in ionogram F, made at H + 33 minutes.

Beginning about H + 33 minutes, an additional traveling disturbance echo was first noted, appearing at a virtual height of about 500 km at a frequency near 1.5 Mc. This echo descended in height, appearing at H + 39 minutes as shown in Figure 64F between 1.5 and 2 Mc, and disappeared by about H + 50 minutes. The spread echo, with a fairly well defined lower edge, continued to decrease slowly in height, and over the next few hours several more oblique echoes were observed moving toward Tern, and these echoes gradually merged with those from overhead. The frequency range over which echo returns were observed varied with time, but in general, as shown in Figure 65, f-min values greatly exceeded the normal values and also exceeded those observed immediately following the detonation.

A representative echo return at approximately H + 4 hours is shown in Figure 64H where it may be seen that the upper frequency of the return is limited by the ionosonde equipment. It may also be observed that the minimum frequency of the echo return is around 5 Mc, and yet, noise and interference signals at frequencies as low as 0.25 Mc are readily observed. This

48

SECRET

characteristic suggests that the high absorption regions are relatively small in extent and are located essentially overhead of Tern. Thus, they do not affect the ionospheric regions through which distant signals pass in arriving at Tern.

Only weak returns, in the vicinity of 15 to 17 Mc, from the same echo shown in Figure 64H were observed during the period H + 5 hours to H + 6 hours. This was probably due to the increased absorption created by solar effects at sunrise. At H + 8 hours, the echo returns had evolved into a strong blanketing sporadic-E echo with, as yet, no F-layer returns visible although the sun had been up for several hours. As the blanketing frequency of the sporadic-E layer decreased, weak F-layer returns began to appear about H + $8\frac{1}{2}$ hours, which showed considerable spread in the echo return. By H + $10\frac{1}{2}$ hours, ionospheric reflections produced echo returns which were more nearly normal than any since the detonation; however, f-min values were substantially greater than normal, and F-layer critical frequencies were several megacycles below usual values. This condition of higher f-min and lower critical frequencies than normal existed throughout the daylight hours as may be seen in the f-plots of Figure 66. Also in Figure 66, echoes are indicated at three different times during the period 0500 to 1600 GMT on 2 November (H + 17 hours to H + 28 hours). The strong sporadic-E echoes may have resulted from debris arriving in the vicinity of Tern. A similar effect of strong sporadic-E echoes for several hours beginning at H + 29 hours following Check Mate (see Figure 32, 1300 GMT 21 October) was also noted.

The passage of the principal traveling disturbance is clearly indicated in the 1 November curves of Figure 88.

King Fish, Midway.

The shot occurred at about 8 Mc on ionogram A in Figure
67. Prior to the event, there was some forking and oblique
reflections in the F2 echoes.

Figure 67B, the ionogram taken immediately after the
shot, shows considerable local absorption (almost a blackout),
which mostly disappeared in about one and a half minutes.

Figure 67C (H + 11 minutes) is an extended range ionogram
(0 to 1400 km) showing forked traces, but no unusual echoes.
In Figure 67D (H + 17 minutes) there are indications of oblique
echoes——the fuzzy patch at 1300 km and just to the right of
the 2-Mc marker, and another short streak at 1300 km and about
4 Mc. Both echoes decreased in range in succeeding ionograms,
and the echo at 2 Mc by H + 20 minutes developed into a thin
line extending from about 1.7 to 3.5 Mc with a range near 1100
km, which increased slightly with increasing frequency. These
echoes disappeared shortly afterward.

The ionogram for H + 35 minutes (Figure 67E) shows consider-
ably increased critical frequencies, and the traces are no
longer forked. The change can also be seen in Figure 68 which
shows that the rise in critical frequencies started about 10
minutes after the event and returned to normal in about 60
minutes. The change in critical frequency was also accompanied
by a change in h'F2 from 330 km at H + 17 minutes to 220 km at
H + 45 minutes. This indicates that the increased ionization
density may have been largely the result of compression due to
a traveling disturbance. There was no indication on the ionograms
of the moving-in of ionized particles which would have shown
initially as oblique echoes rather than a gradual decrease in
virtual height and increase in critical frequency. Changes in

f-min after H + 45 minutes were not seen because the ionogram sweep started at 1.0 Mc and f-min was below the lower limit of the recorder much of the time.

By H + 67 minutes (Figure 67F), the critical frequencies were near normal and an oblique reflection can be seen above the second multiple near fxF2. This echo was first seen a minute before this record. Figure 67G shows how it changed in 4.5 minutes more (H + 71.5 minutes). By H + 74 minutes (Figure 67H), the oblique trace was moving in overhead and had become associated with the traces at the critical frequencies. By H + 78 minutes (Figure 67I), the former traces near foF2 and fxF2 had become spurs. Within a minute thereafter, the two pairs of traces had merged, and the stratification appears as a small ripple farther down each trace. A new oblique echo is seen in ionogram I at H + 74 minutes at 600 km. This echo was seen for only about 5 minutes.

Weak sporadic-E was seen at detonation time and immediately thereafter, but was not seen again for approximately 4 hours.

There was a possible long-delayed effect shown in Figure 67J, for 0400 GMT on 2 November. Complete blanketing by Es was observed for a time (see also Figure 69).

The shot-induced effects were the enhanced critical frequencies between H + 15 minutes and H + 60 minutes accompanied by a fairly rapid decrease in layer height (Figure 89) and one more well-marked traveling disturbance, first seen 66 minutes after detonation. A possible delayed effect was the occurrence of blanketing Es nearly 16 hours after the explosion.

King Fish, Canton.

Figure 70A shows an ionogram completed before shot time.

51

SECRET

The ionosphere was approximately normal with moderately heavy spread-F, but with a fairly well defined critical frequency; f-min was about 1 Mc.

The explosion took place at 1.2 Mc on the next ionogram (not shown). The immediate effect was the disappearance of the 2nd-hop sporadic-E echo and weakening of the other echoes. The next record (not shown) is very much like Figure 70B. The additional absorption had virtually disappeared by H + 4 minutes.

Beginning about H + 10 minutes, the character of the F2 echo changed, and by H + 20 minutes, as shown in Figure 70C, the echo was a moderately spread horizontal trace on the ionogram, and the turn up at the maximum frequency is no longer seen. There was also a considerable increase in the maximum echo frequency to 11 Mc. The sporadic-E echo was still relatively simple. In Figure 71, the rise and fall of the vertical lines indicating spread echoes between about H + 20 minutes and H + 40 minutes is indicative of the passage of a traveling disturbance.

The range spreading of the F-layer echo continued to be more pronounced with two ranges predominant at about 400 and 600 km. See Figure 70D. The sporadic-E echoes in this ionogram had also become more complex. The absorption had decreased to about normal as indicated by an f-min value of 0.6 Mc. By H + 112 minutes, Figure 70E, the F-layer was diffuse and showed a number of poorly defined traces. The sporadic-E echoes also showed multiple ranges. Subsequently the blanketing effect of the sporadic-E became more pronounced until complete blanketing of F2-echoes occurred at H + 2 hours, (1410 GMT) and from 1516 to 1520 GMT. Figure 71, showing blanketing (symbol A) after H + 117 minutes, merely indicates that very little of the F-layer returns were observed. During this

52

period, the F-layer height increased, and echoes were very diffuse.

By H + 5 hours, the F2-layer had largely returned to normal, with only a little spread-F. Thereafter, the ionograms appeared to be normal as shown in the f-plots of Figure 72.

The shot-induced effects were an early moderate increase in absorption followed by fairly large diffusing effects in the F-echoes, plus increased complexity of sporadic-E echoes and indications of a traveling disturbance. The total duration of the effects of the event appeared to be about five hours.

King Fish, Tutuila.

The shot occurred as the ionosonde was passing 2.5 Mc on the ionogram in Figure 73B, and the onset of strong absorption was instantaneous. The absorption increased in strength for about $\frac{1}{2}$ minute. The echoes in the ionogram made 30 seconds after Figure 73B (15 seconds before 73C) had almost disappeared. But by H + 1.5 minutes (Figure 73D), f-min was back down to about 1.5 Mc. Also in this figure is a trace of sporadic-E at about 80 km near 2 Mc. Referring to Figure 74, f-min returned to approximately the pre-shot value by H + 3 minutes, but increased again beginning about H + 3 minutes, and remained abnormally high the remainder of the night. At sunrise (Figure 75), it increased again to abnormally high morning values, but subsided to approximately normal values by late morning.

Again, referring to Figure 74, and the 1 November sections of Figures 75 and 90, the F2-layer remained relatively undisturbed until about H + 30 minutes, when the critical frequencies began to increase, and virtual heights to decrease. The crit-frequencies reached daytime values near H + 65 minutes, and the relative thickness of the underside of the F-layer decreased

considerably. Figure 74 shows another slight increase in critical frequencies near H + 150 minutes, but the magnitude of this is hardly more than a natural fluctuation. It should be noted that there was a tendency for the critical frequencies to increase sharply near 1200 GMT on other days (see 31 October in Figure 75, 19 and 22 October in Figure 41 and 25 October in Figure 58). The large excursion in critical frequency was probably caused by an influx of ionization from above and/or a compression of the original ionization which took place in such a way that no stratification occurred below the height of maximum density.

At about H + 2 hours, a fuzzy patch appeared near 11 Mc (about 4 to 5 Mc above the critical frequency) at a little beyond 500-km range. In a few minutes this was seen on an extended range ionogram (not shown) to extend backward with increased range (apparently retardation) to about a megacycle below foF2. In Figure 73F, a portion near 11 Mc can be seen just beyond the 500-km range marker. The range near 11 Mc gradually decreased to about 400 km before it disappeared near sunrise. None of the fuzzy echo showed on the ionograms after 0720 GMT (H + 5 hours and 10 minutes). Thereafter, the ionograms appeared normal but with weak echoes. Comparing the virtual height curves for Tutuila in Figure 26 (Star Fish) with those for King Fish in Figure 90, note the absence of the initial disturbance in the King Fish curves, but the general similarity thereafter.
King Fish, Tonga.

Ten ionograms, F through 0, of Figure 42 illustrate this event for Tonga.

Ionogram F, 1210 GMT, was being made just before shot time. The characteristics were f-min less than 1 Mc; h'Es 95

km, fEs 1.6 Mc; h'F2 250 km, foF2 6.9 Mc. The shot took place just after 1 Mc in ionogram G. The sporadic-E echo at 100 km was promptly cut off at about 1.1 Mc. F-region echoes are not seen at frequencies below 3.4 Mc, and the number of interfering signals was reduced considerably. Otherwise, there was no immediate change in the F2-echoes.

Ionogram H, H + 14 minutes, shows an echo from 1.9 to 2.5 Mc at a range of 380 km. This echo is at a frequency and range appropriate to the third multiple of Es. On the other hand, the absence of the second multiple of Es suggests that perhaps this is an oblique echo which may be related to the shot. Ionogram I, H + 19 minutes, shows the new echo fading out as the range decreased slowly. All other characteristics remained unchanged.

Ionogram J, H + 37 minutes, shows the appearance of another oblique echo at a range of 410 km. By H + 75 minutes (K), its range had decreased considerably. That the echo is not from overhead is indicated by the lack of interference with the first multiple reflection from the F2-region.

In ionogram L, H + 92 minutes, the critical frequencies in first-hop F2-echo are nearly obscured by the oblique echoes. h'F has decreased to 210 km, and foF2 has decreased to 7.5 Mc. The weak return from the E-region may be due to the variable nature of Es rather than to absorption. Ionogram M, H + 116 minutes, shows still further development of the oblique echoes.

In ionogram N, H + 145 minutes, the oblique echoes have nearly vanished. The oblique echoes were last seen at about H + 230 minutes.

55

SECRET

Ionogram 0, H + 265 minutes, marks the start of a blackout period which began at sunrise and persisted about three hours. Recovery was slow, and normal-appearing records were not obtained until about 2240 GMT, or nearly noon.

Figure 76 shows the wave-like fluctuations of the F2 critical frequencies associated with traveling disturbances. The corresponding variations in virtual height appear in the curves at the bottom of the figure.

Figure 77 gives f-plots for October 31, November 1 and 2. These days are typical for this latitude. The event of November 1 is marked by a slight increase in f-min at 1215 GMT followed by a disturbance in the F-region and finally by a sunrise blackout at 1700. At 2245, the f-plot has returned to normal. Tight Rope, Maui.

Figure 78A is the pre-shot ionogram. The shot took place just after the ionogram. Effects seem to be confined to disturbances of the F-region which occurred beginning at H + 23 minutes. Figure 78B, the record for H + 24 minutes, shows an inflection of the traces near the critical frequency which indicates an increase in electron density above a height just below level of maximum electron density. The inflection was in evidence only about 3 minutes. Later, about H + 41 minutes, another inflection appeared for about 2 minutes (Figure 78C). At about H + 53 minutes, still another appeared for about 1 minute (Figure 78D). The satellite traces paralleling the 2nd- and 3rd-hop echoes near 2 Mc in Figure 78D may be echoes from an oblique irregularity. Another manifestation of a traveling disturbance appeared about H + 3 hours and 15 minutes (Figure 78E). This lasted about 20 minutes. There

SECRET

is little evidence of disturbance in Figure 78 and the 4
November curves of Figure 87.

Figure 80 gives the diurnal f-plots for this event.

Tight Rope, Tern.

The effects of Tight Rope at Tern, if any, were so mild
as to be indistinguishable from normal fluctuations. There was
no discernible prompt absorption, not even a discernible effect
on the background of interfering signals. Therefore, no iono-
grams and no f-plots are presented.

The evidence presented is in Figures 81 and 88. The in-
crease in critical frequencies, reaching a maximum at about
H + 50 minutes (Figure 81), may be bomb-associated, but takes
place much later than the disturbances produced by the other
bombs. The 4 November virtual height curves in Figure 88
likewise show nothing unusual.

Tight Rope, Midway.

Figure 67K shows an ionosonde sweep completed at H + 3
seconds; i.e., the bomb went off at about 14 Mc in this iono-
gram. Figure 67L shows an ionogram started at H + 4 seconds.
No change is evident except for a possible diminution of inter-
ference indicating increased absorption elsewhere.

Evidence of traveling disturbances, possibly bomb-generated,
appeared in subsequent ionograms, as at Maui. There were a
number of fairly rapidly moving oblique echoes over a period
of about 3 hours. By 1225 GMT, the ionosphere appeared to have
returned to normal.

Notice the similarity of the critical frequency variation
in Figure 82 and the 4 November virtual height variation in
Figure 89 to those for Tern (Figures 81 and 88).

Figure 83 gives the diurnal f-plots for this event.

SECRET

Tight Rope, Canton.

No effects on the vertical incidence soundings were observed. There may have been a slight attenuation of interference. No ionograms covering this event and no detailed plots of critical frequency and f-min and virtual height are included in this report. The diurnal f-plots are shown in Figure 84.

Tight Rope, Tutuila.

The ionograms showed no recognizable evidence of a bomb effect. The 4 November virtual height curves in Figure 90 show no effects. The diurnal f-plots are given in Figure 85.

Tight Rope, Tonga.

Two ionograms, P and Q, included in Figure 42 illustrate this event. No recognizable effects of the bomb were found in the ionograms. The f-plots for November 3, 4, 5, and 6 are given in Figure 86. These plots are typical of undisturbed days at this latitude.

DISCUSSION

Star Fish.

The changes in the ionosphere resulting from the Star Fish
shot as indicated by ionosonde data were greater at stations
located near the magnetic meridian passing through the point
of explosion than at the other stations. This was the case
even though some of the stations not on the magnetic meridian
were closer to the point of explosion.

The greatest duration of total blackout, approximately
85 minutes, occurred at Tern Island which lies near the point
at which the magnetic line through the explosion enters the
earth. Following total blackout, a high degree of absorption
persisted for several hours, and only weak spread echoes from
the F-region were observed. It is likely that HF radio com-
munications for radio paths requiring ionospheric reflection
in the vicinity of Tern Island would have been interrupted, or
poor, for several hours following the explosion.

At Tonga, near the southern conjugate area of Tern, an
extended period of total blackout also was observed. Although
equipment difficulty prevented continuous observation, total
blackout apparently persisted until H + 51 minutes. It should
be remembered, however, that the ionosonde at Tonga was an older
less sensitive model than those at some of the other stations,
Tern in particular.

The F-layer reflections at Tonga were entirely different
from the weak spread-type echoes observed at Tern. It seems
likely, following the total blackout at Tonga, that HF com-
munication circuits with reflection points in the ionosphere
over Tonga would have been able to operate satisfactorily

SECRET

much sooner than those circuits with paths in the vicinity of
Tern Island.

The various layers formed over Tonga may have been the
result of ionized bomb debris which travelled along the magnetic
field and deposited in the southern conjugate area. Some of
these layers may have been in existence at times earlier than
those observed with the ionosonde, but echo returns were pre-
vented by the high absorption at lower heights in the D-region.

At Tutuila, which is some 900 km north and somewhat east
of Tonga, very dramatic ionospheric effects were also observed.
It is interesting to note that the ionization density over
Tutuila following Star Fish was on the order of 4 times the
diurnal maximum value for a normal July day, when the critical
frequencies reach the vicinity of 12 Mc. The increase of F-
region critical frequency from a value of 4 Mc to over 20 Mc
indicates that the shot promptly produced a greater than 25-
fold increase in electron density.

The perturbation of the ionosphere in the equatorial
region over Canton, while significant, was much less than
observed at the other ionosonde stations along the magnetic
meridian. Blackout occurred for only a little over a minute
following the shot, and a transient F1 layer echo was returned
for about two minutes beginning at H + 3 minutes. No F2-layer
effect was observed until about H + 7 minutes when the critical
frequency began to increase, rising to a value of 11.5 Mc at
H + 20 minutes. This increase of critical frequency corresponds
to an increase in electron density of more than 2.5 times that
which existed prior to the shot.

The effects observed at the islands of Maui, Midway, and

60

SECRET

Wake were smaller in magnitude than at the other locations
discussed above. At these three stations, a prompt increase in
absorption occurred which resulted in a blackout for about 8
minutes at Midway, and for more than a minute at Maui. At Wake,
f-min increased to at least 6 Mc momentarily but dropped to 1
Mc within a minute. At Maui and Midway, f-min decreased more
slowly, requiring more than an hour before reaching 1 Mc.

F-region critical frequencies increased by about half a
megacycle at H + 15 minutes at Midway corresponding to an increase
in electron density of about 20 per cent. At Wake, a very slight
rising trend in the critical frequencies, which had begun prior
to the detonation, continued after the explosion, and it is not
certain that there was any effect in the F-region caused by the
shot within the first 15 minutes. The Maui station did not
record any increase in critical frequency, but, instead, fre-
quencies were slightly depressed in the period H + 5 to H + 10
minutes, after which time they decreased more rapidly, and to
values lower than normal for that period of day. Critical
frequencies at Midway and Wake also decreased at a rate greater
than normal, after the initial increase. The rapid decrease of
critical frequency at Midway contributed to a second period of
blackout at H + 35 minutes when the critical frequencies were
less than the value of f-min for a brief period.

Near the time of local sunrise at each of the seven
stations on the morning after Star Fish, D-region absorption
increased more rapidly and remained considerable higher through-
out the day than on normal days. A slight excess of absorption
on the following day was also noted. F-region characteristics
and critical frequencies returned to normal at all stations after
sunrise on the morning following the shot.

Most HF communication circuits crossing the Pacific Ocean should have suffered only a small amount of outage time due to absorption effects resulting from Star Fish. Notable exceptions would have been those circuits with paths traversing the ionosphere in the vicinity of the northern and southern conjugate areas around Tern and Tonga. The rapid decline in critical frequencies soon after the detonation to values lower than normal for the time of day, observed in the north at Maui, Midway, and Wake, may have caused MUF (maximum usable frequency) failure on circuits with ionospheric reflection points in those areas. Such circuits could probably have operated successfully by lowering the operating frequency. Ionospheric layers formed over Tonga, and the spread-F condition which developed there and at Tutuila could have resulted in deleterious effects on some types of circuits because of changes in multipath and fading conditions.

Check Mate.

All stations showed an immediate though moderate increase in local absorption, although the increase at Tonga may have been fortuitous. At all stations, except Tonga, there were indications of traveling disturbances after the explosion. At Tern, there was a well-marked increase in critical frequencies beginning about H + 8 minutes, and at Maui and Midway less well-marked increases beginning about H + 20 minutes at Maui and H + 20 to 25 minutes at Midway. These times imply average speeds of traveling disturbances of about 1.9 km/sec, 1.3 km/sec, and 1.0 to 1.3 km/sec, respectively, to Tern, Maui, and Midway.

A disturbance manifested by an oblique echo from an

62

SECRET

approaching disturbance followed by spread echoes seemed to
arrive at Canton about H + 53 minutes and at Tutuila about
H + 90 minutes. The corresponding average speeds would be
0.7 km/sec to Canton and 0.65 km/sec to Tutuila. Such iden-
tification of the disturbance at Tutuila may be erroneous,
because the corresponding echoes seemed to grow out of new
echoes which first appeared on the Tutuila ionograms at H +
6.5 minutes!

Blue Gill.

There were prompt increases in local absorption at all
stations, the most pronounced being at Tern, and the least,
apparently, at Canton. Apparent recovery time was variable,
but seemed to be about 10 minutes at most stations. Only at
Tutuila did there appear to be a relatively unambiguous delayed
increase in absorption (H + 2 hours to H + 3.5 hours) aside
from abnormal increases at sunrise.

F-region traveling disturbances of substantial magnitude
were indicated by the ionograms for Maui and Tern; a somewhat
weaker indication appears on the Midway ionograms; and none
is recognizable at the other stations. At least 3 and pos-
sibly more disturbances are recognizable in the Maui and Tern
records. Each of these disturbances is characterized by a
marked decrease in critical frequency followed by the develop-
ment of a higher layer with a greater critical frequency. As
the higher layer developed, it took the place of the previous
layer. The advent of the next disturbance was then marked
by another decrease in critical frequency, followed by the
appearance of another higher layer as the cycle repeated.

Taking the time at which the critical frequencies at

63

SECRET

Tern began to decrease at the onset of the first large disturbance as H + 25 minutes, the value obtained for the average velocity of travel from Johnston Island, assuming travel began at the instant of the explosion, is 0.6 km/sec. The decrease which began at H + 60 minutes for Maui would correspond to a velocity of 0.4 km/sec.

King Fish.

An immediate increase in local absorption occurred at all stations, but seemed to be least at Canton. The increase was greatest at Tern and Tutuila. There was substantial recovery at all stations after a few minutes, but at Tutuila the absorption increased rather rapidly again at about H + 10 minutes and remained high the rest of the night. At Tern, also, the absorption increased again in a more gradual manner after about H + 80 minutes and remained high the rest of the night.

F-region changes were dramatic at Tern and Tutuila; they were also well marked at Maui, Midway, and Tonga, but somewhat subtle at Canton. The increases in critical frequency which began about H + 17 minutes at Maui and about H + 40 minutes at Tutuila took place without marked stratification, whereas marked stratification appeared at Tern and Midway. At Tonga the effect was principally an increase in oblique echoes and spreading of the F-region echoes.

The above-mentioned times for the beginnings of the critical frequency increases at Maui (H + 17 minutes) and Tutuila (H + 40 minutes) both yield 1.5 km/sec for the average velocity of the disturbance. The beginnings of critical frequency disturbance at the other stations, including Canton, are in good agreement with this velocity. Except at Canton and Midway, the times of the maxima are proportional to

64

SECRET

distance from Johnston Island within a few percent. At Midway, the arrival was late. Again excepting Canton, a depression followed the main enhancement of critical frequencies, which was in turn followed by another small increase. The times of these minima are also approximately proportional to distance, arrival at Midway again being relatively late, and at Tonga relatively early.

Tight Rope.

Only Tonga showed evidence (an increase in f-min) of a prompt increase in local absorption, and this increase could have been fortuitous. No clear effects were recorded at Tern, but both Maui and Midway ionograms showed evidence of traveling disturbances, beginning at about H + 24 minutes at both places. The disturbances occurred over a period of about 3 hours in both cases. H + 24 minutes for these stations corresponds to a velocity of about 1.0 km/sec.

Comparison of Events.

The magnitudes of the effects of a shot tended to be a strong function of the detonation altitude, as well as the yield. Thus, Check Mate produced more disturbance at Tutuila than did Blue Gill, which was more than ten times as strong, because of the difference in altitude. The differences in the heights of Blue Gill and King Fish, which had similar yields, made a great difference in their effects, especially in the southern region.

Star Fish, of course, had a big advantage in both altitude and yield, and thus had by far the greatest effect at all stations. Tight Rope, on the other hand, though having about the same yield as Check Mate, had the lowest altitude of all,

65

SECRET

and thus produced scarcely recognizable effects at any station.

The effects of King Fish were similar in some ways to those of Star Fish. A notable difference is the practically instantaneous buildup of ionization density in the F-region at Tutuila by Star Fish, which was entirely lacking following King Fish. In both events, however, the major disturbances seemed to be at those stations near the conjugate areas, namely, Tern and Tutuila.

Although the altitude of Check Mate was substantially greater than that of King Fish, the effects of Check Mate at Tutuila were less like those of Star Fish than those of King Fish, presumably because of the low yield of Check Mate.

The overall effects of Check Mate and Blue Gill tended to be about equal, though noticeably different in detail. Thus, the change in critical frequency at Maui, Tern, and Midway, resulting from Check Mate, tended to be greater than that from Blue Gill, but oblique echoes and stratification of the F-region tended to be greater after Blue Gill than after Check Mate. This suggests that the principal traveling disturbance was higher in the ionosphere (mainly above the peak electron density in the F-region) for Check Mate than for Blue Gill.

Abnormally high absorption developed at sunrise or during the day following some events. The tendency was greatest for Star Fish, but nothing of the sort appeared after Check Mate and Tight Rope. Enhanced f-min occurred at all stations the day after Star Fish, at all stations but Maui and Midway after Blue Gill, and at all but Midway and Canton after King Fish. It is conceivable that some of the extra absorption following King Fish was caused by the airdrop on 30 October.

66

SECRET

CONCLUSIONS AND RECOMMENDATIONS

As this project was primarily concerned with data gathering, the interpretation given in this report is sketchy and speculative. Much work remains to be done, especially in correlating the results of measurements by the various projects, before an adequate understanding of bomb effects can be achieved.

The sweep-frequency ionosonde has proved capable of providing much useful data on immediate and delayed effects on absorption in the lower ionosphere and electron density in the E-and F-regions, but changes in virtual heights are not per se reliable indications of true height changes, because the retardation at a given frequency depends on the retardation at all lower frequencies. Thus, to convert virtual heights into true heights, the complete ionogram for all frequencies below the critical frequency is necessary, in principle, although certain gaps can be tolerated without excessive error. Another condition necessary for the conversion, however, is that the ionosphere over the station be plane stratified, and this condition may not be well met when traveling disturbances are present.

Most of the ionosondes used in our measurements provided ionograms adequate for reasonably accurate true-height calculations under undisturbed conditions. The performance could have been improved with better antennas, but it is doubtful whether, even with the best performance, the ionograms would have been adequate for true-height calculations under the disturbed conditions following the Fish Bowl shots. Thus, no true-height analysis was attempted for this report.

The deployment of the available ionosondes seems in retrospect to have been quite good, especially in view of

SECRET

the locations of ionosondes operated by other projects.

Although intended for and used in continuous operation, the ionosondes were not really properly designed for this mode of operation and tended to break down frequently. For a future Fish Bowl, it would be wise to use new ionosondes designed with the 1962 Fish Bowl experience in mind.

APPENDIX

CONVENTIONS AND SYMBOLS FOR f-PLOTS

1. When definite and well defined, the ordinary wave critical frequencies are plotted as open circles.

2. Definite x- and z- critical frequencies, when plotted, are plotted as x's and z's respectively. No Z echoes appeared in the ionograms described in this report.

3. If the value of a critical frequency, as defined by the standards of accuracy, or the magnetoionic identity is in doubt, a filled circle is plotted. This applies to all the components; o, x, or z. When a filled circle is used, and the reason for the doubt is not obvious from the representation on the f-plot, the appropriate descriptive letter is written on the f-plot near the filled circle. When the values for a particular ionogram plotted on the f-plot are all doubtful for the same reason, the descriptive letter is noted at the top margin. This procedure facilitates transcribing the data to the daily tabulation sheets.

4. Any spread of the echo about the critical frequency is plotted as a straight vertical line extending over the frequency range covered by the spread. If a critical frequency is seen through the spread, its value is plotted at the appropriate frequency.

5. All values of fbEs are plotted as filled circles; consecutive 15-minute observations associated with the same Es trace are connected from one sounding to the next by a straight line. When fbEs exceeds foF2, the value of foEs may be plotted and connected to adjacent values of fbEs.

69

SECRET

6. f-min is represented by a filled circle with a vertical line connecting it to the effective lower frequency limit of the ionosonde.

7. "v" represents "less than" and is used primarily with f-min. Normally, "v" will be plotted for f-min at the lowest frequency at which echoes are received when this "lowest frequency" is determined by noise or interference.

8. "Λ " represents "greater than" and will most often be used with foF2. It is plotted at the highest frequency obtained within the accuracy rules.

9. Missing data: Prolonged periods of no echoes due to equipment difficulty or absorption may be indicated on the f-plot by _____C_____ or _____B_____ .

10. Qualifying and descriptive letters:

   A   Measurement influenced by, or impossible because of, the presence of a lower thin layer, for example, Es.

   N   Conditions are such that the measurement cannot readily be interpreted, for example, in the presence of oblique echoes.

   R   Measurement influenced by, or impossible because of, absorption in the vicinity of a critical frequency.

   S   Measurement influenced by, or impossible because of, interference or atmospherics.
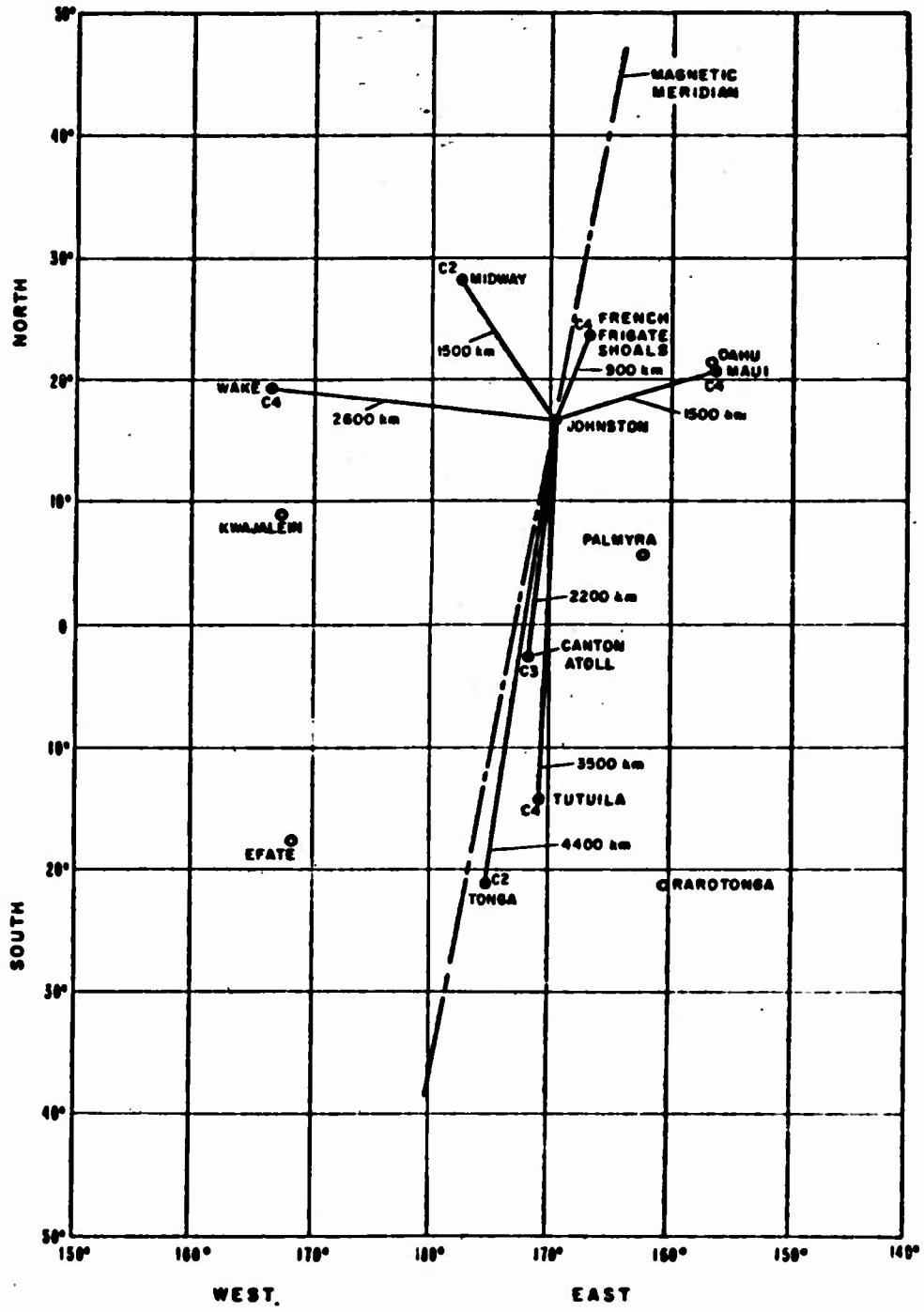
Figure 1 Ionosonde locations.

71
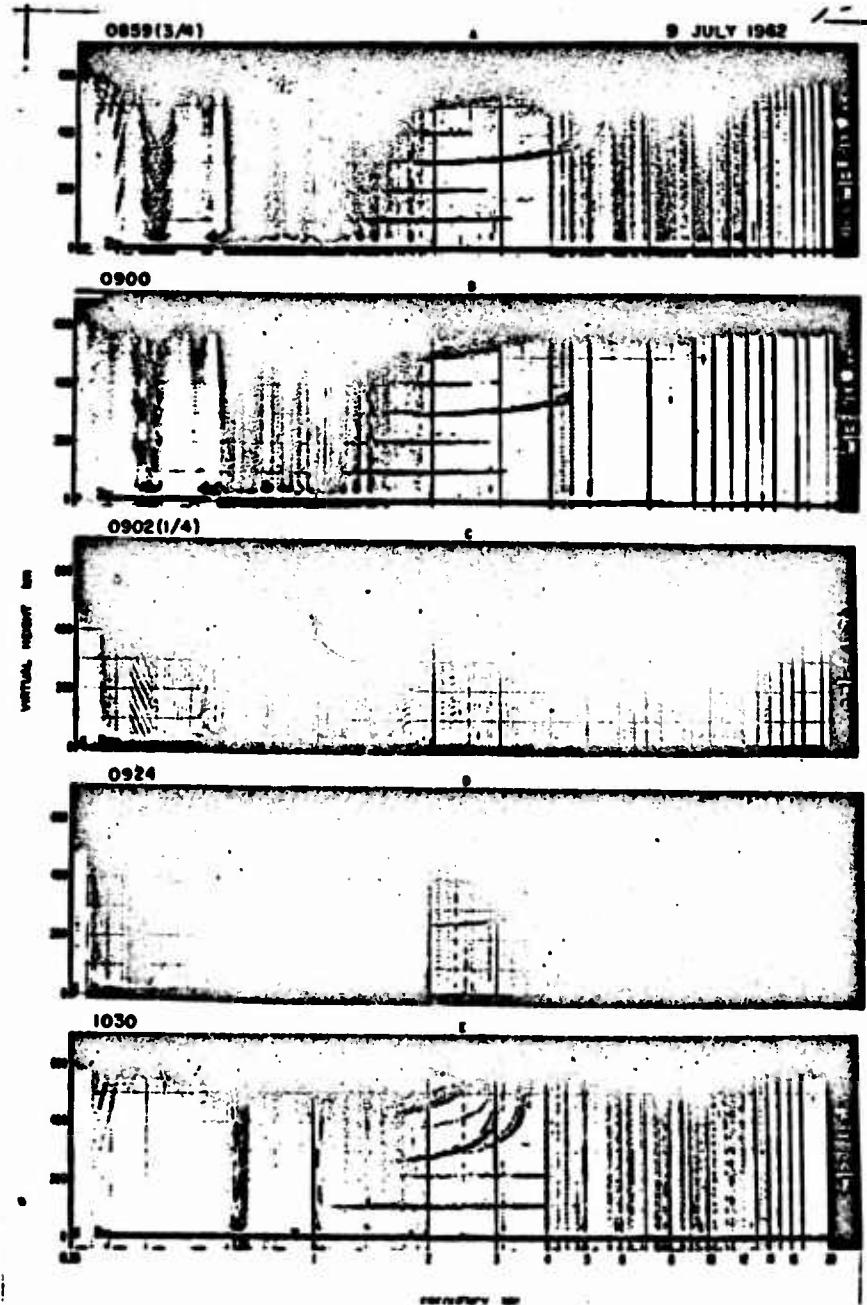
SECRET

Figure 2 Star Fish, Maui, selected ionograms.
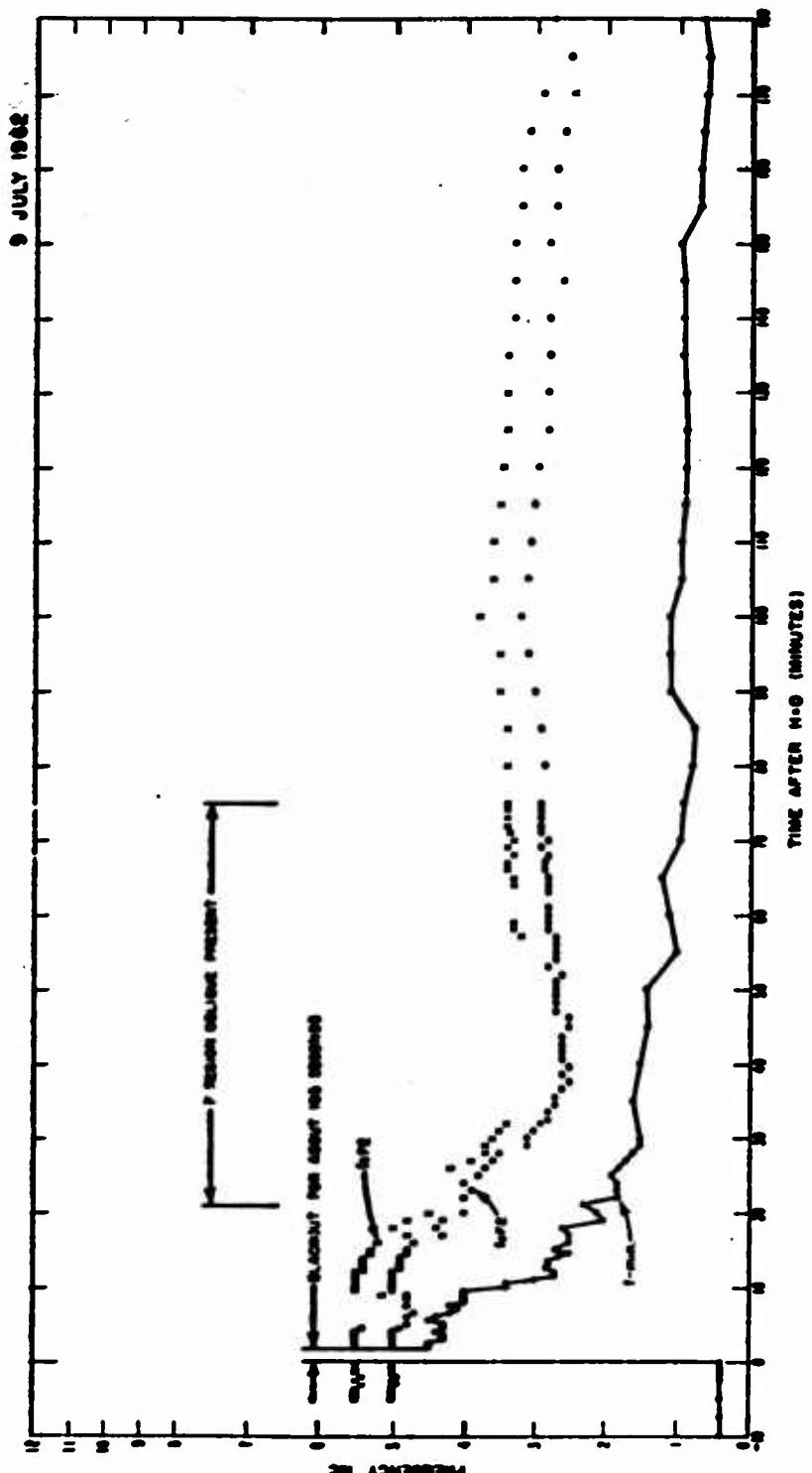
SECRET

Figure 3 Star Fish, Maui, 3-hour frequency plot.
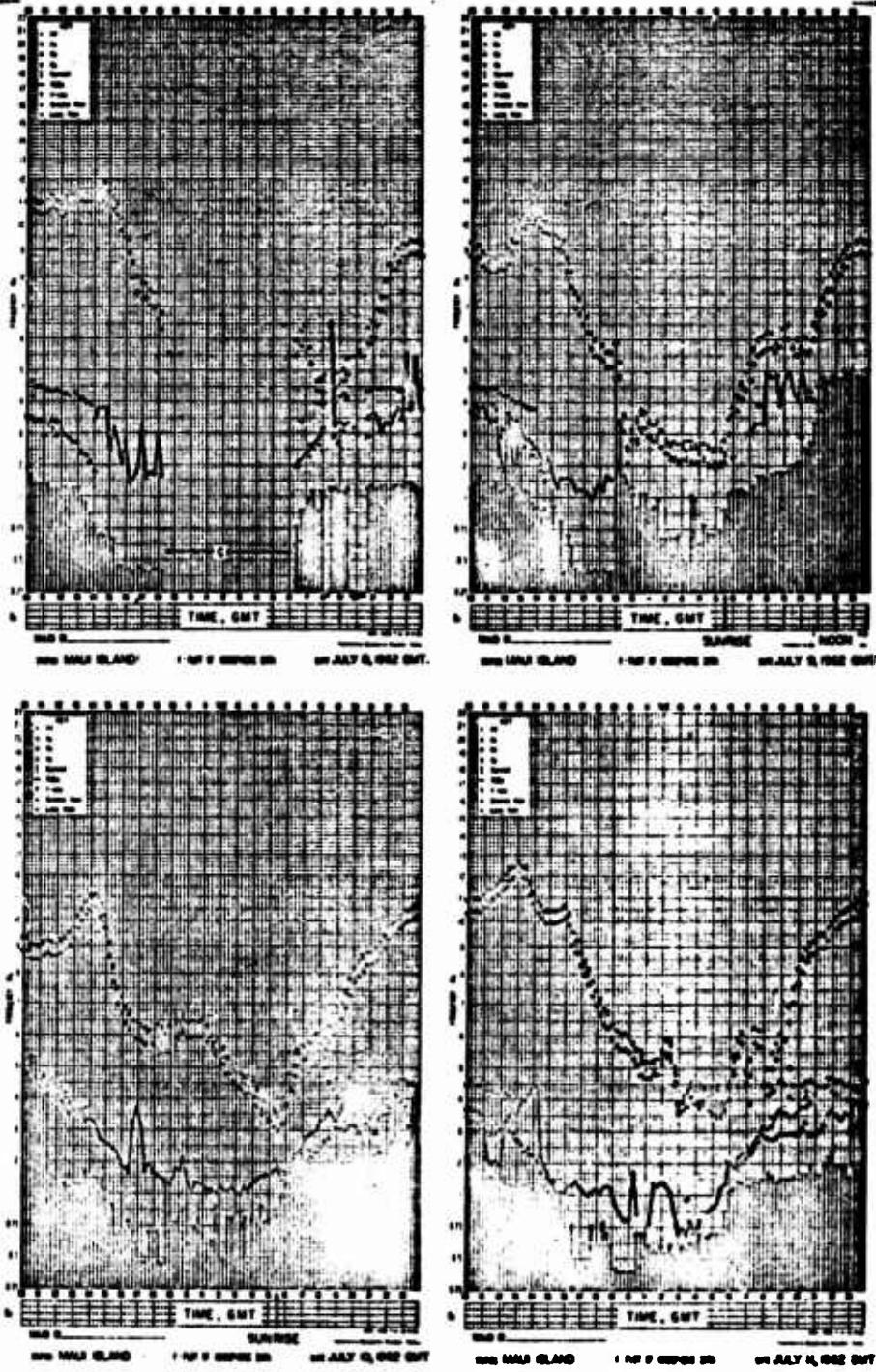
Figure 4 Star Fish, Maui, f-plots

74
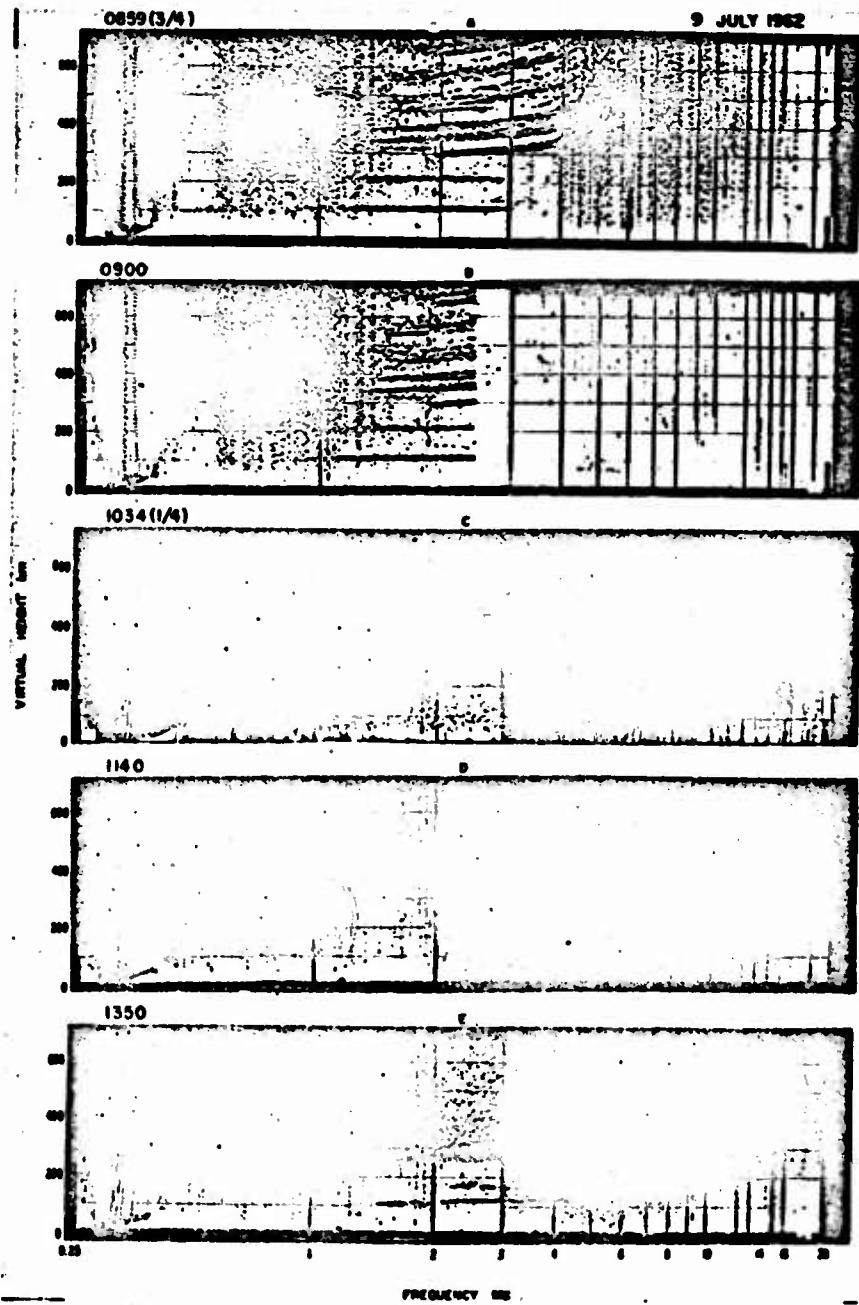
Figure 5 Star Fish, Tern, selected ionograms.
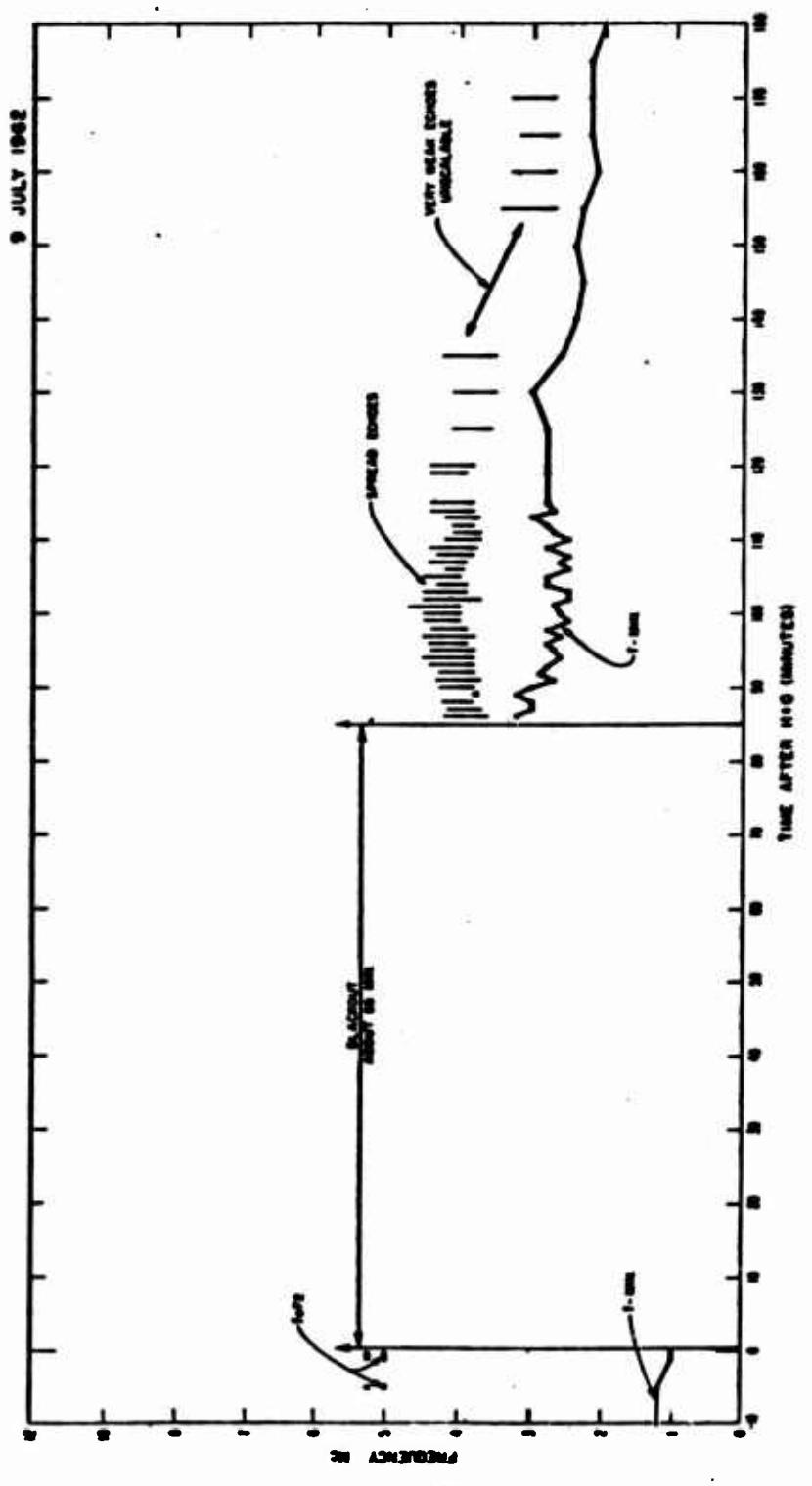
SECRET

Figure 6 Star Fish, Tern, 3-hour frequency plot.

76
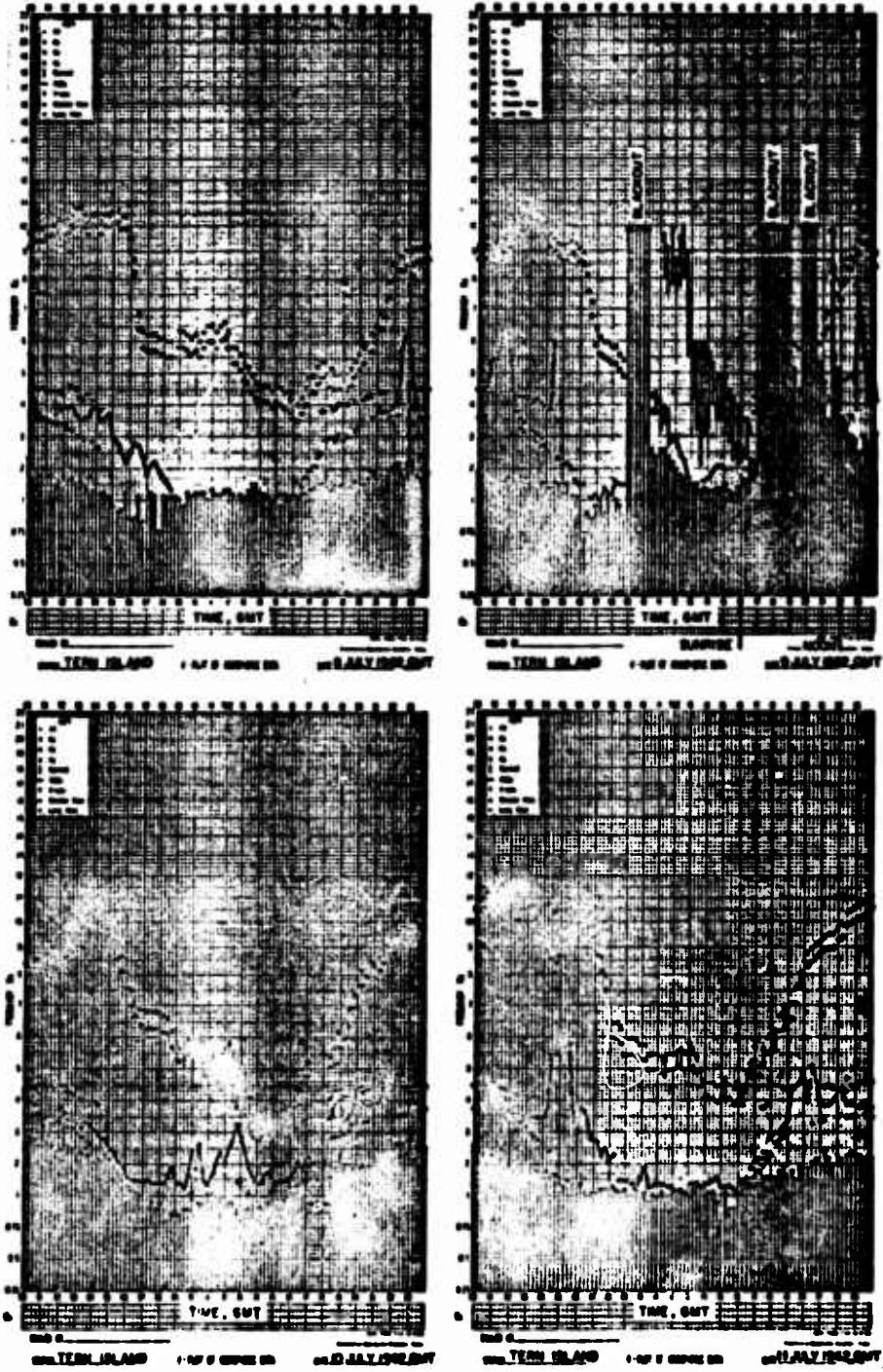
Figure 7 Star Fish, Tern, f-plots.

77

SECRET
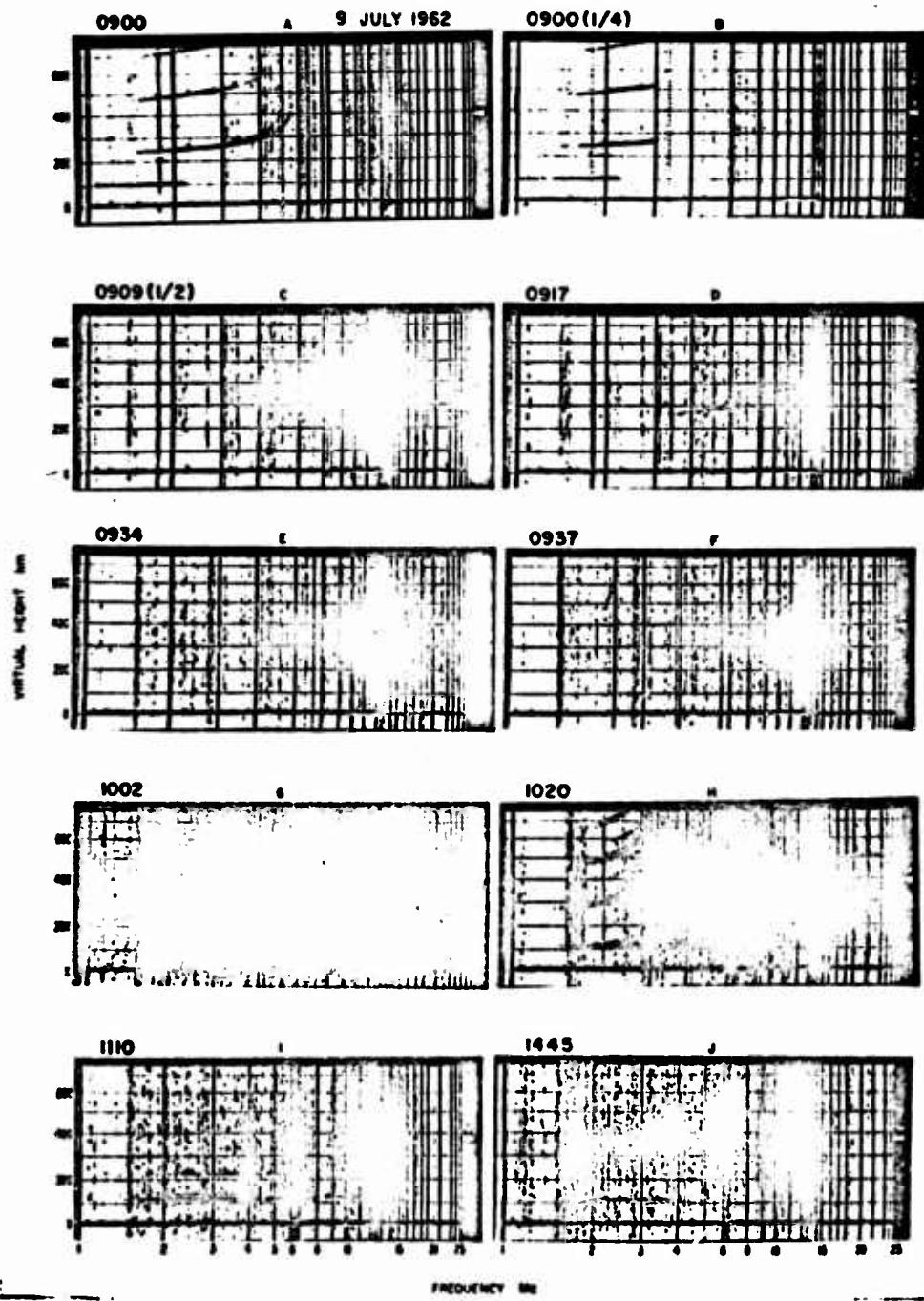
Figure 8 Star Fish, Midway, selected ionograms.
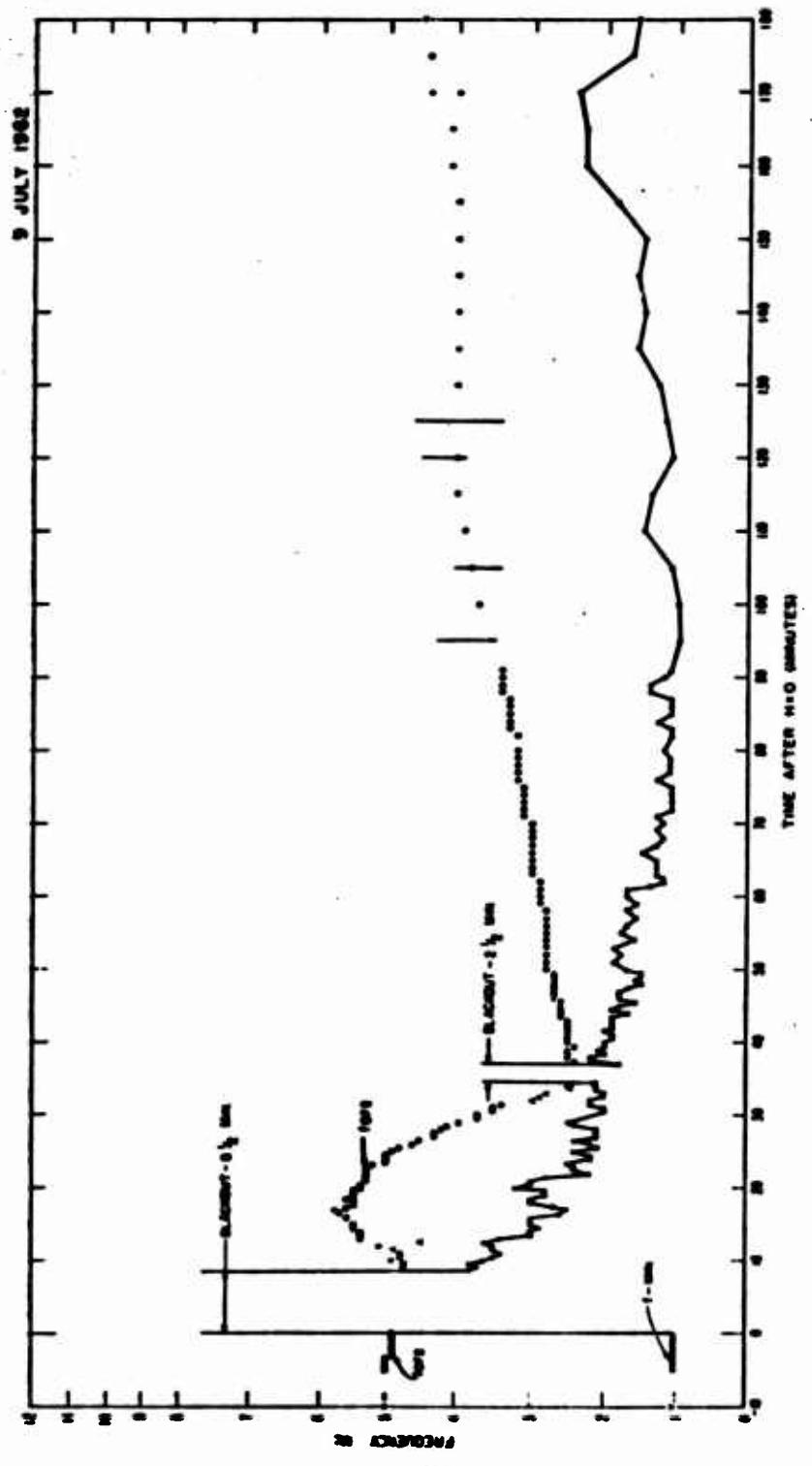
Figure 9 Star Fish, Midway, 3-hour frequency plot.
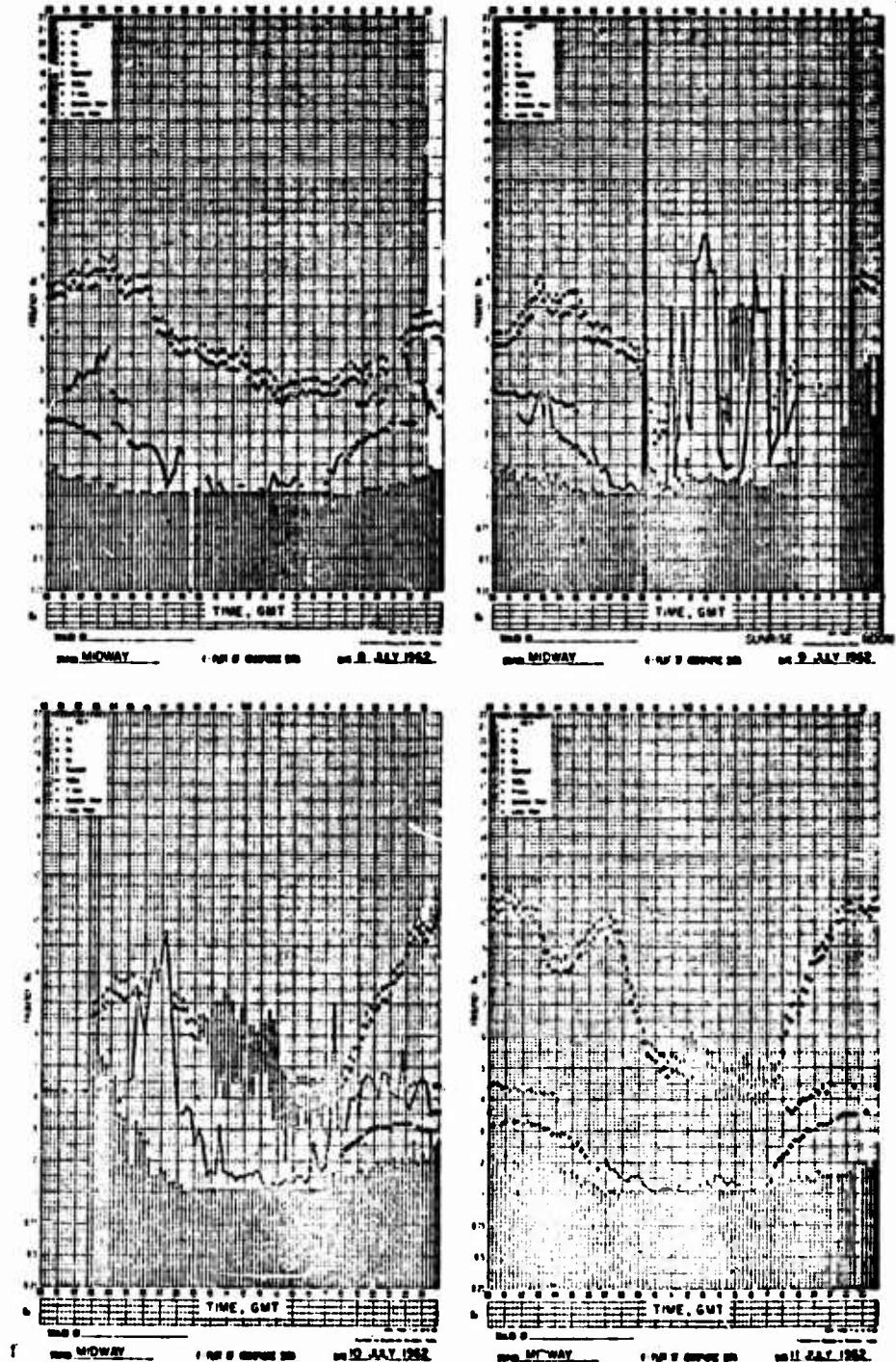
SECRET

Figure 10 Star Fish, Midway, f-plots.
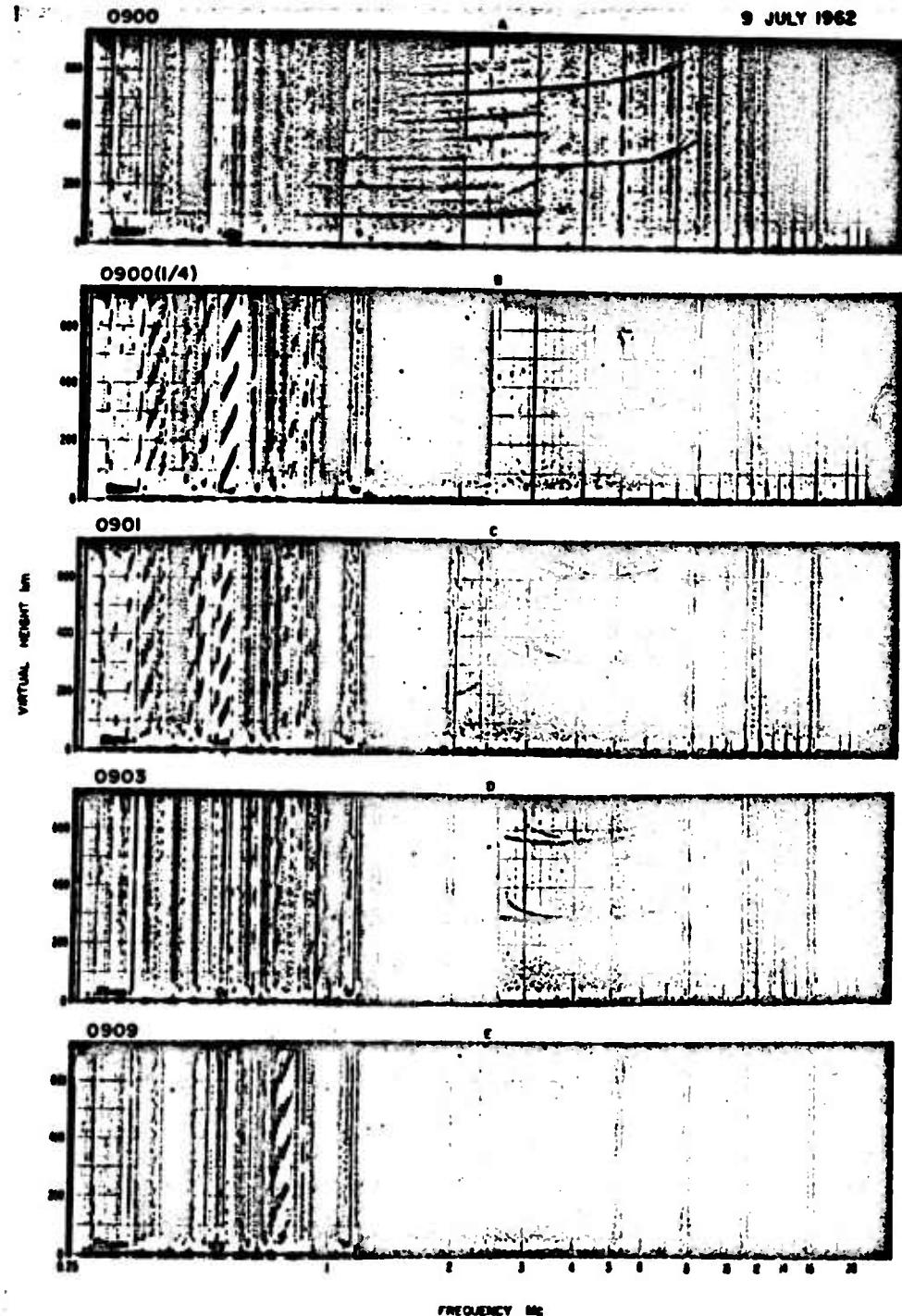
SECRET

Figure 11 Star Fish Wake, selected ionograms.

81
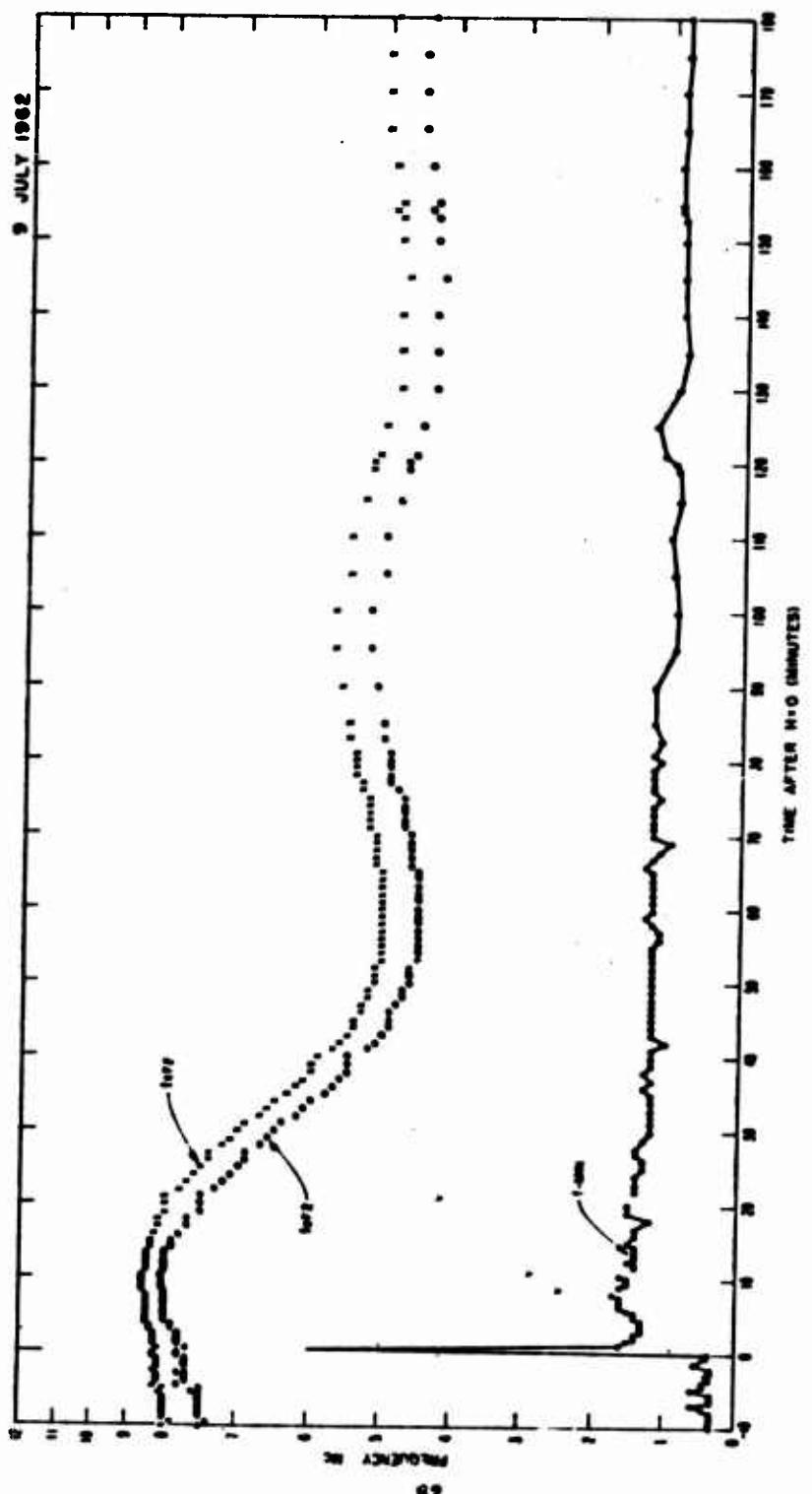
SECRET

Figure 12 Star Fish, Wake, 3-hour frequency plot.
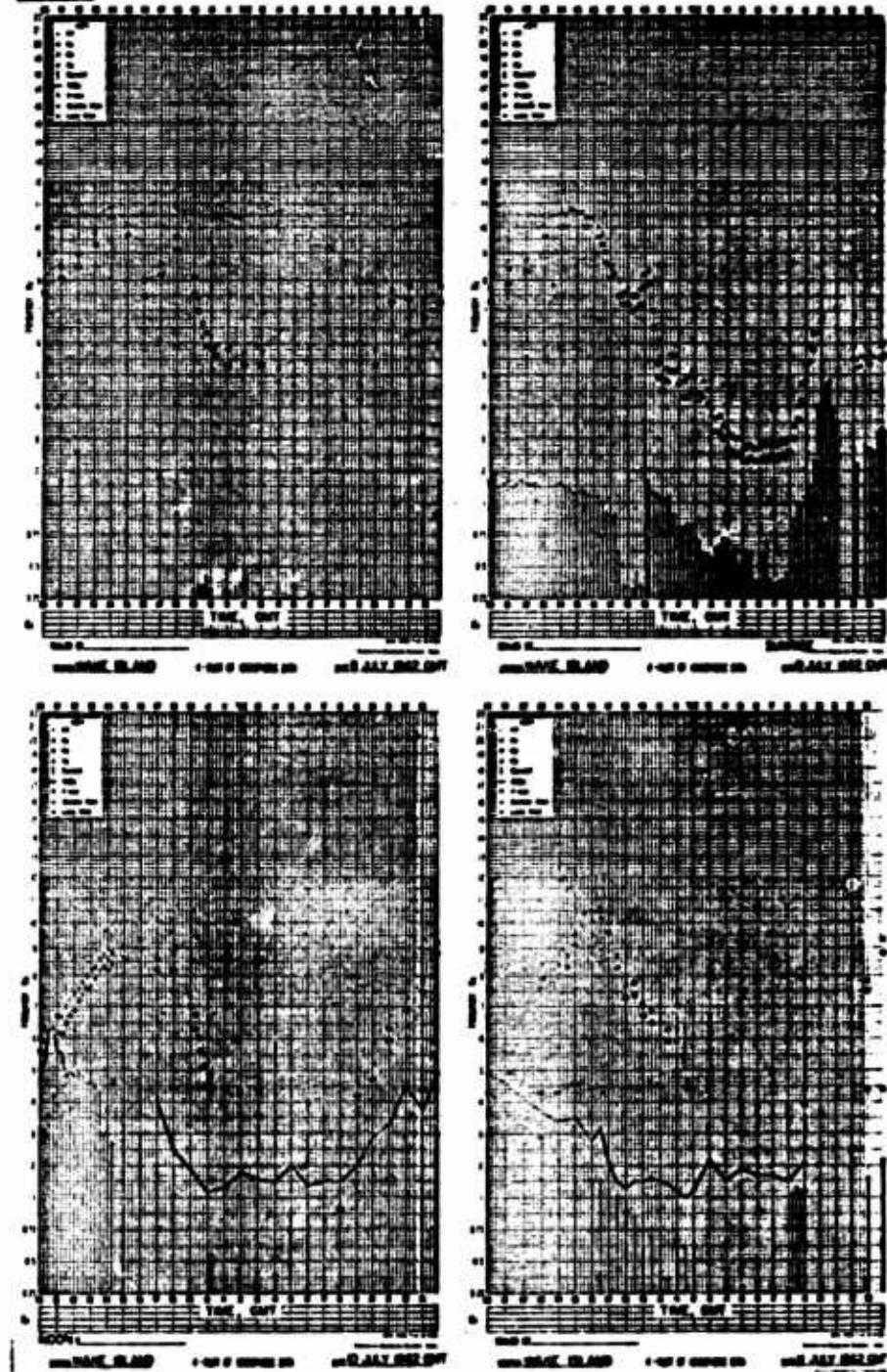
Figure 13 Star Fish, Wake, f-plots.

83

SECRET
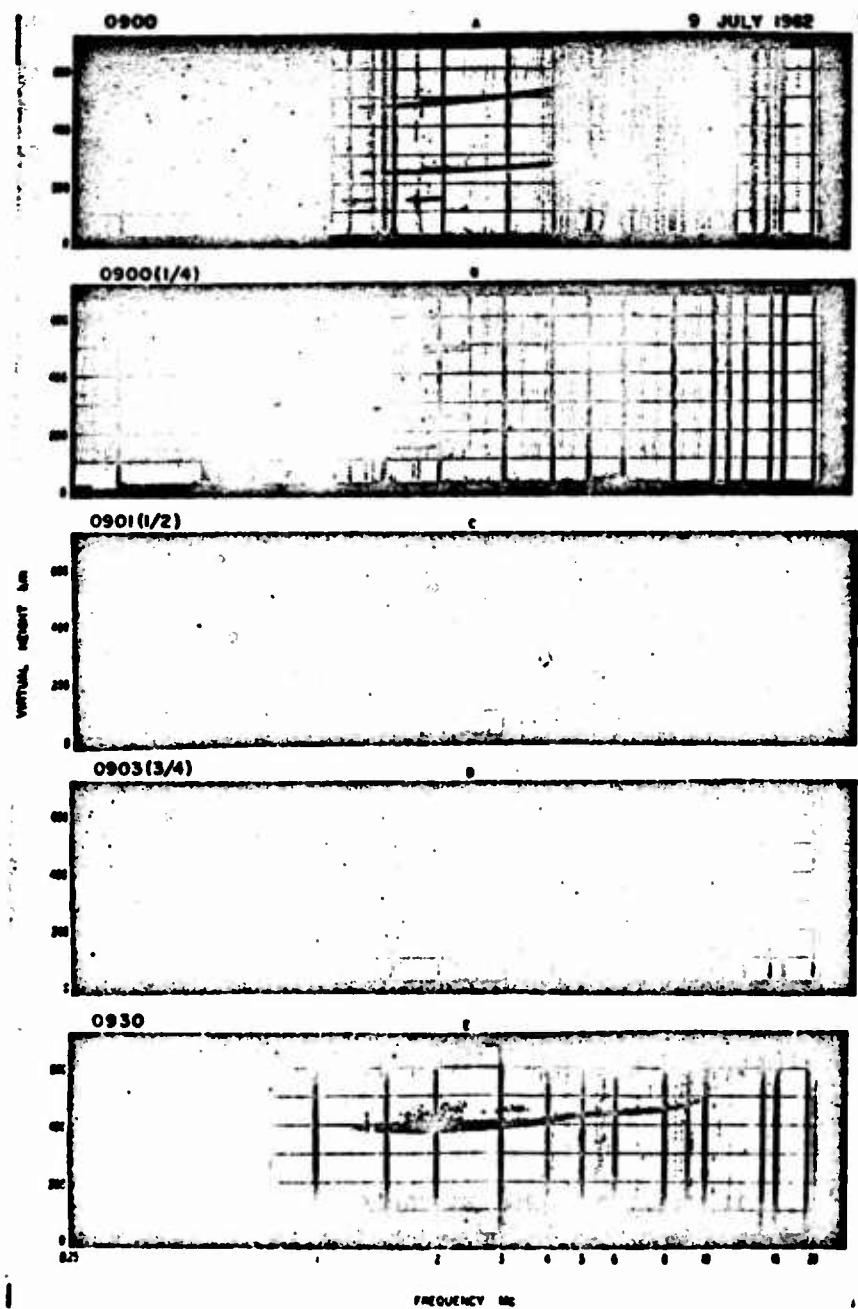
Figure 14 Star Fish, Canton, selected ionograms.

SECRET

Figure 15 Star Fish, Canton, 3-hour frequency plot.

85
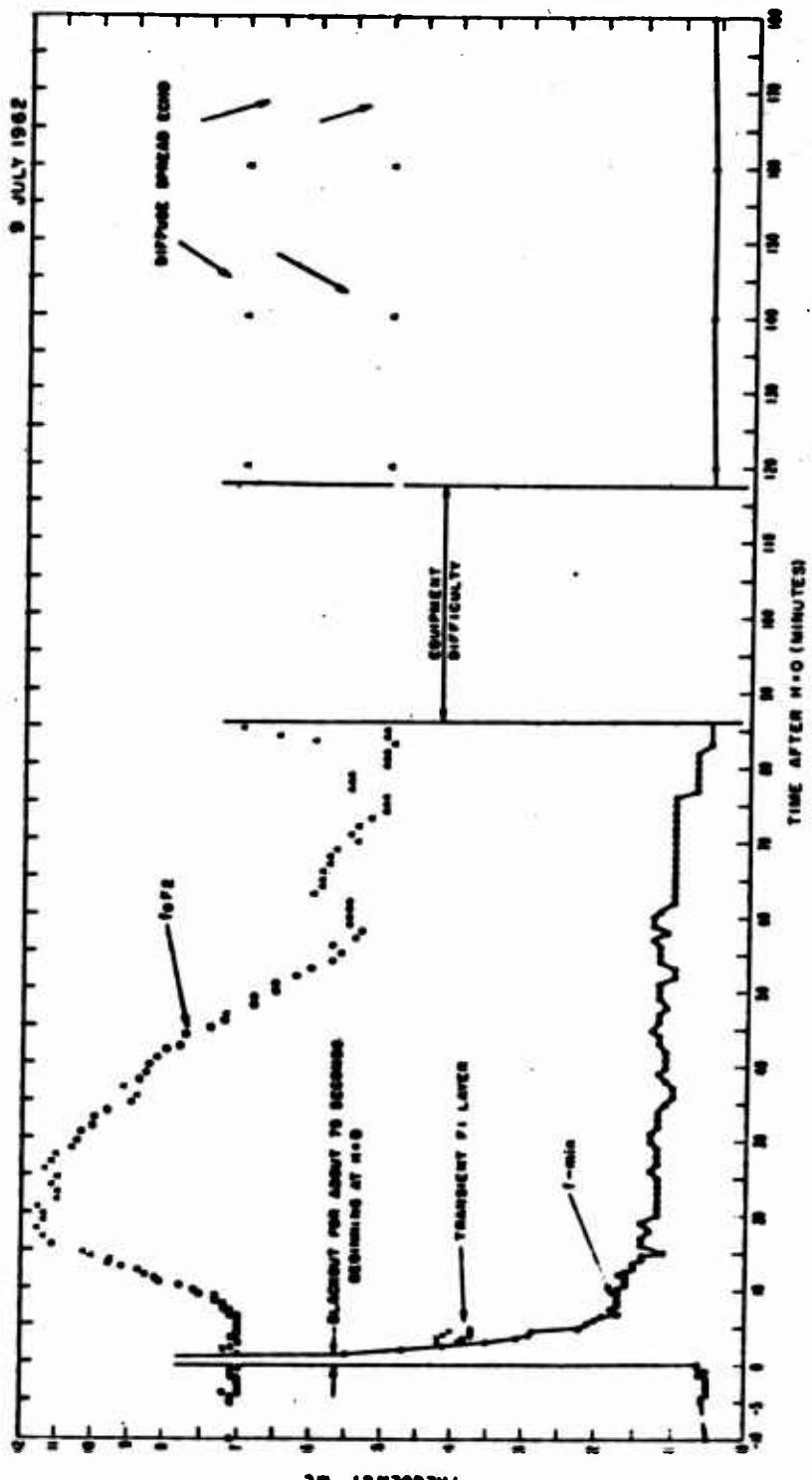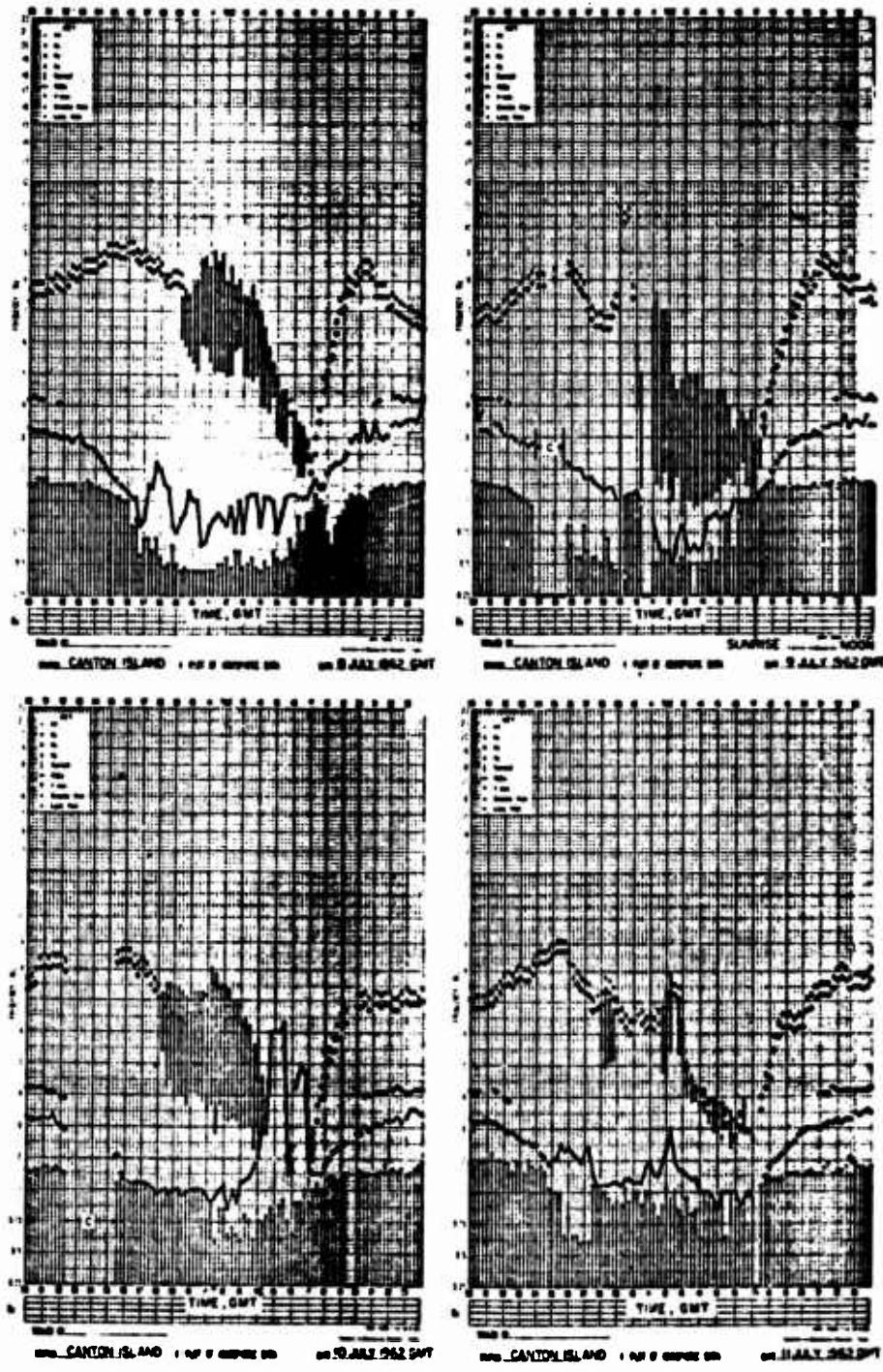
Figure 16 Star Fish, Canton, f-plots.
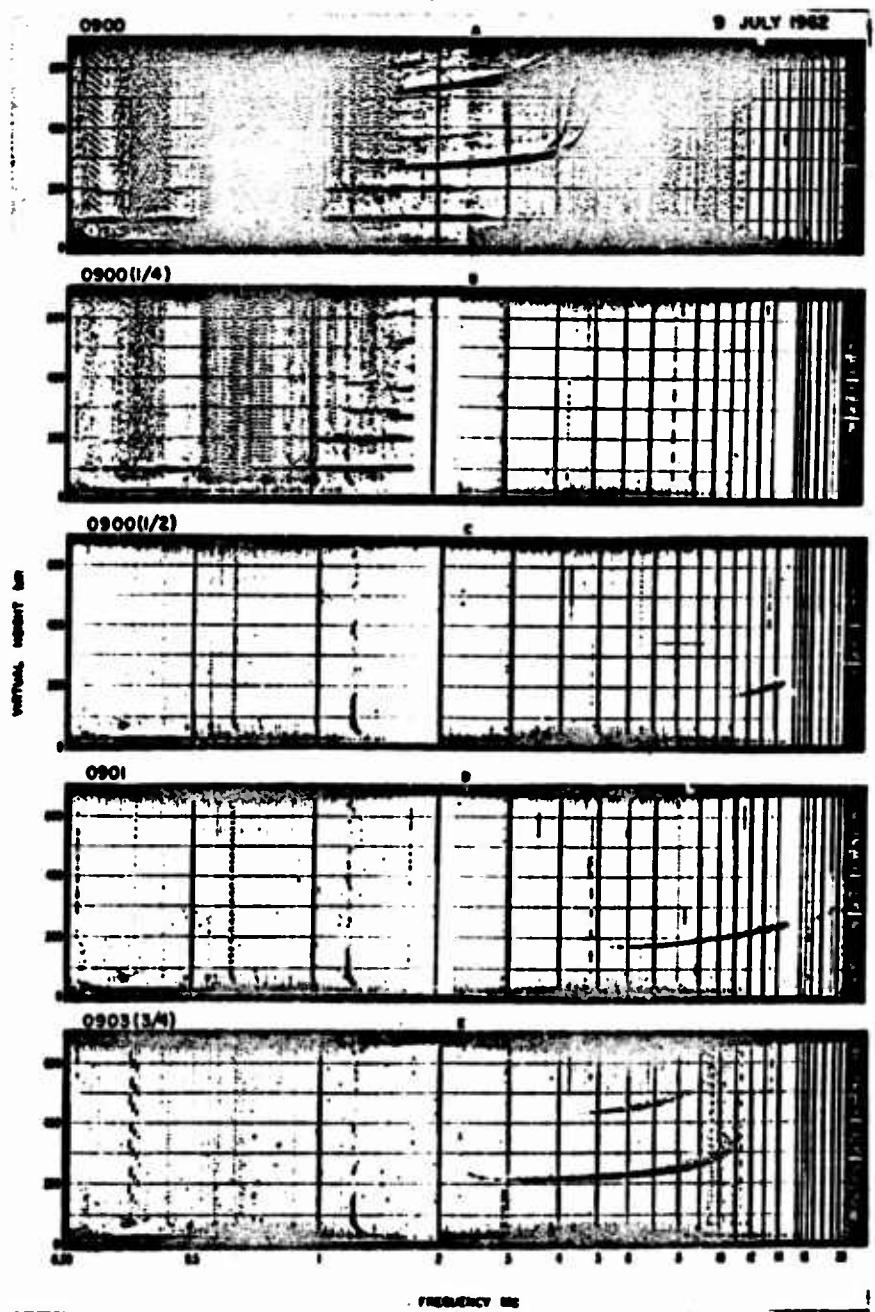
SECRET

Figure 17 Star Fish, Tutuila, selected ionograms.

87
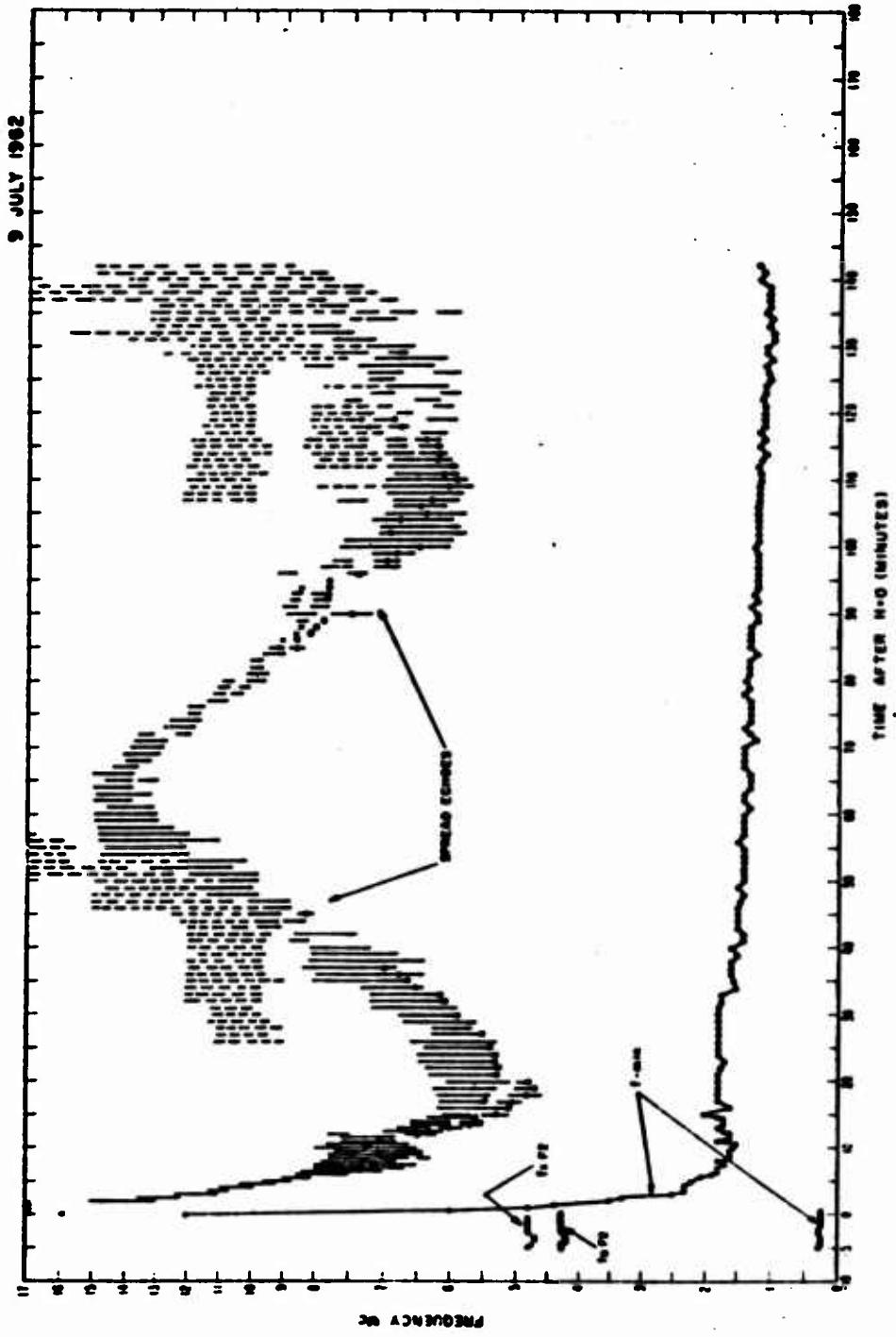
Figure 16 Star Fish, Tutuila, 3-hour frequency plot.
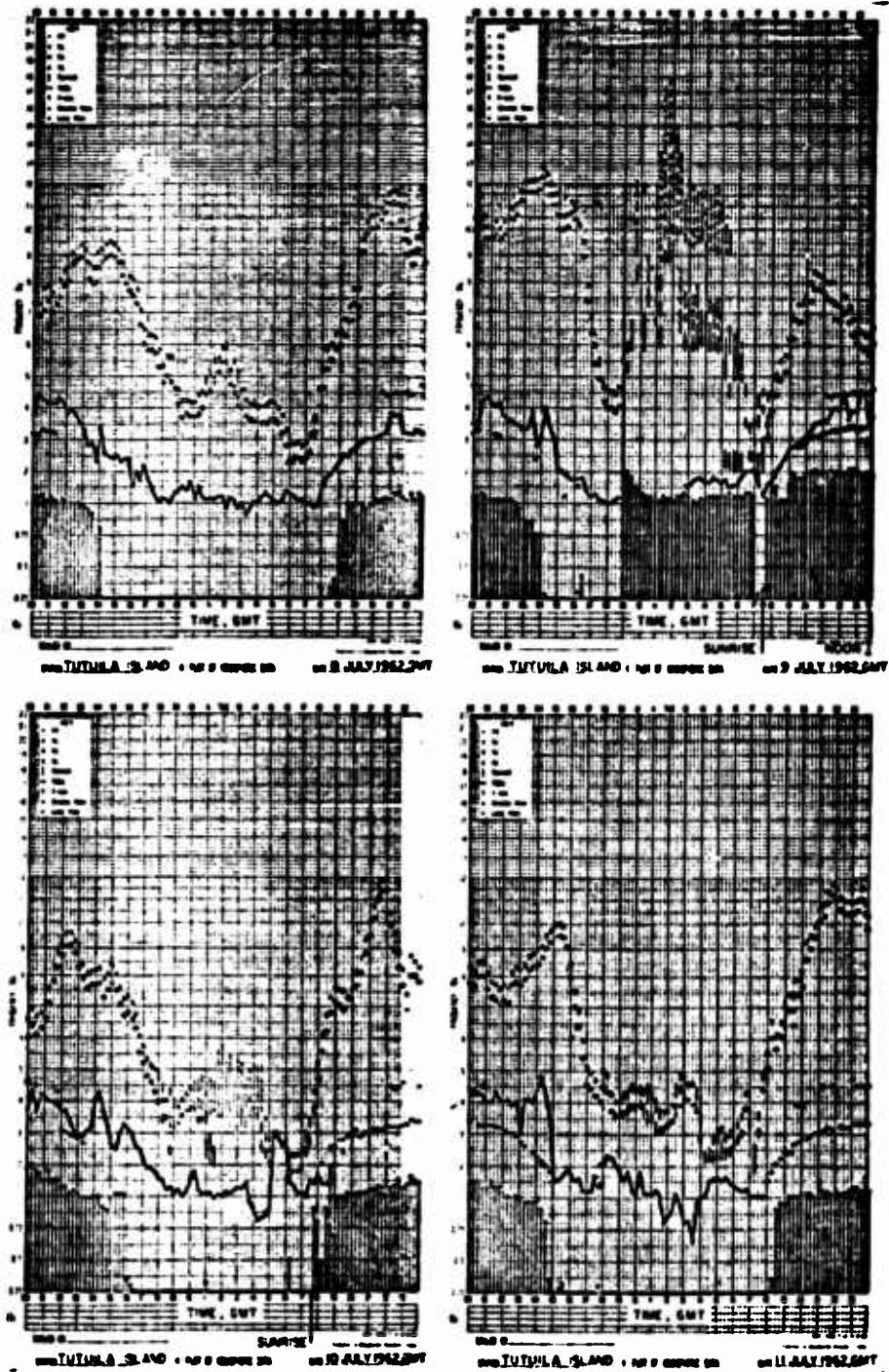
Figure 19 Star Fish, Tutuila, f-plots.

89
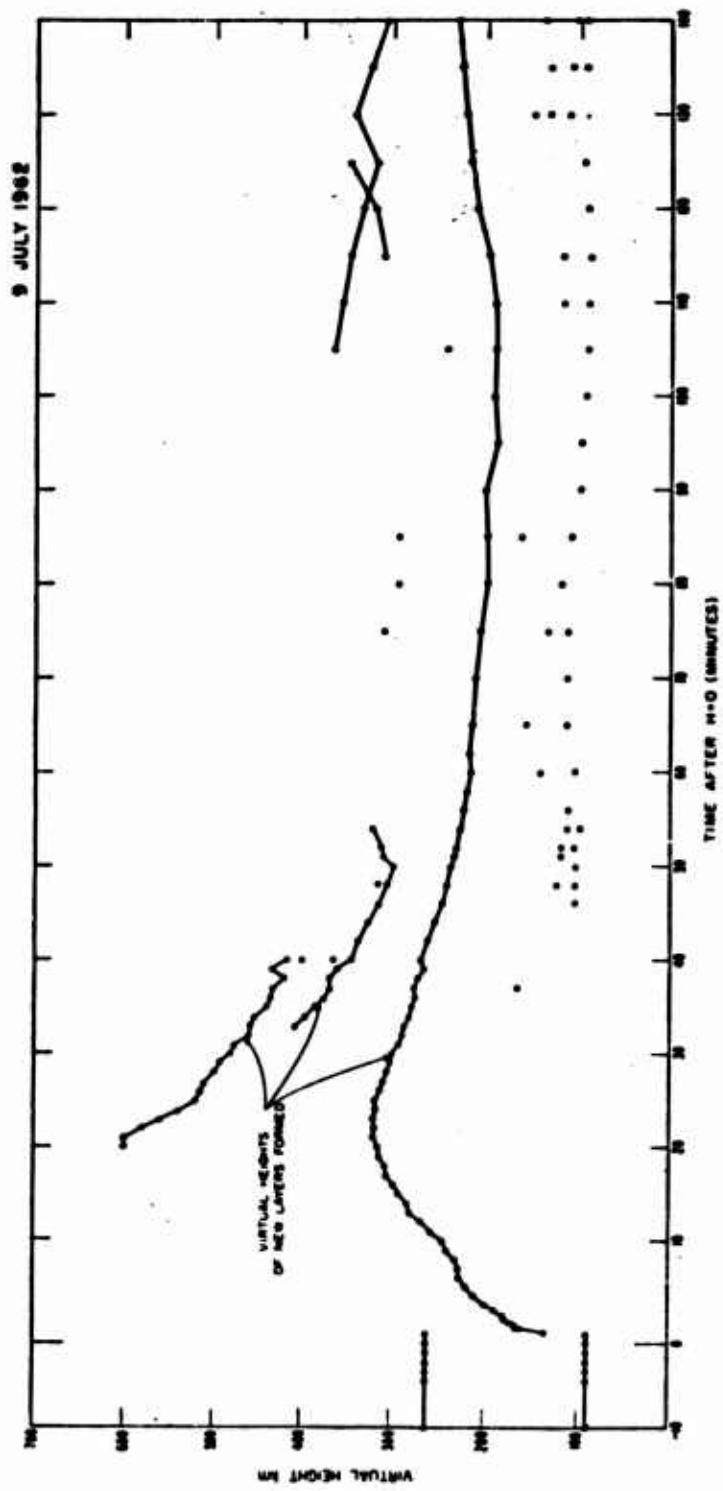
Figure 20 Star Fish, Tutuila, virtual heights of new echoes.
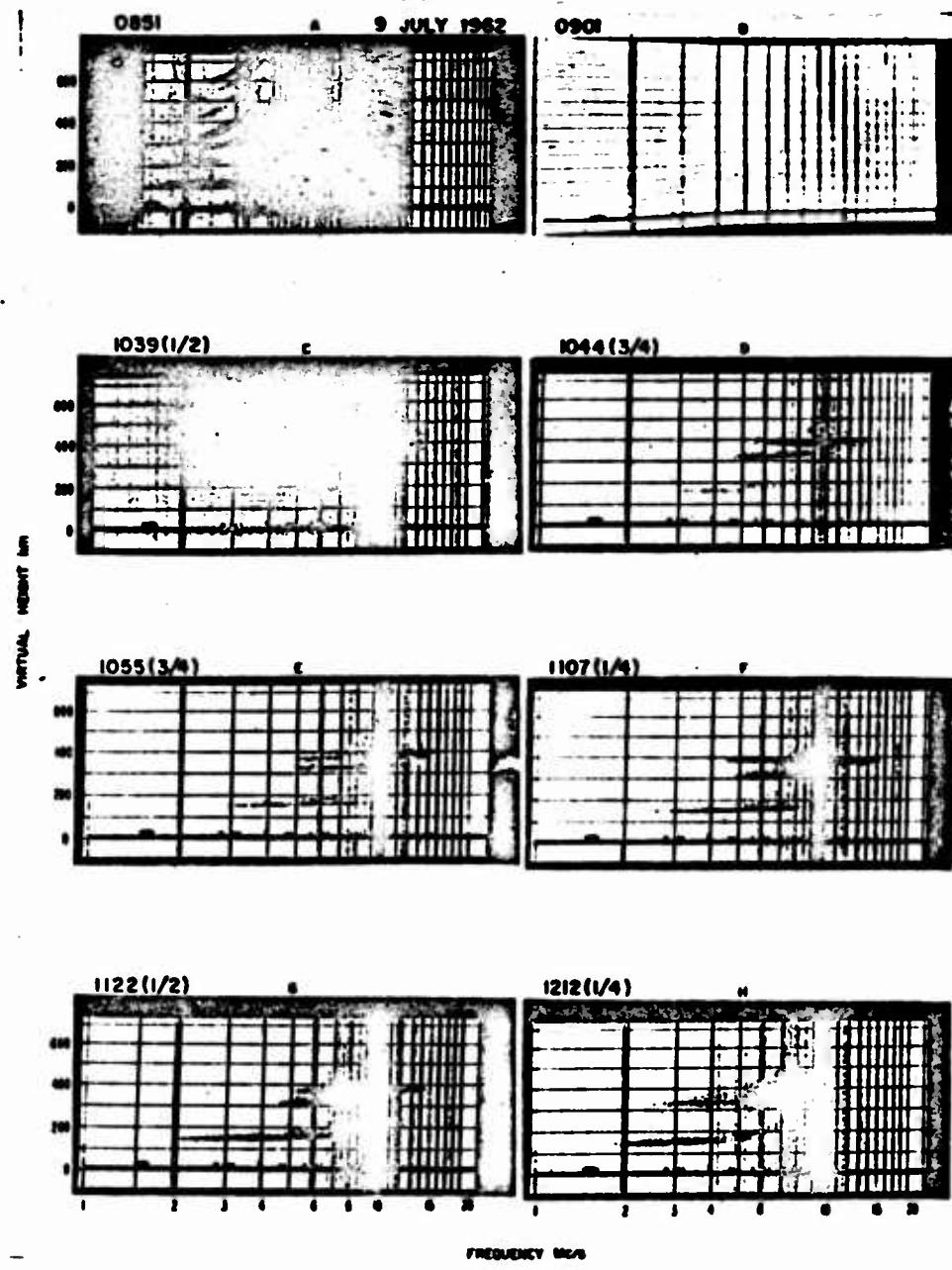
SECRET

Figure 21 Star Fish, Tonga, selected ionograms.
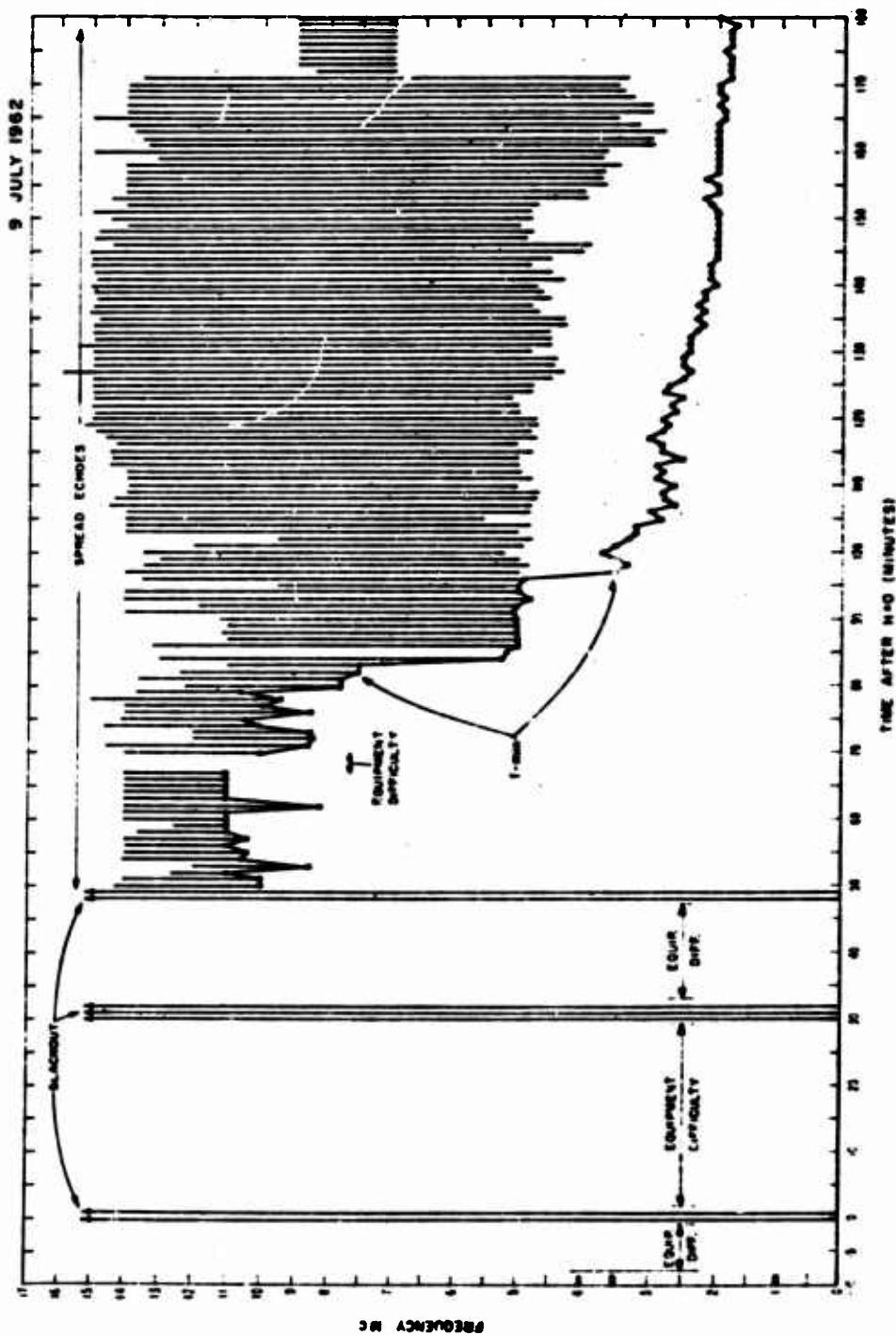
Figure 22 Star Fish, Tongn, 3-hour frequency plot.
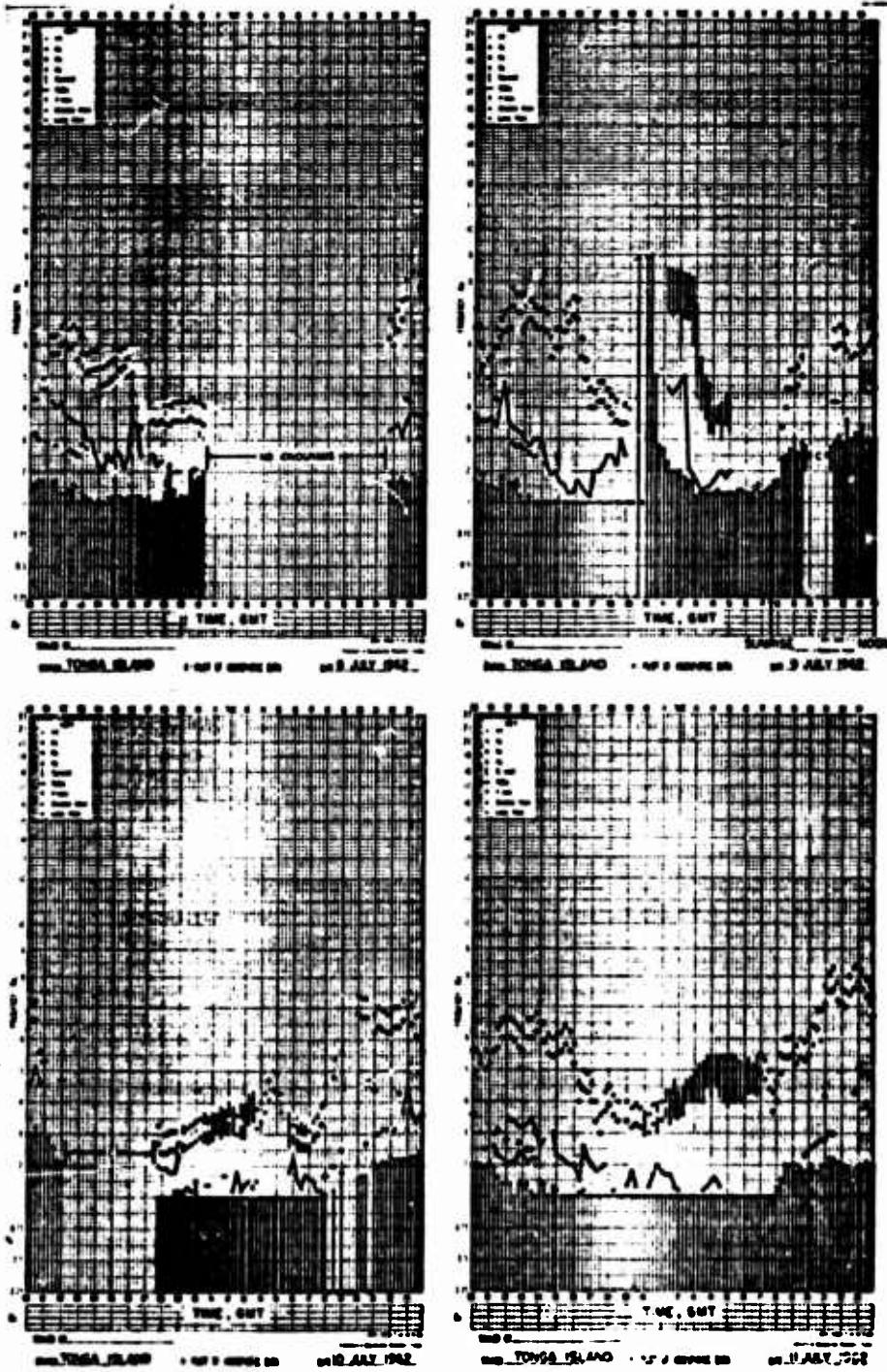
Figure 23 Star Fish, Tonga, f-plots.

93

SECRET
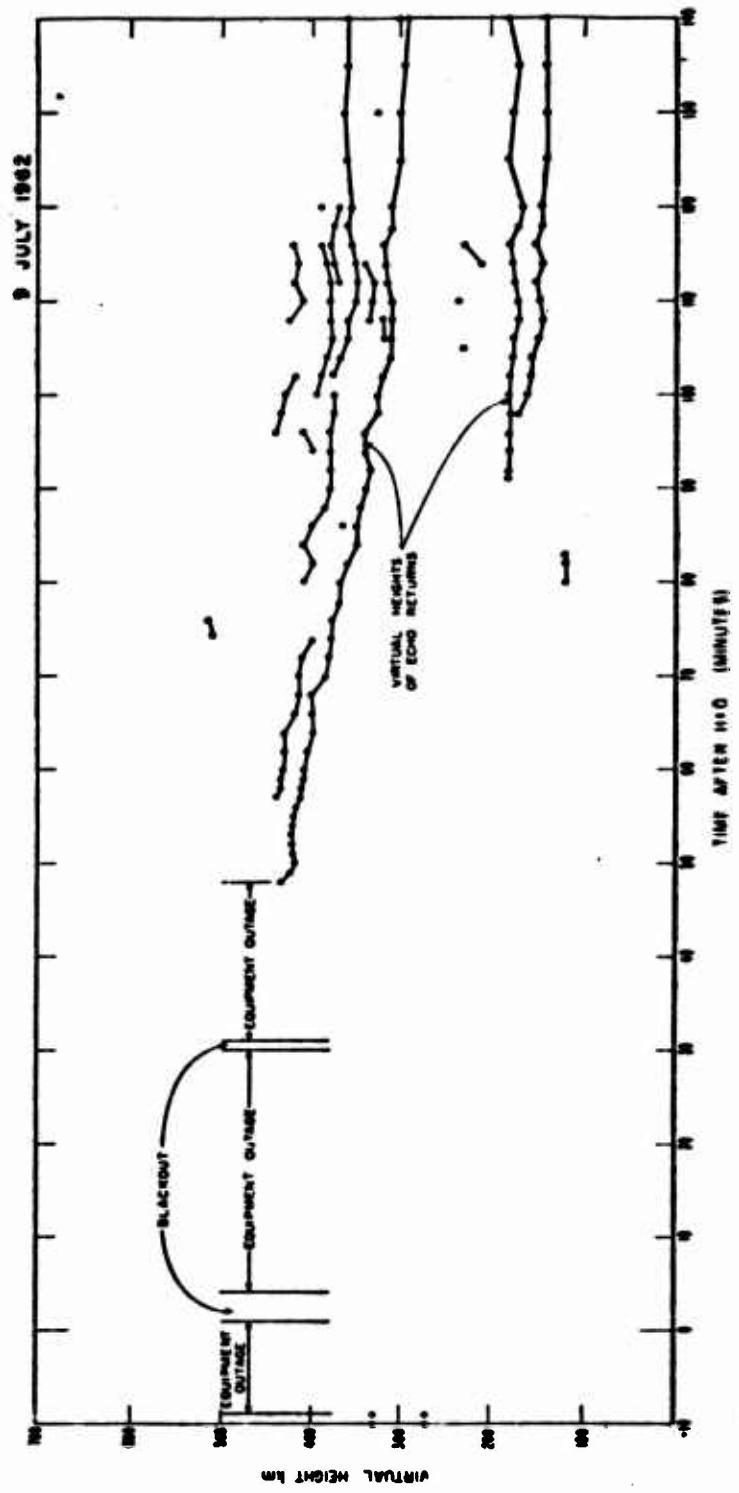
Figure 24 Star Fish, Tonga, virtual heights of new echoes.

94
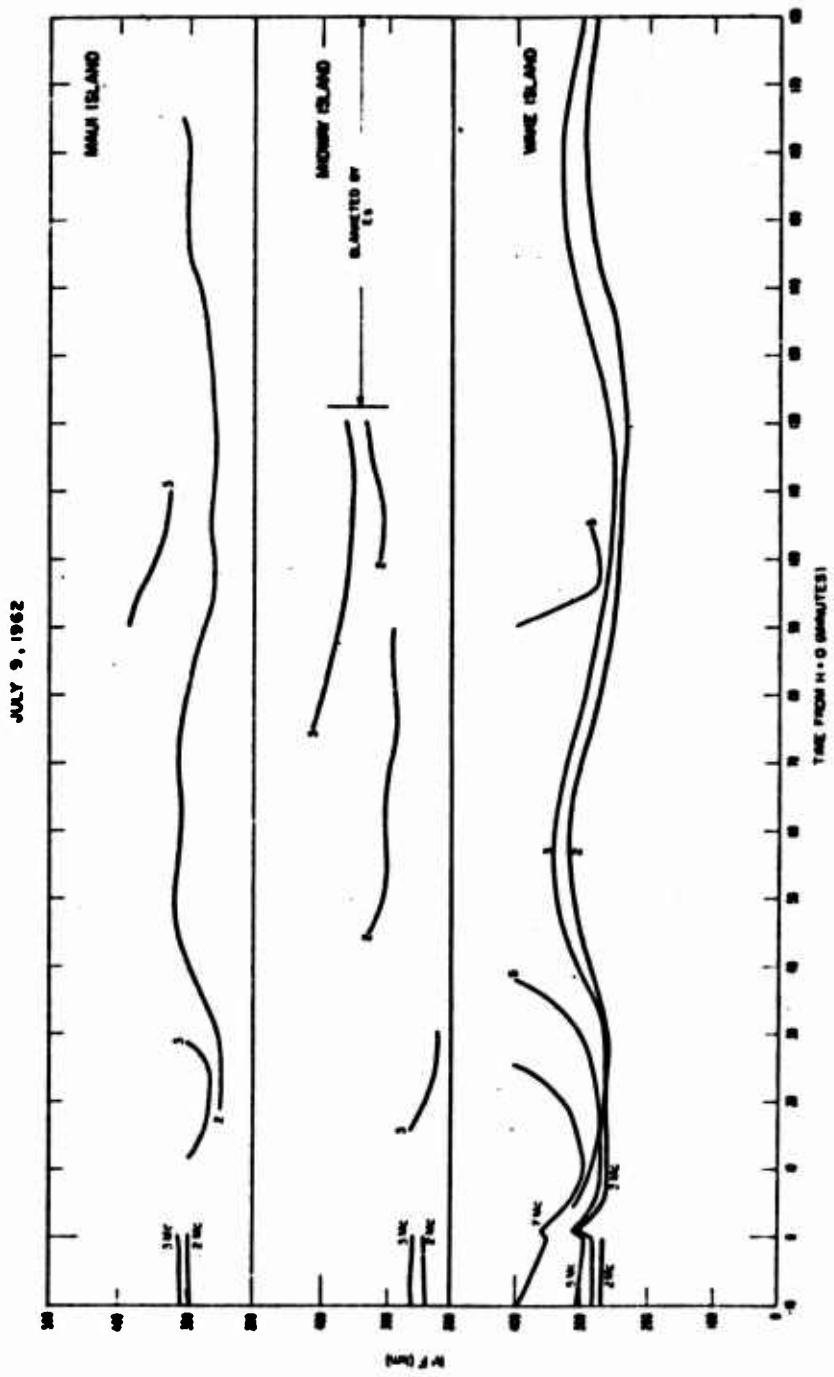
Figure 25 Star Fish, Maui, Midway, Wake, F 2 virtual heights.

SECRET

Figure 26 Star Fish, Canton, Tutuila, F2 virtual heights.

96
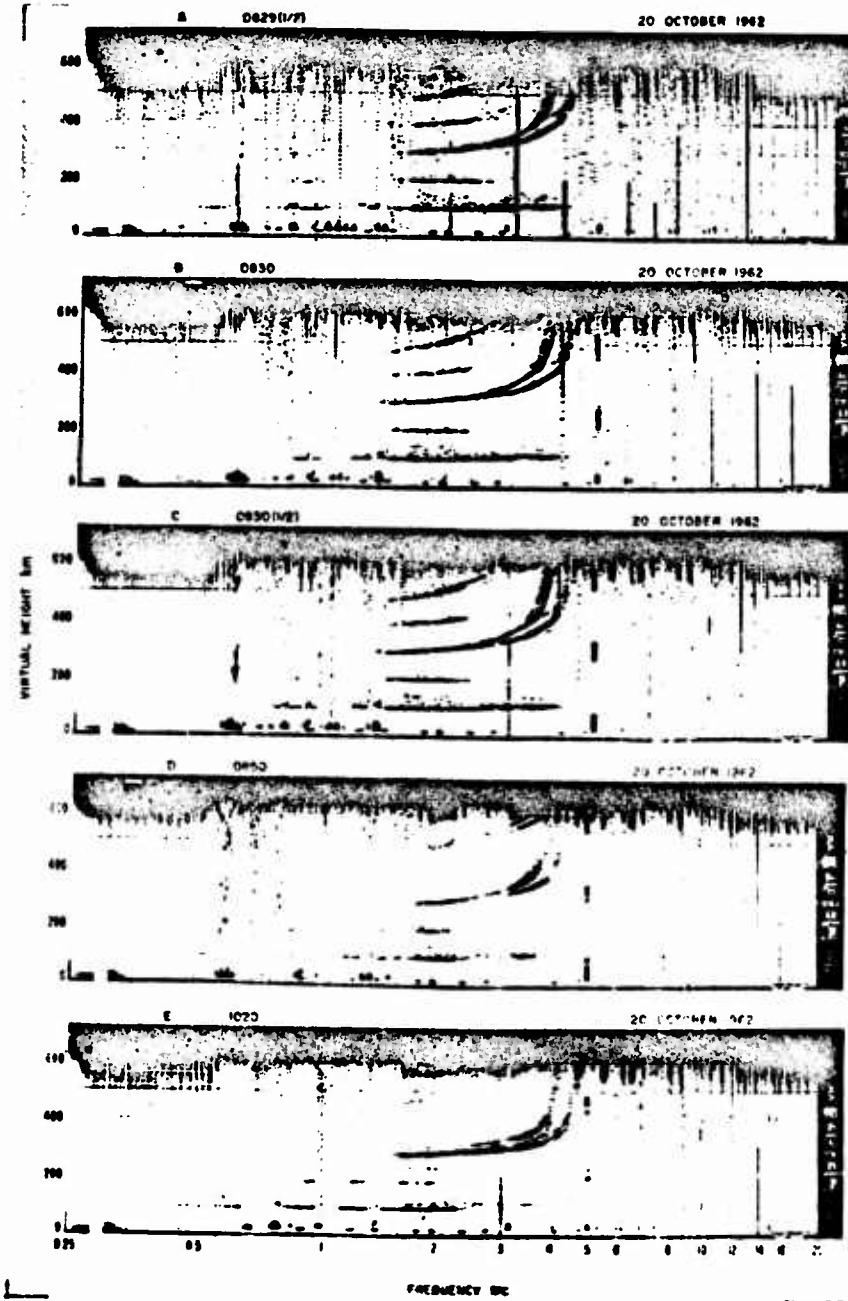
Figure 27 Check Mate, Maui, selected ionograms.
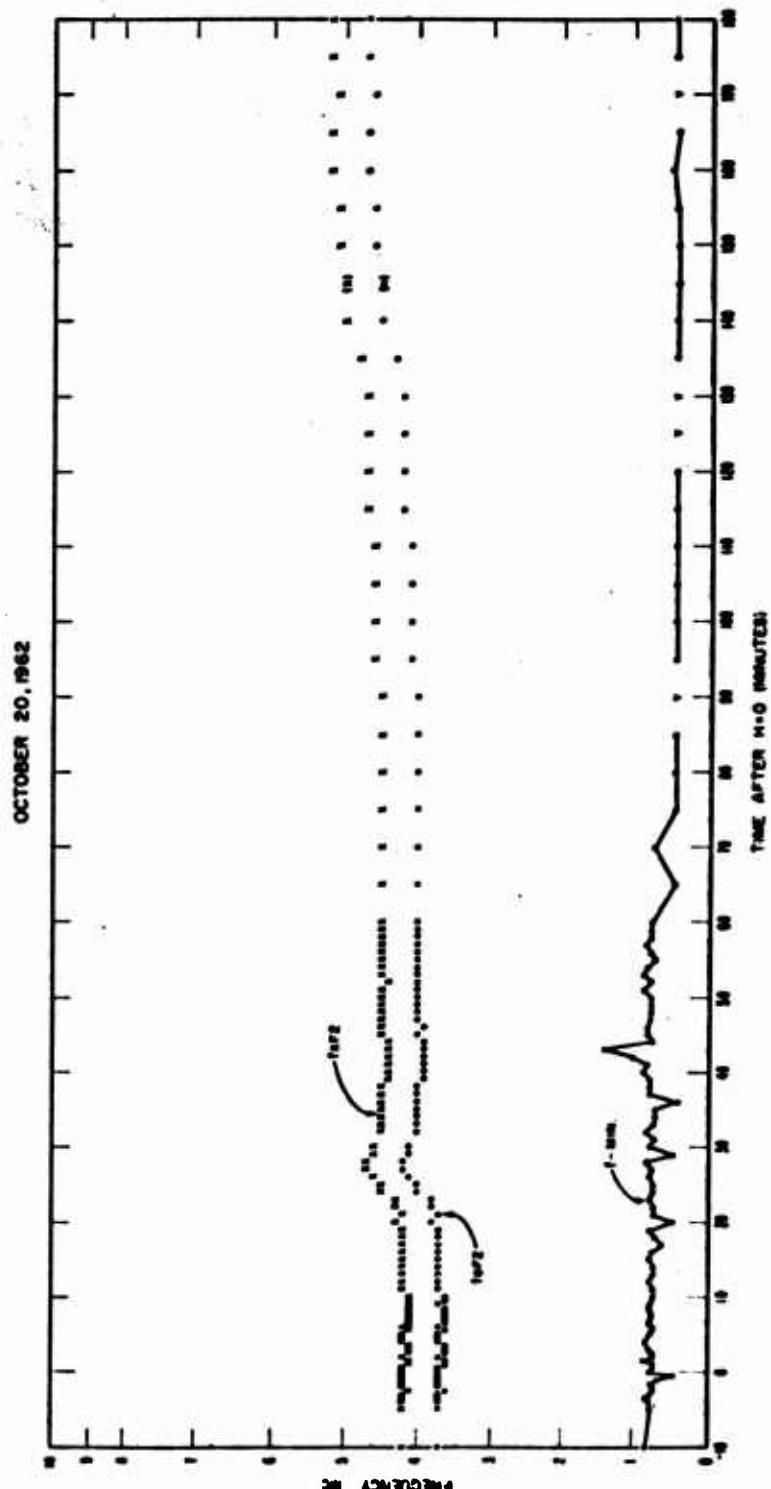
SECRET

Figure 28 Check Mate, Maui, 3-hour frequency plot.

OCTOBER 20, 1962

TIME AFTER H+0 (MINUTES)

FREQUENCY, MC
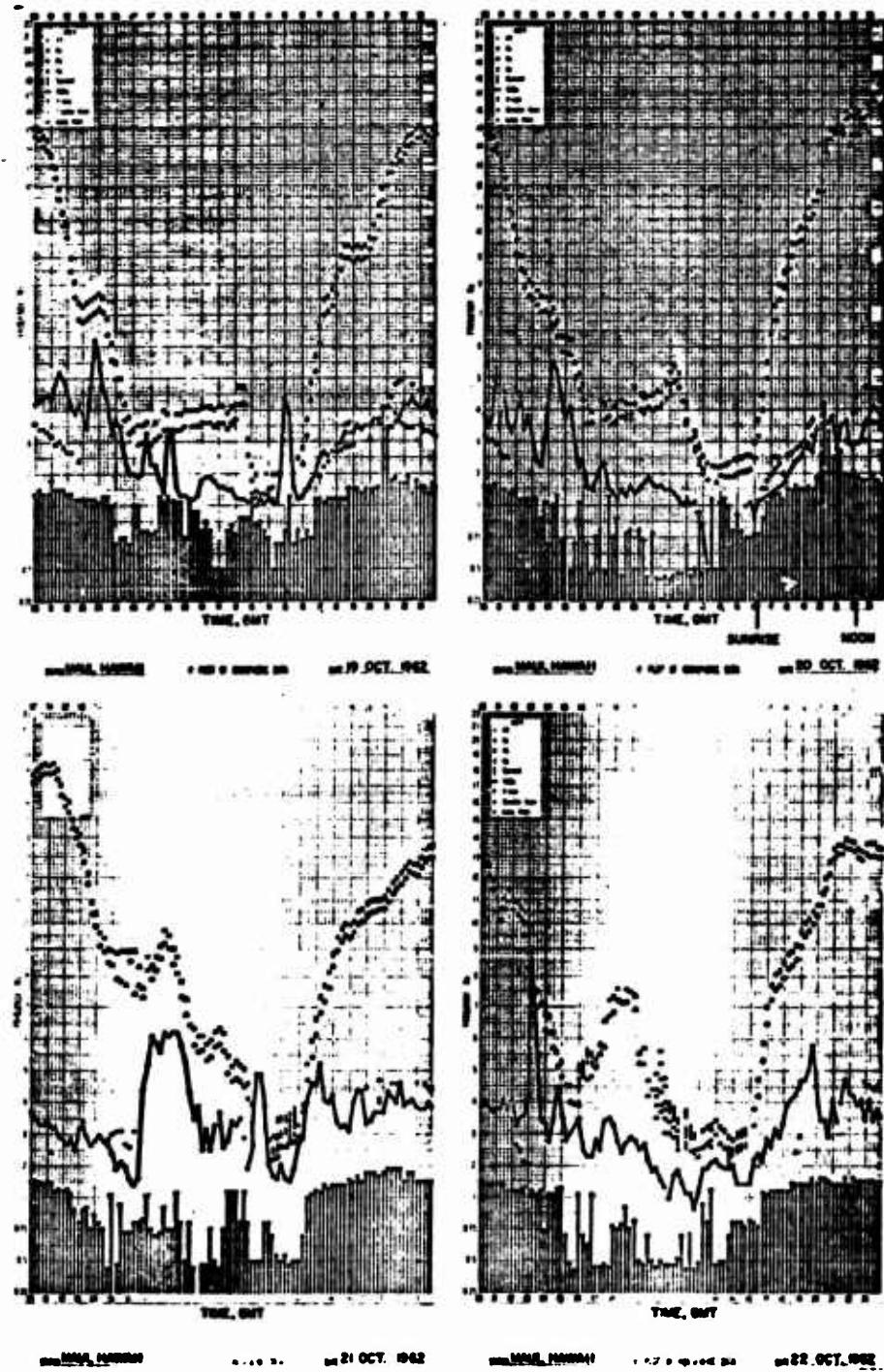
SECRET

Figure 29 Check Mate, Maui, f-plots.

99

SECRET
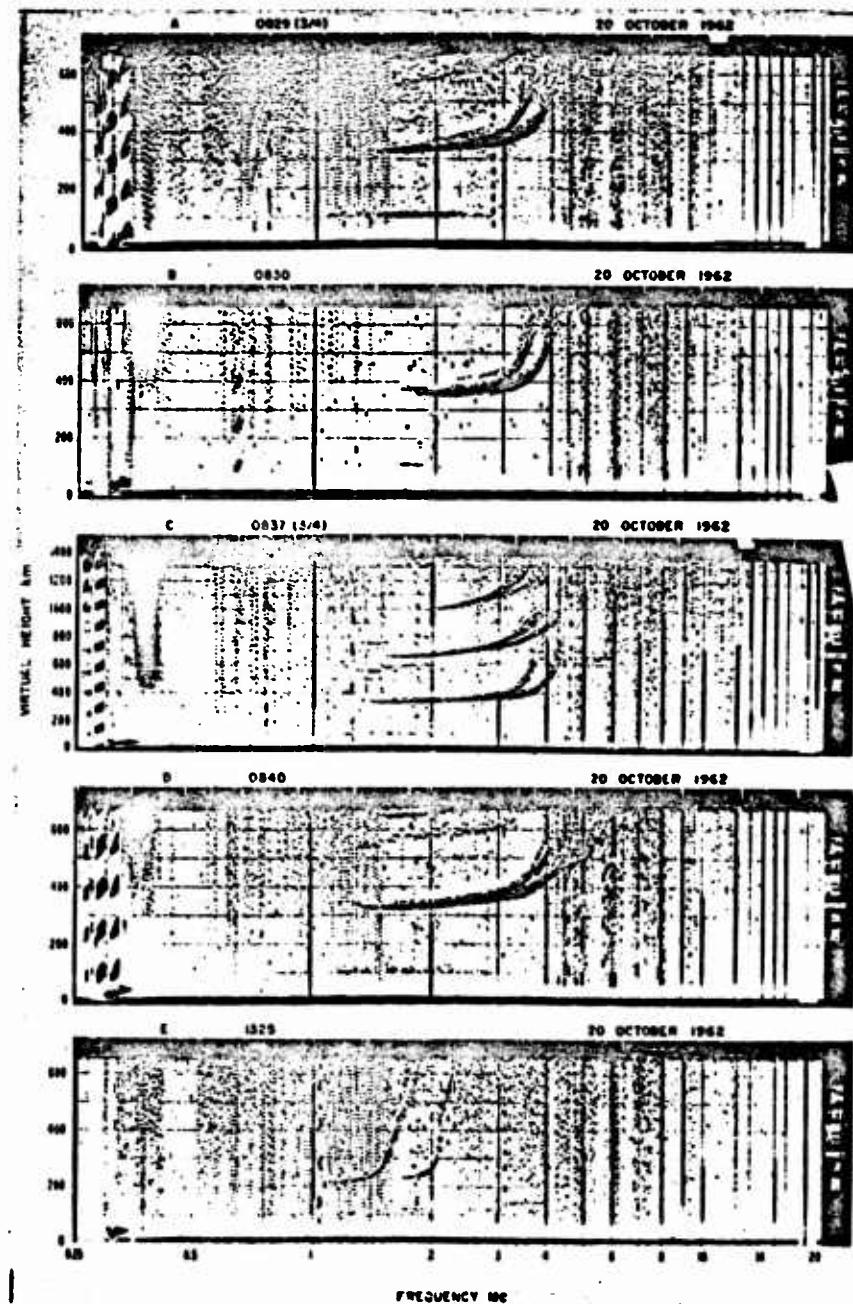
Figure 30 Check Mate, Tern, selected ionograms.
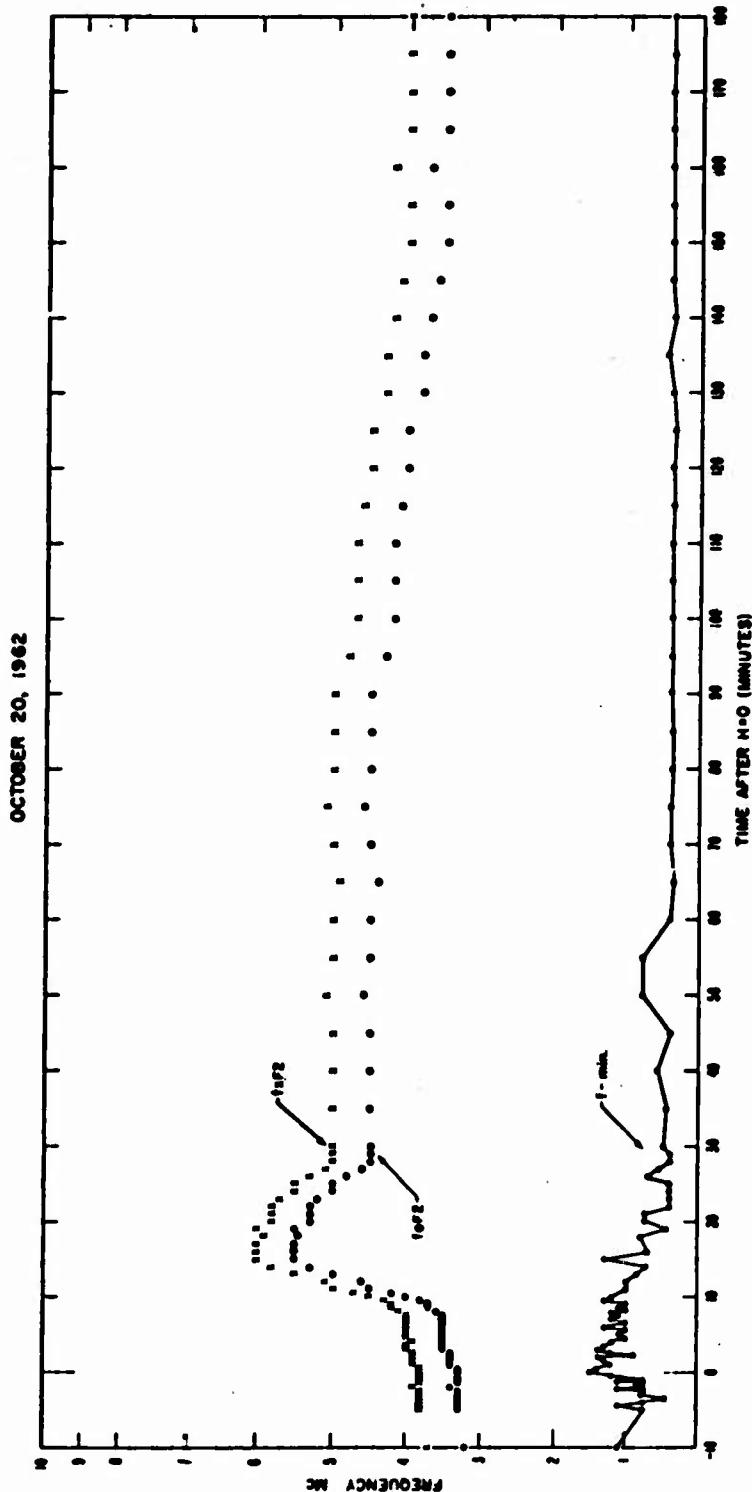
SECRET

Figure 31 Check Mate, Tern, 3-hour frequency plot.
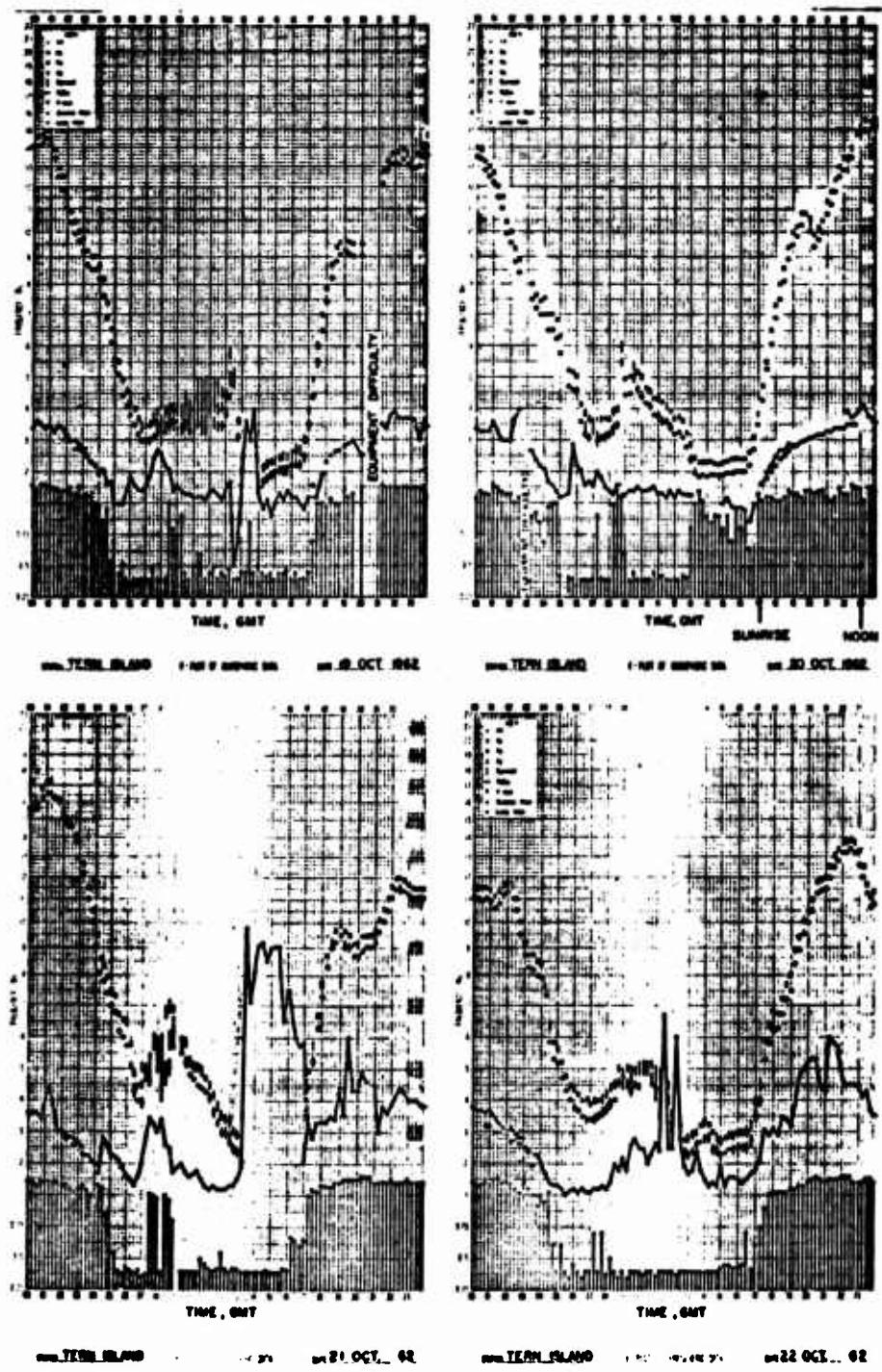
Figure 32 Check Mate, Tern, f-plots.

102

SECRET
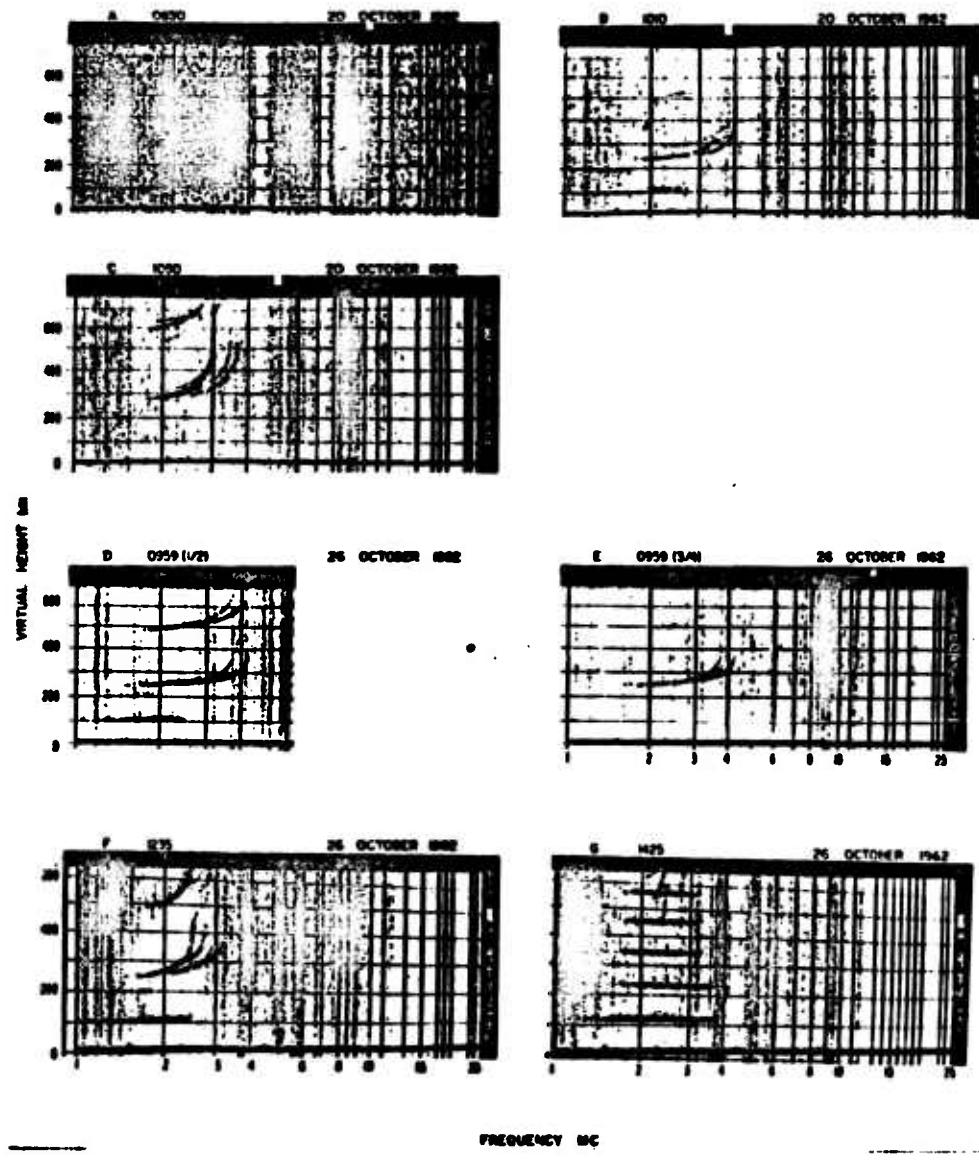
Figure 33 Check Mate, Blue Gill, Midway, selected ionograms.

103

OCTOBER 20, 1962
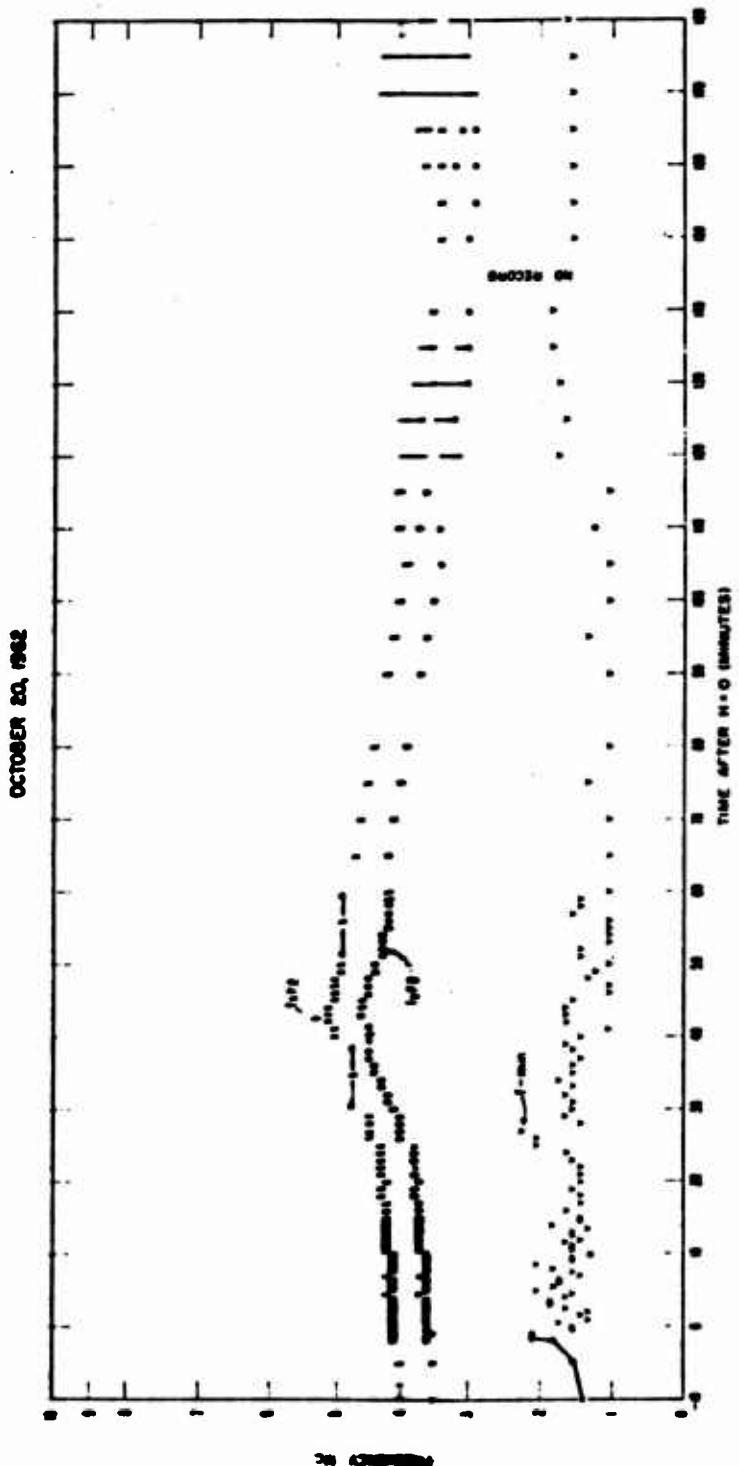
Figure 34 Check Mate, Midway, 3-hour frequency plot.
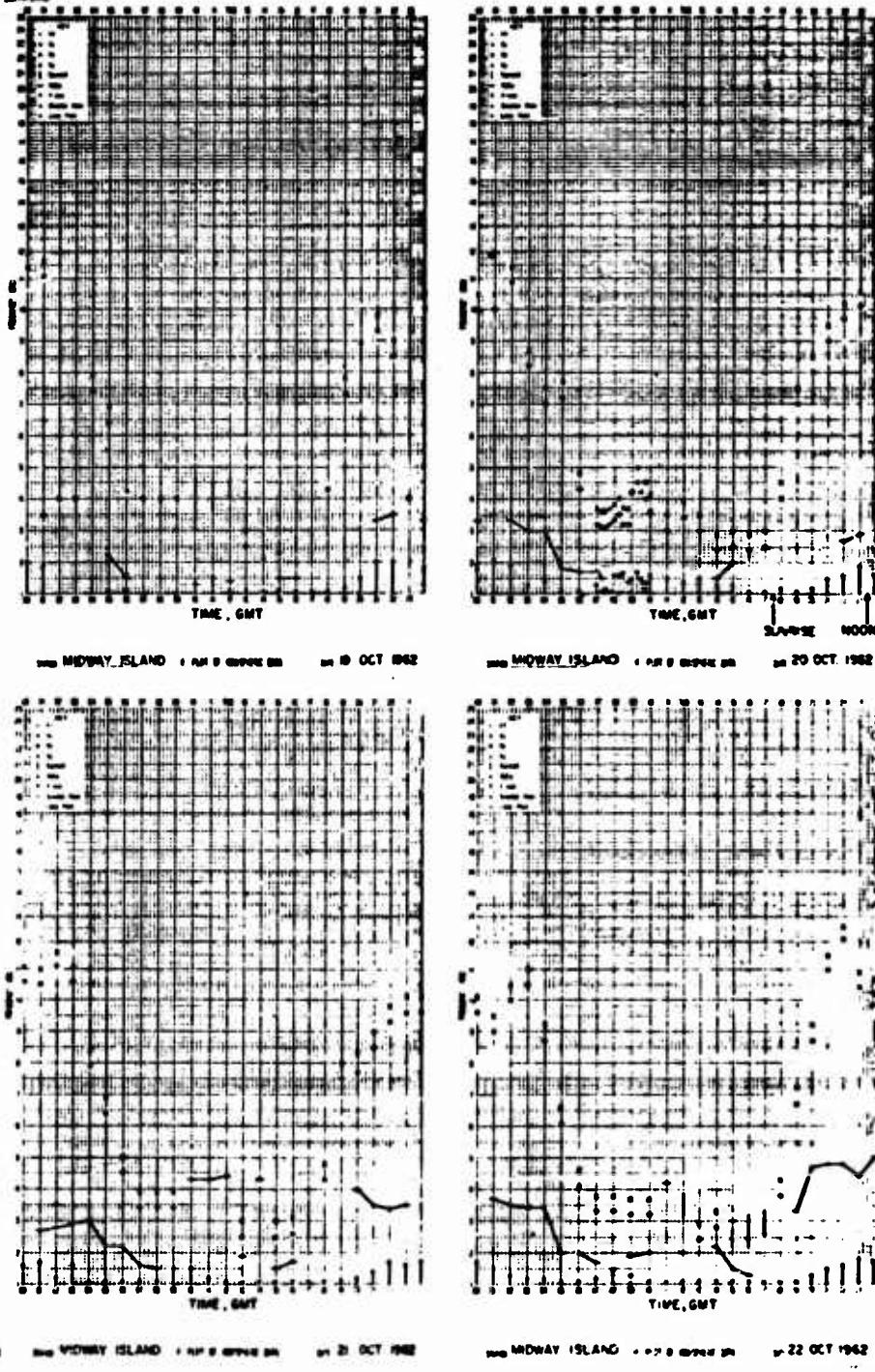
Figure 35 Check Mate, Midway, f-plots.

105
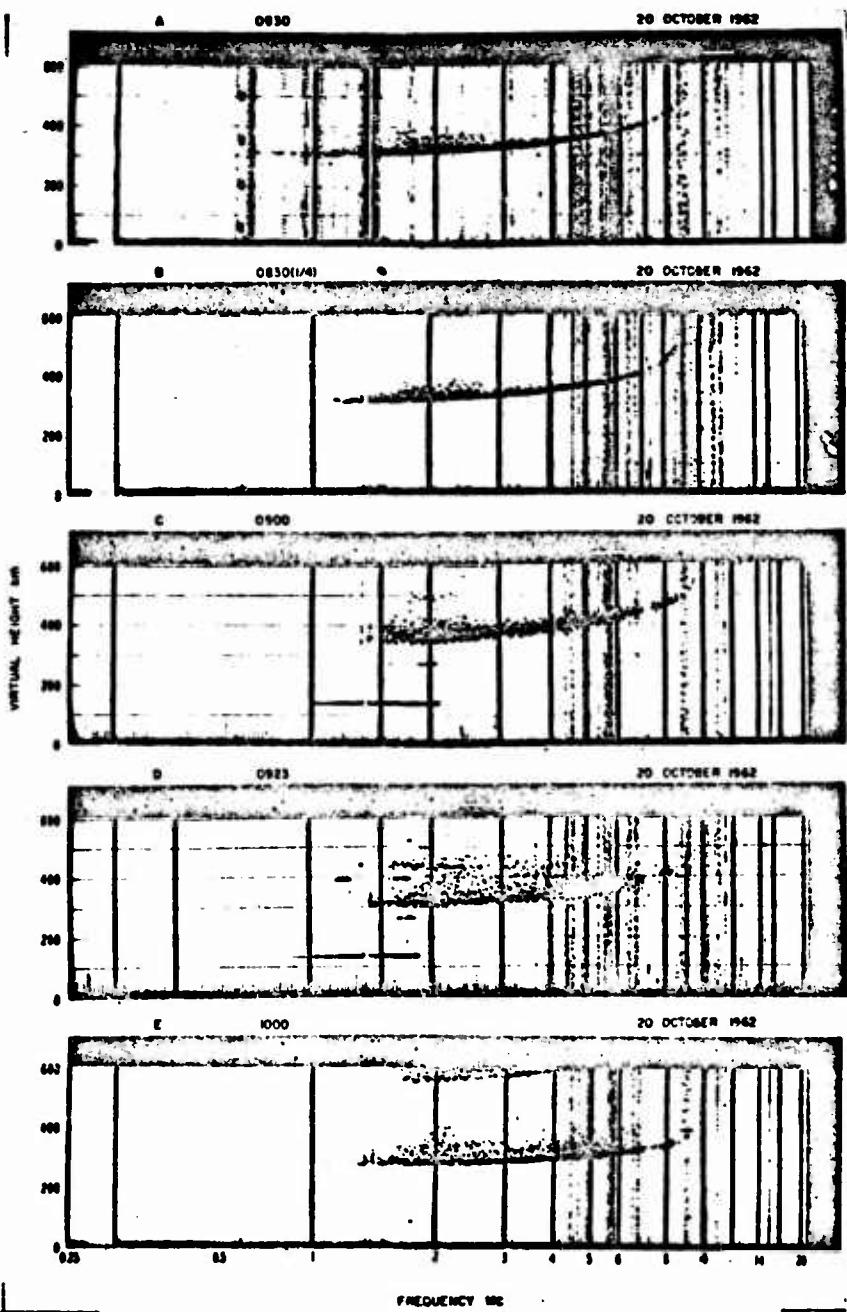
Figure 36 Check Mate, Canton, selected ionograms.
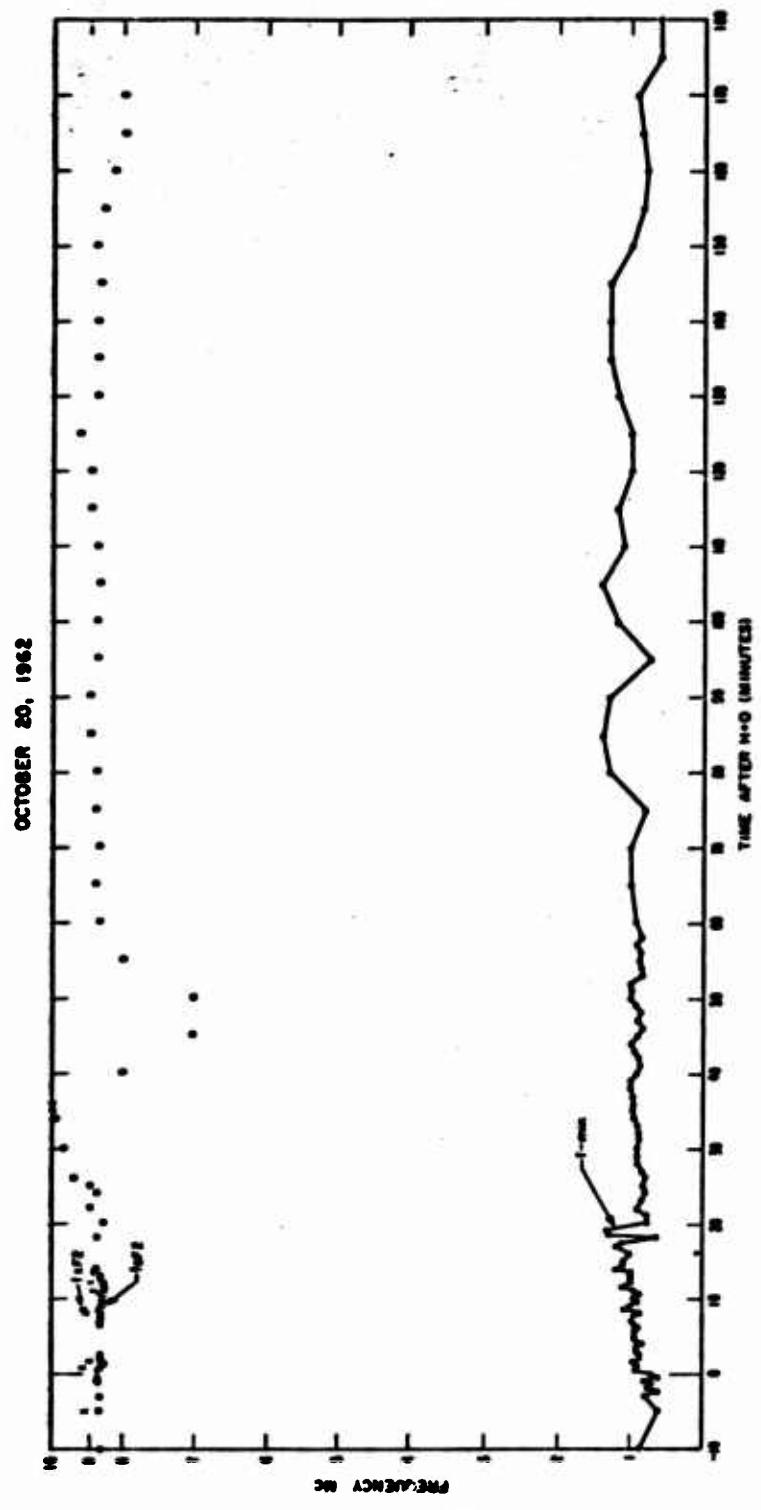
SECRET

Figure 37 Check Mate, Canton, 3-hour frequency plot.

107
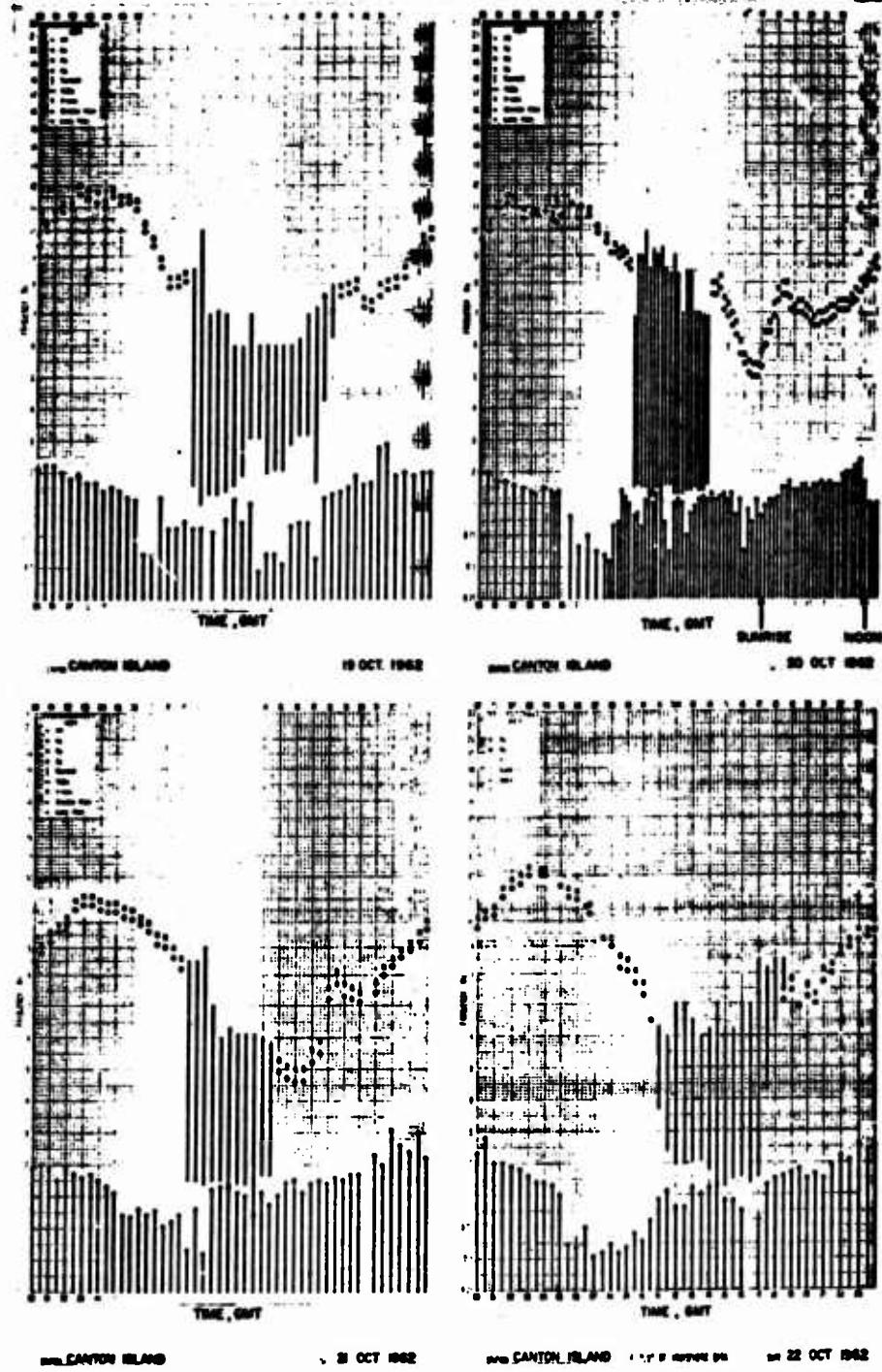
Figure 38 Check Mate, Canton, f-plots.

108

SECRET

Figure 39 Check Mate, Tutuila, selected ionograms.
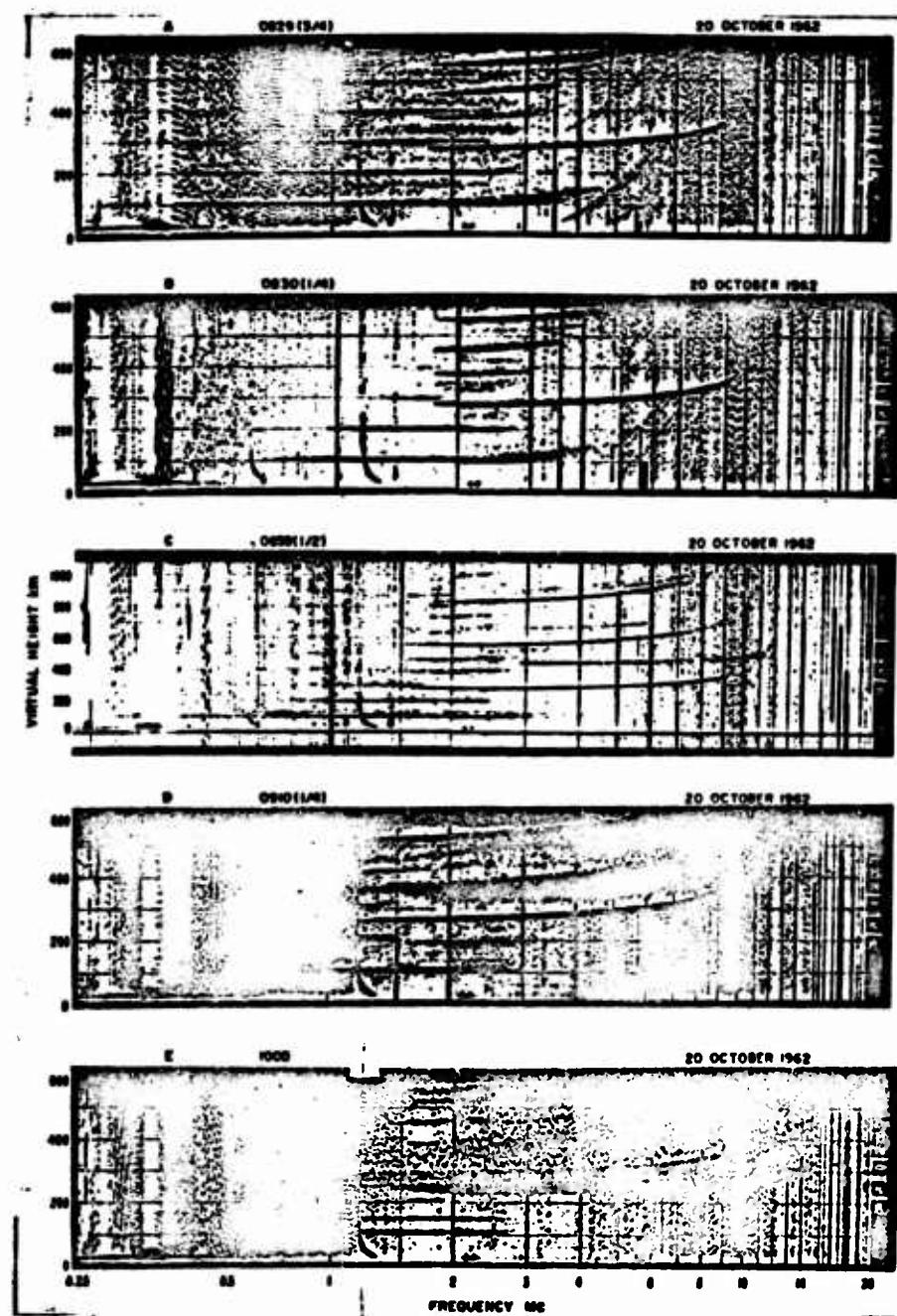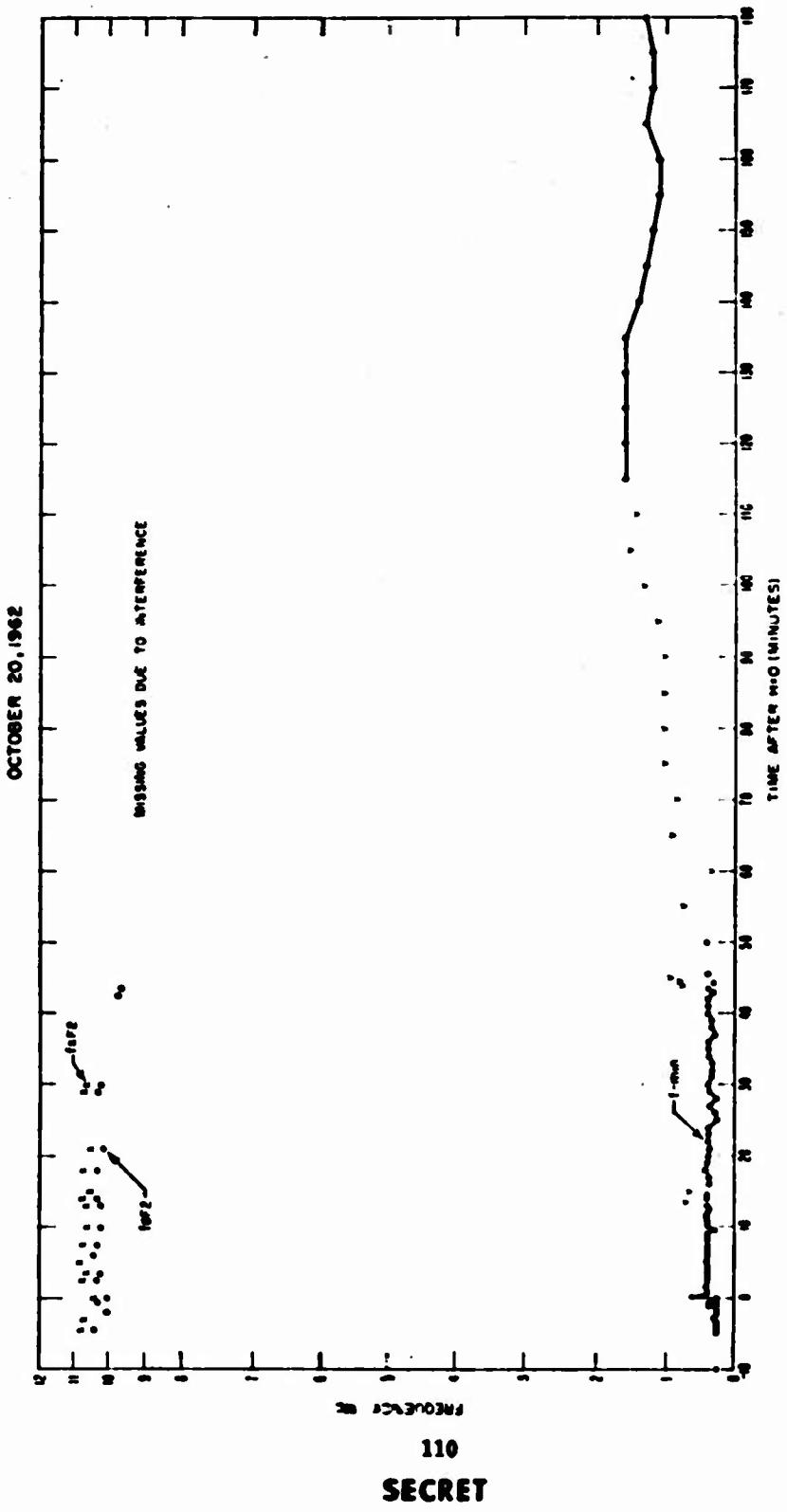
Figure 40 Check Mate, Tutuila, 3-hour frequency plot.
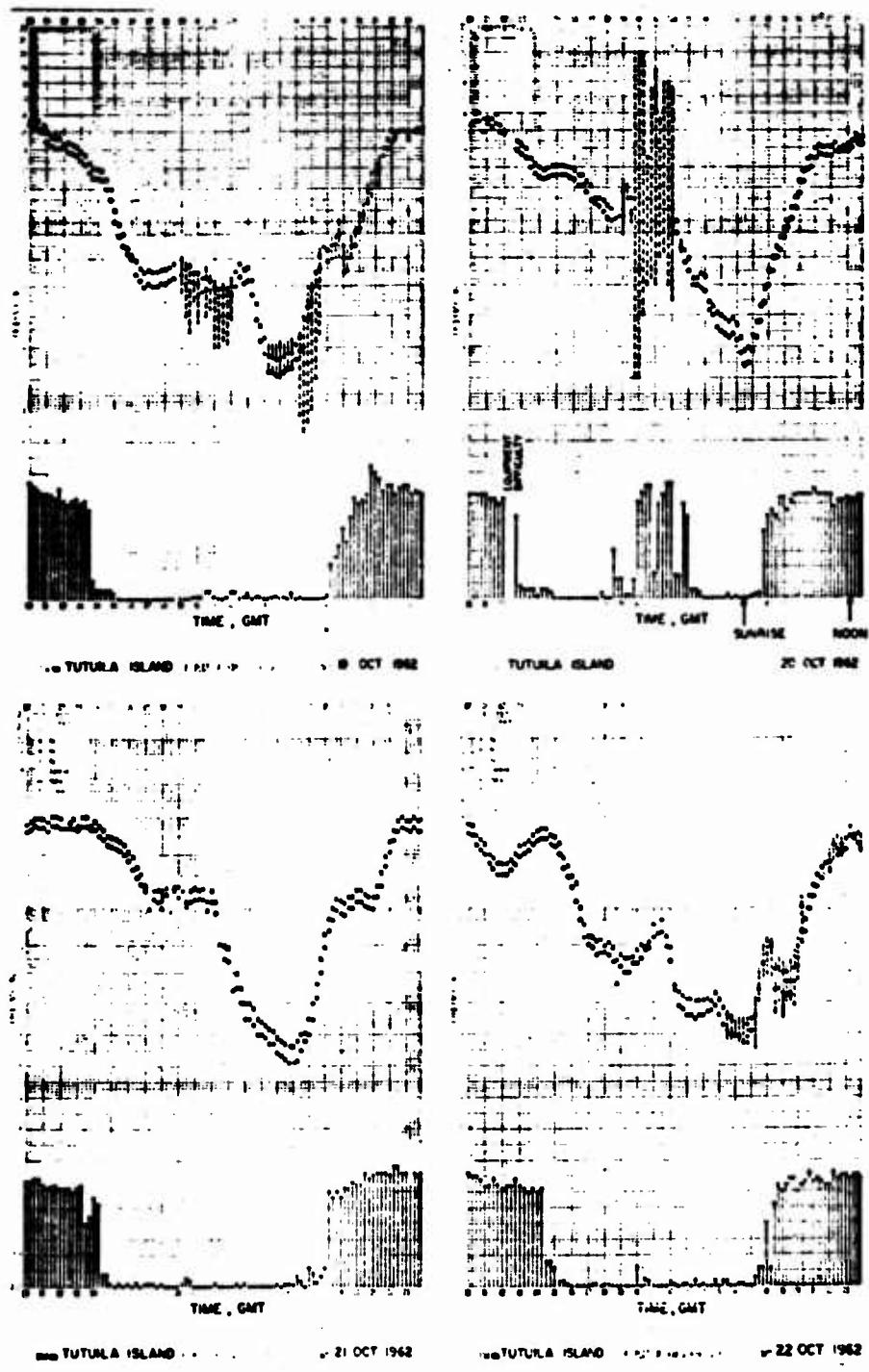
Figure 41 Check Mate, Tutuila, f-plots.

111
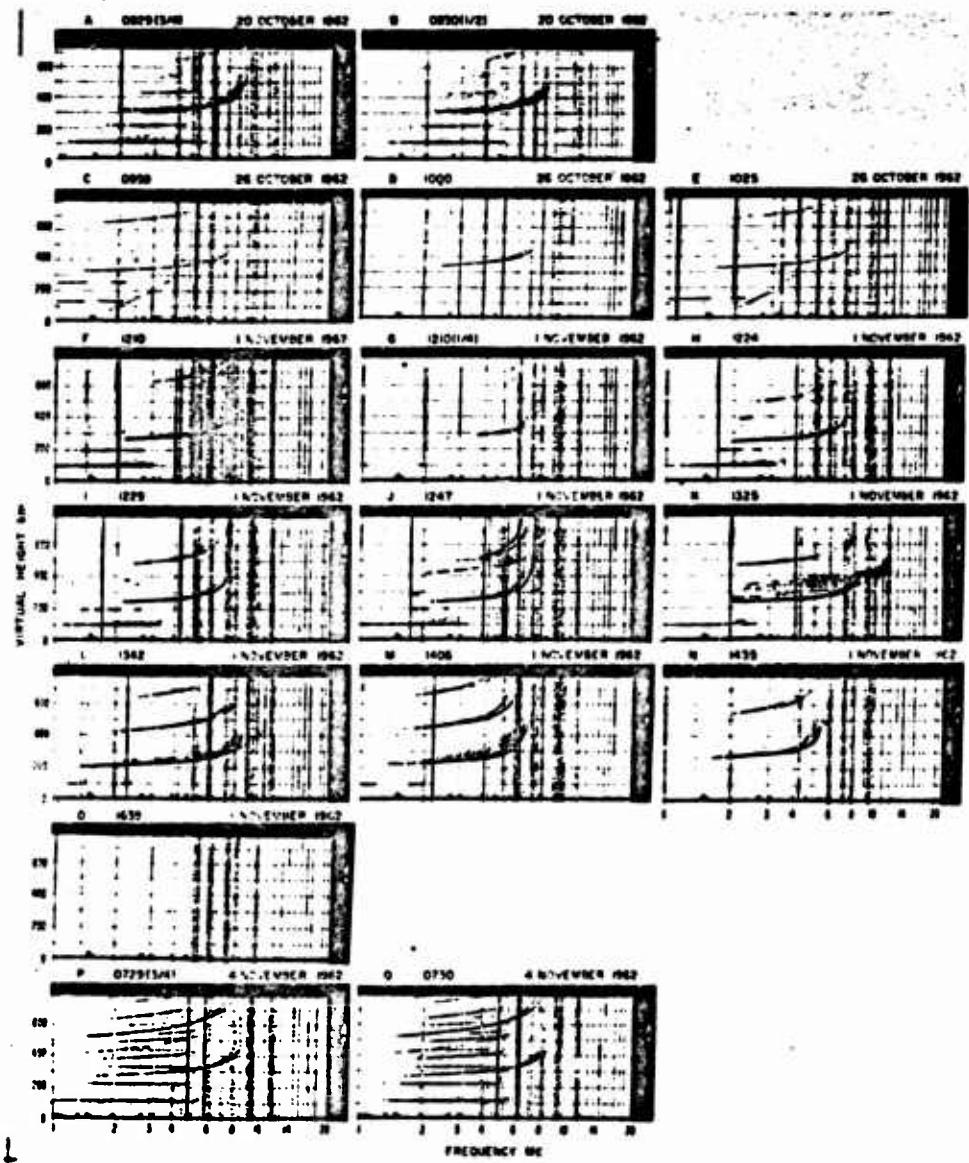
Figure 42 Check Mate, Blue Gill, King Fish, Tight Rope, Tonga, selected ionograms.
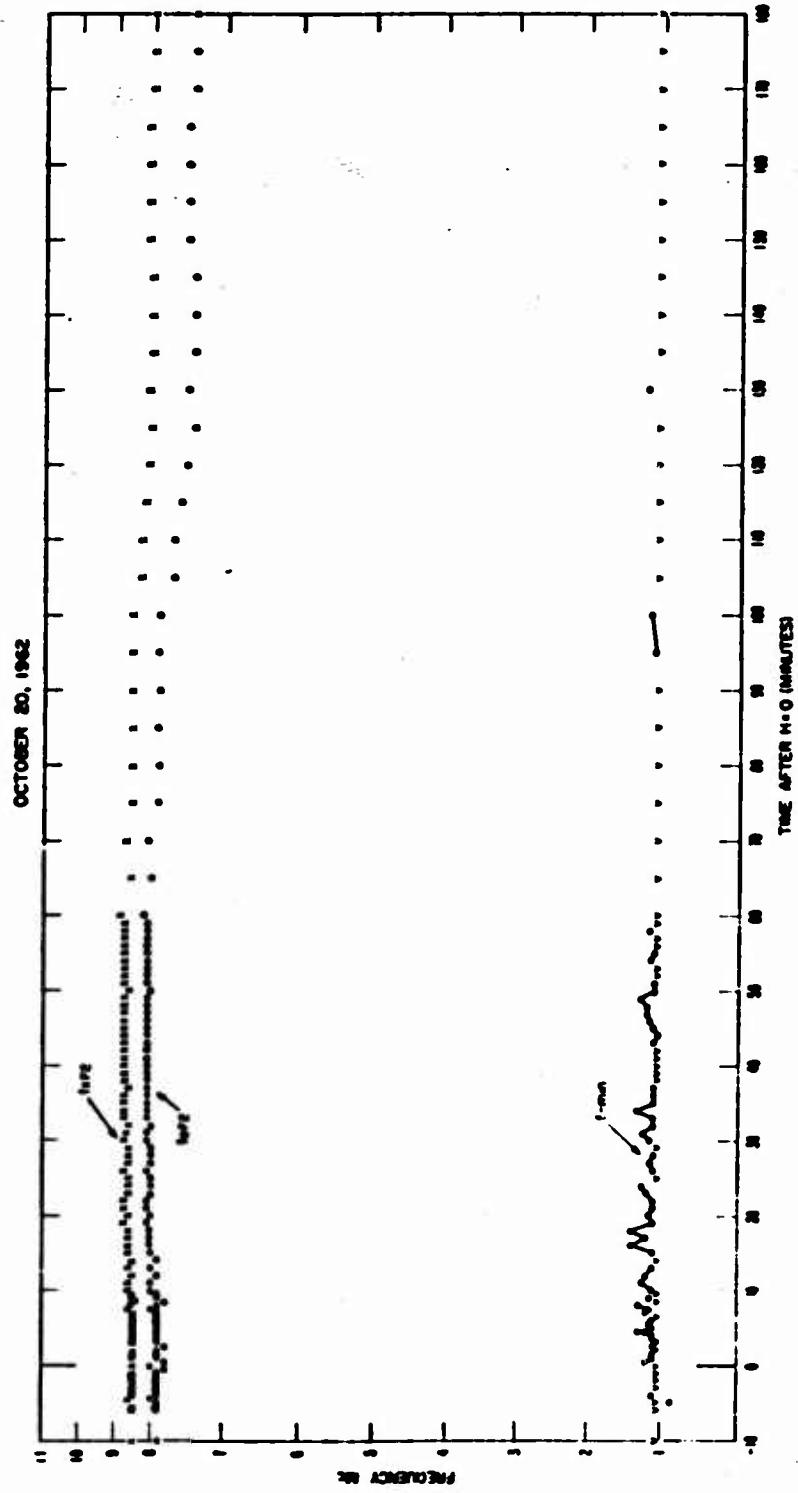
Figure 43 Check Mate, Tonga, 3-hour frequency plot.
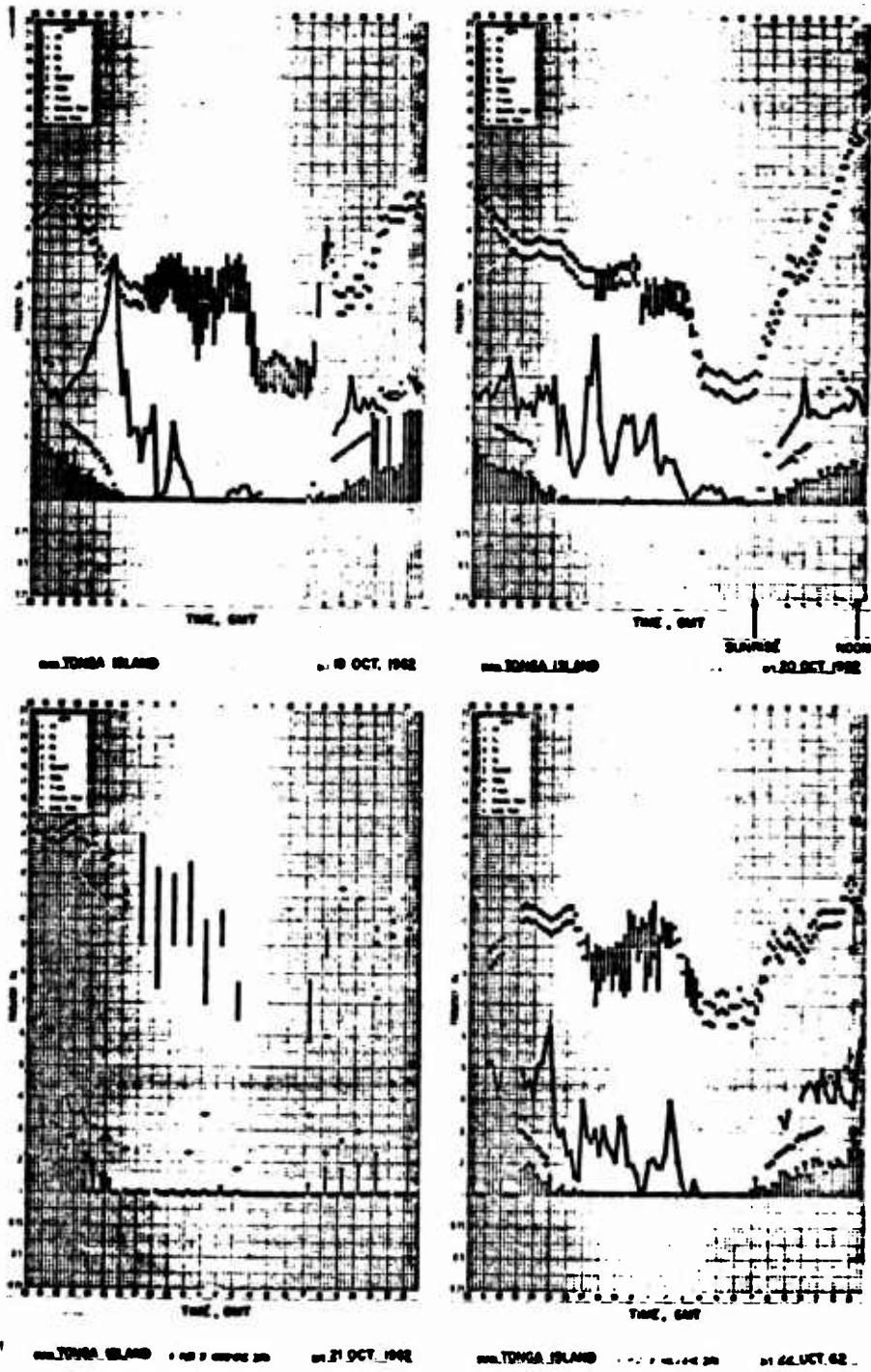
Figure 44 Check Mate, Tonga, f-plots.

114
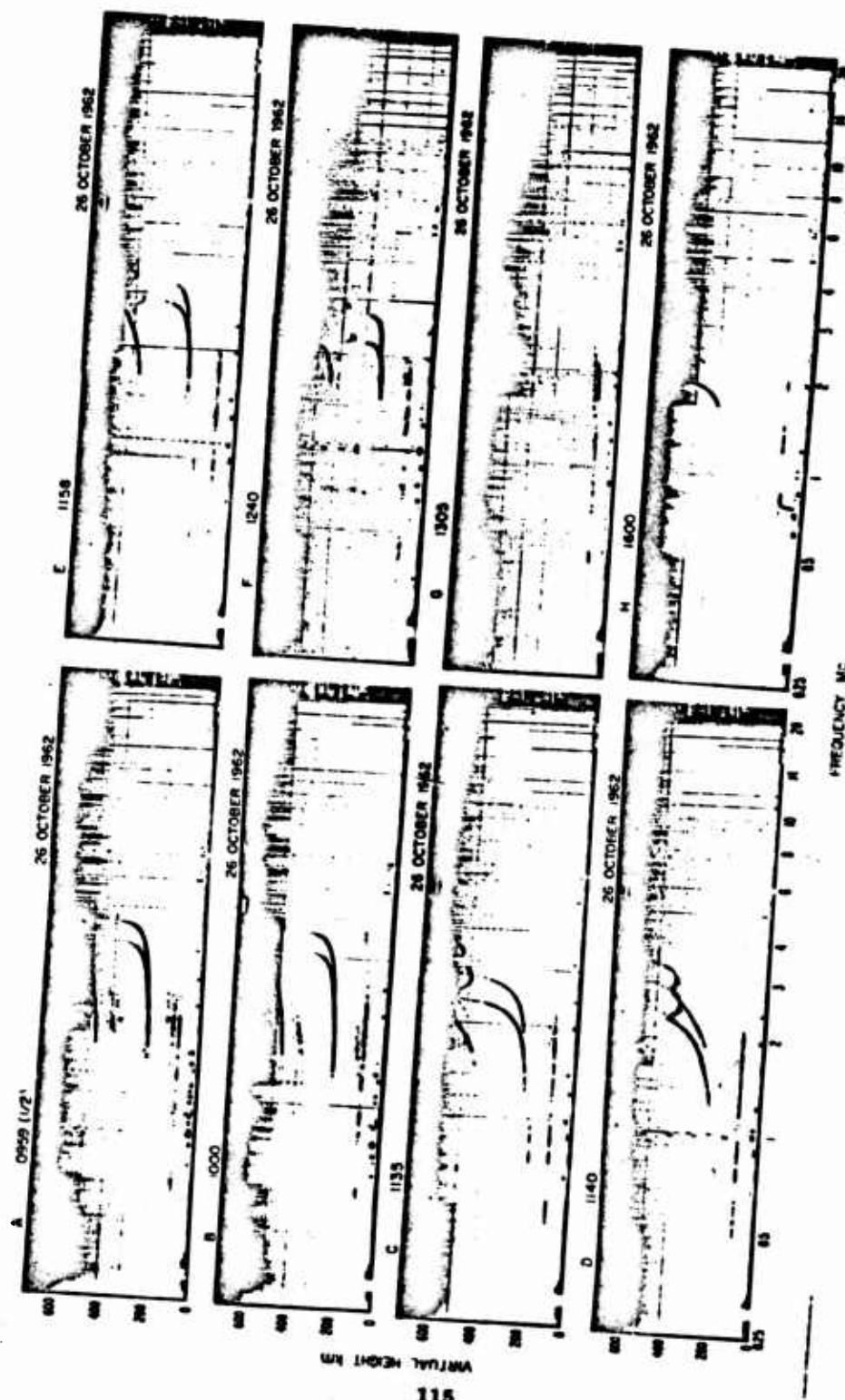
Figure 45 Blue Gill, Maui, selected ionograms.

115
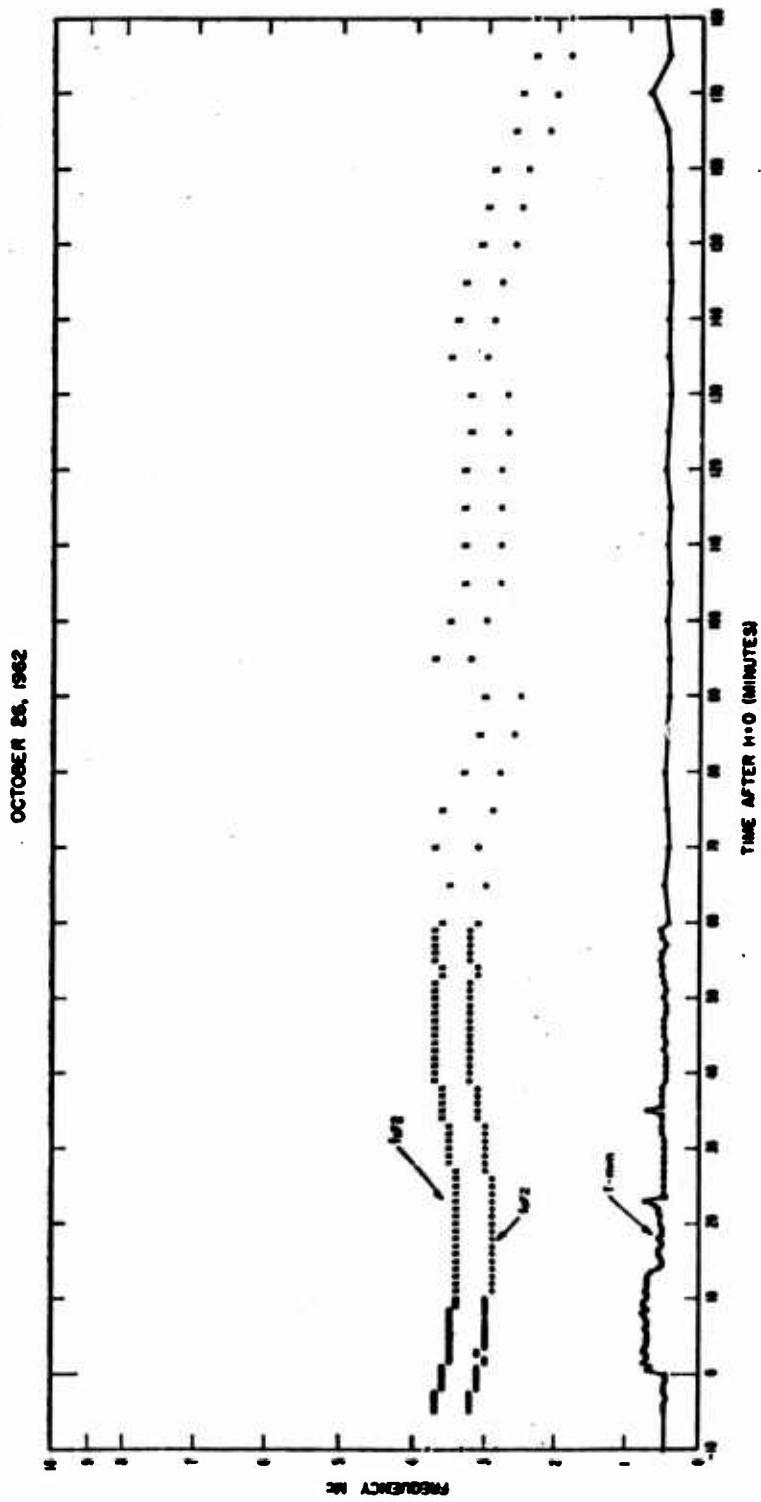
Figure 46 Blue Gill, Maui, 3-hour frequency plot.

116
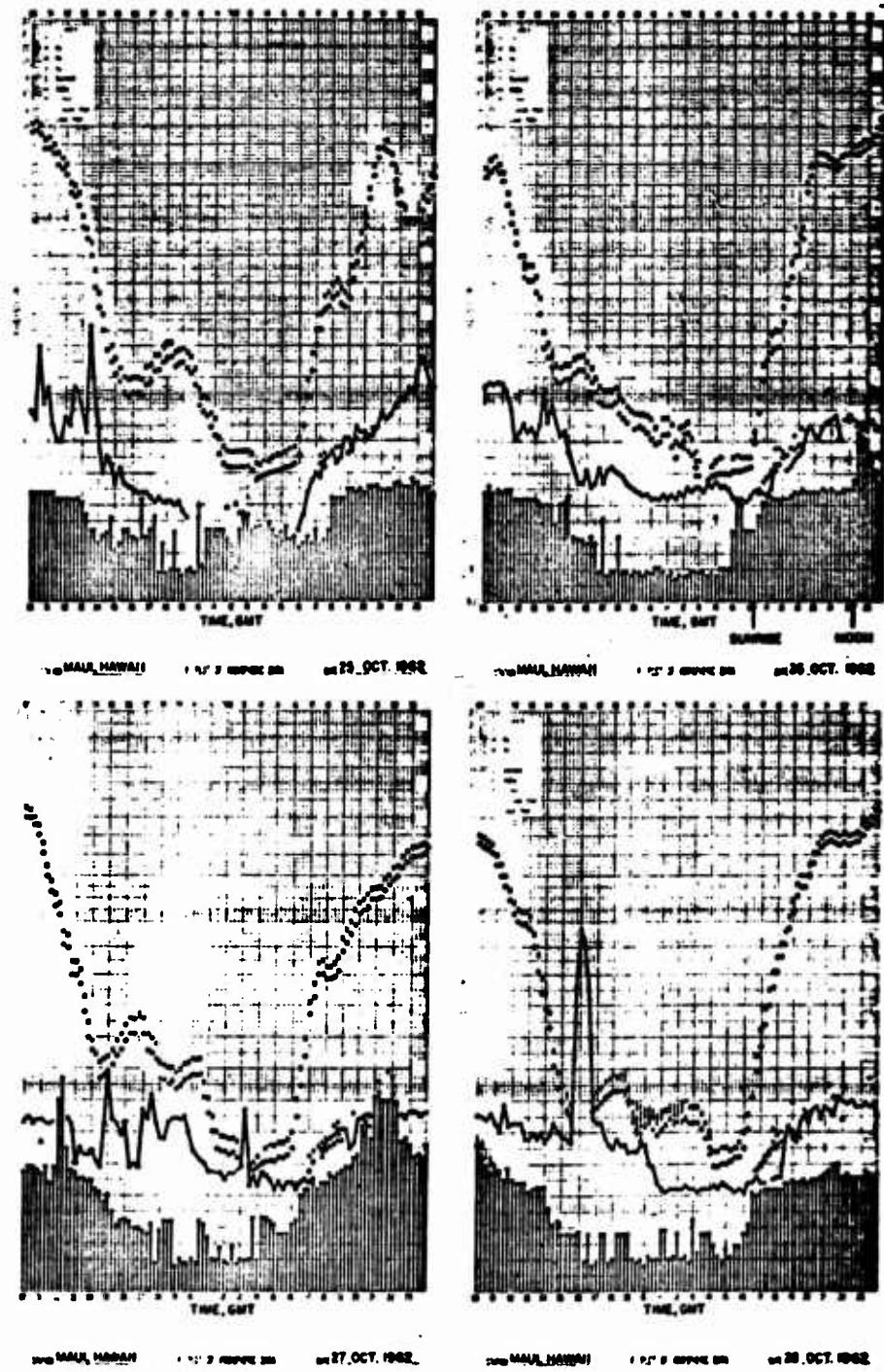
Figure 47 Blue Gill, Maui, f-plots.

117

SECRET
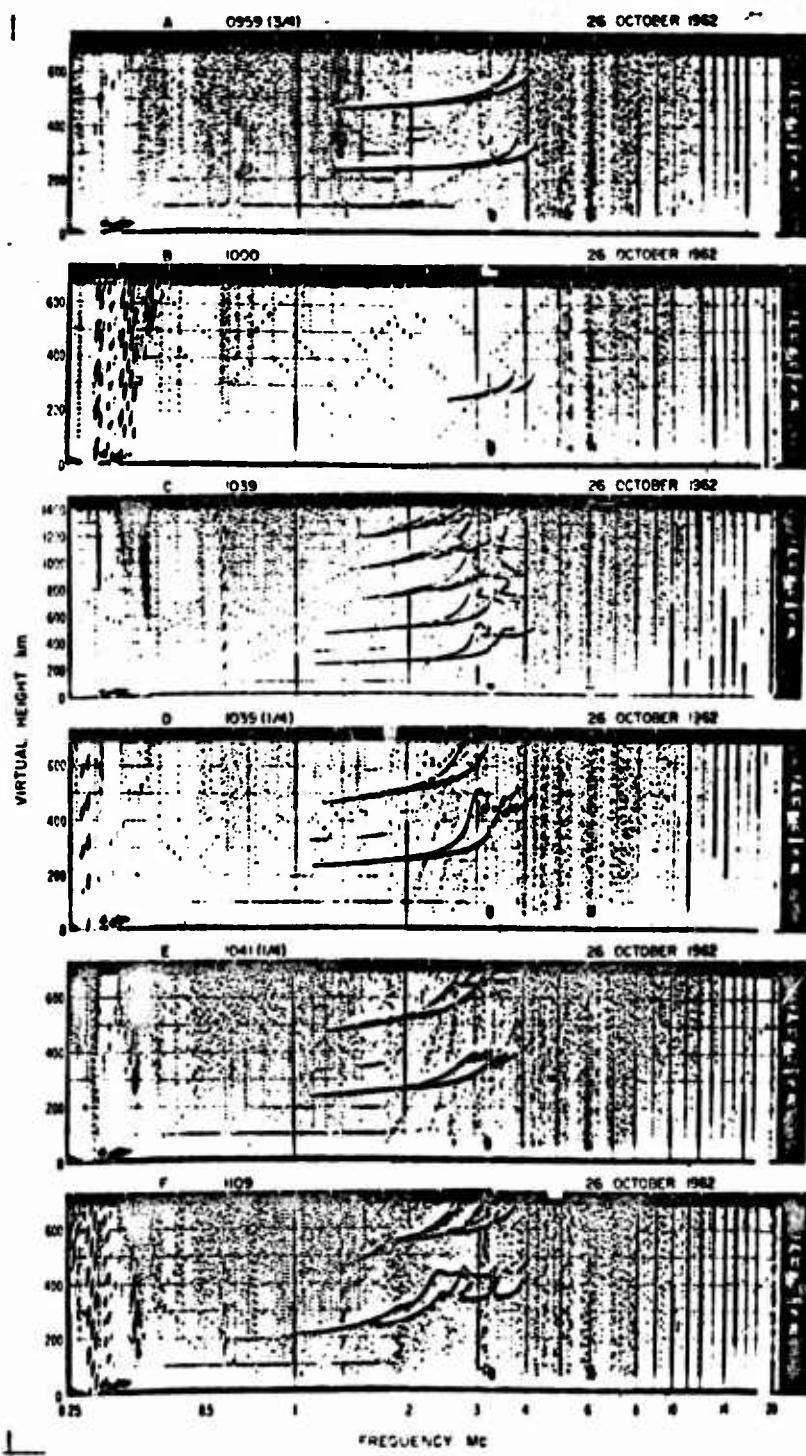
Figure 48 Blue Gill, Tern, selected ionograms.
118
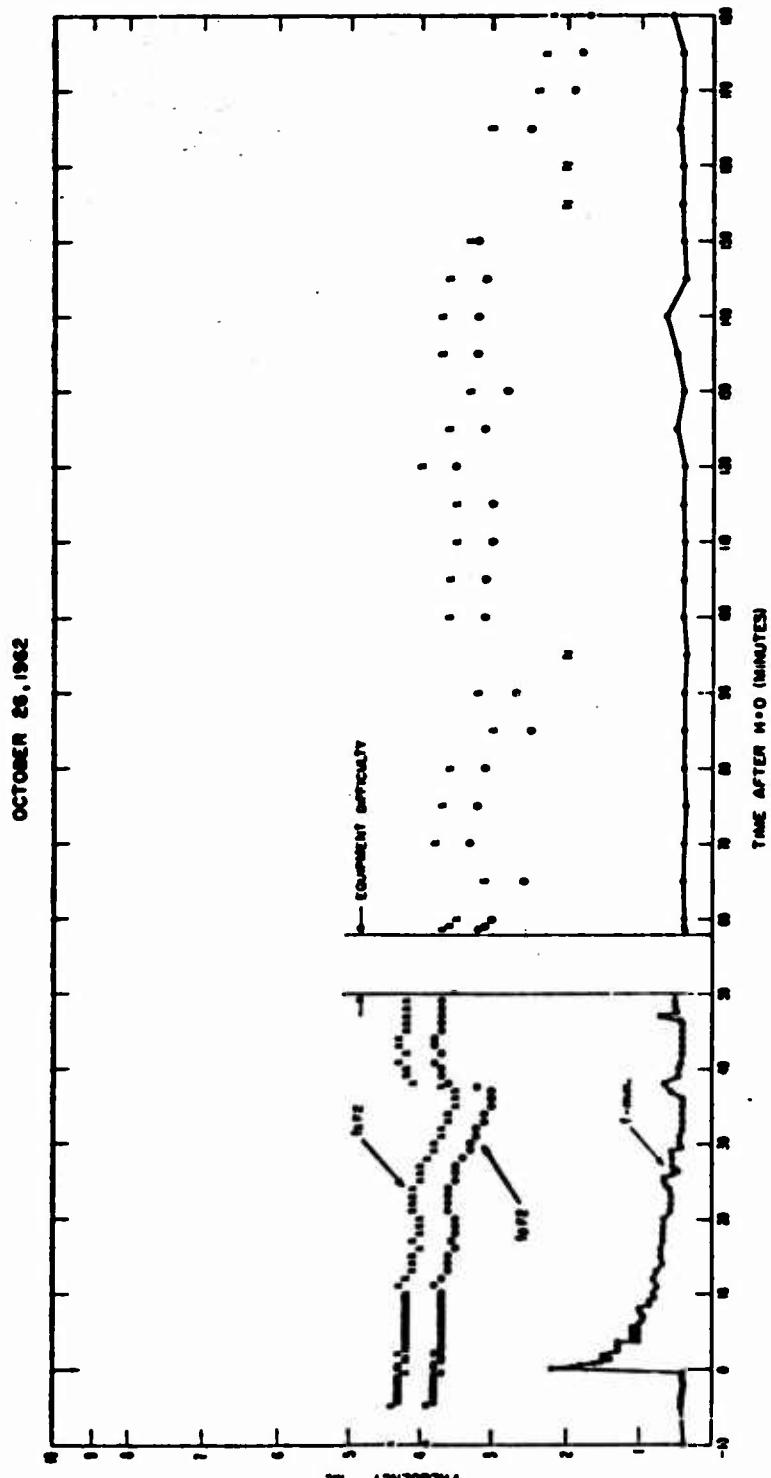
Figure 49 Blue Gill, Tern, 3-hour frequency plot.

119
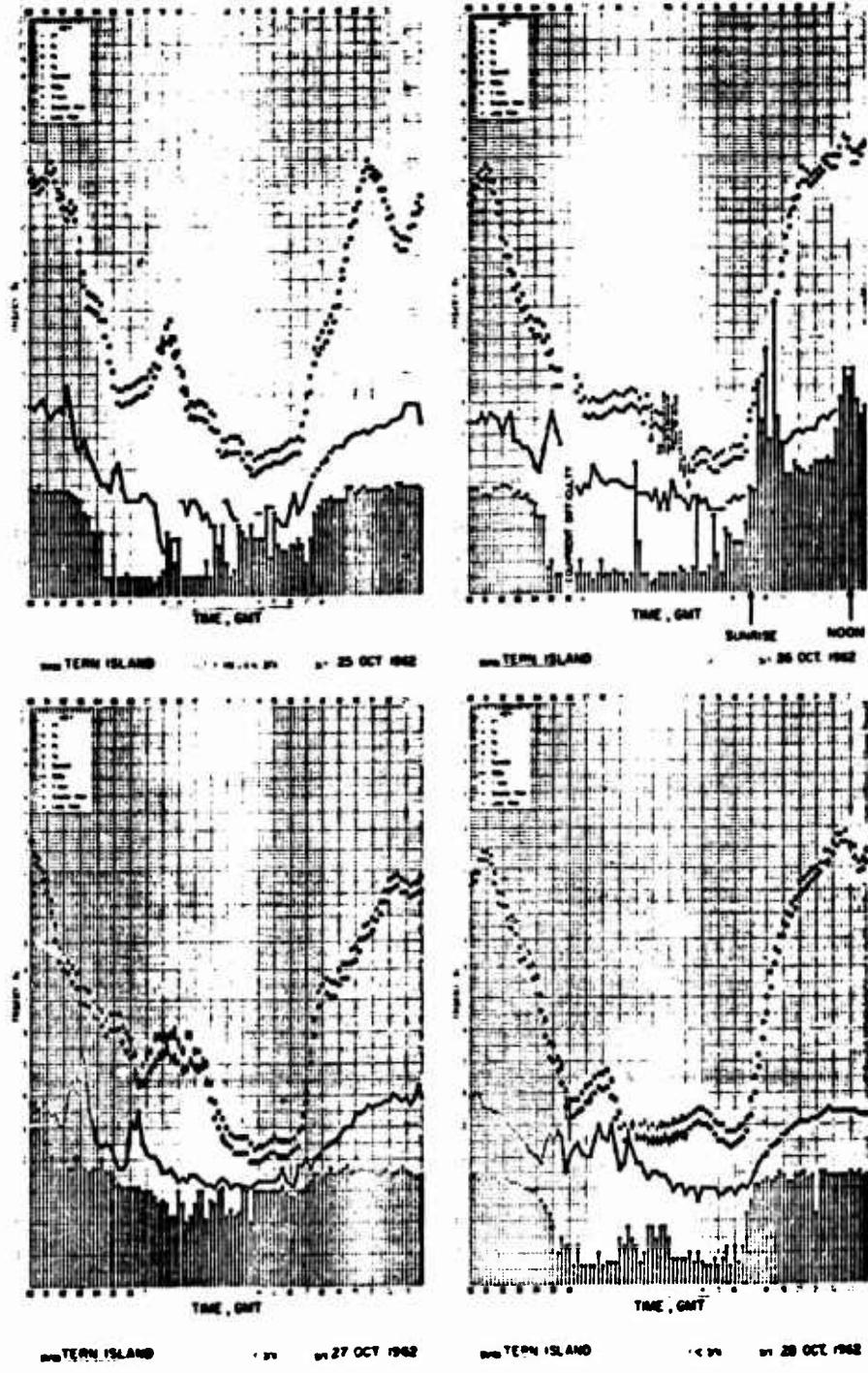
SECRET

Figure 50 Blue Gill, Tern, f-plots.

120
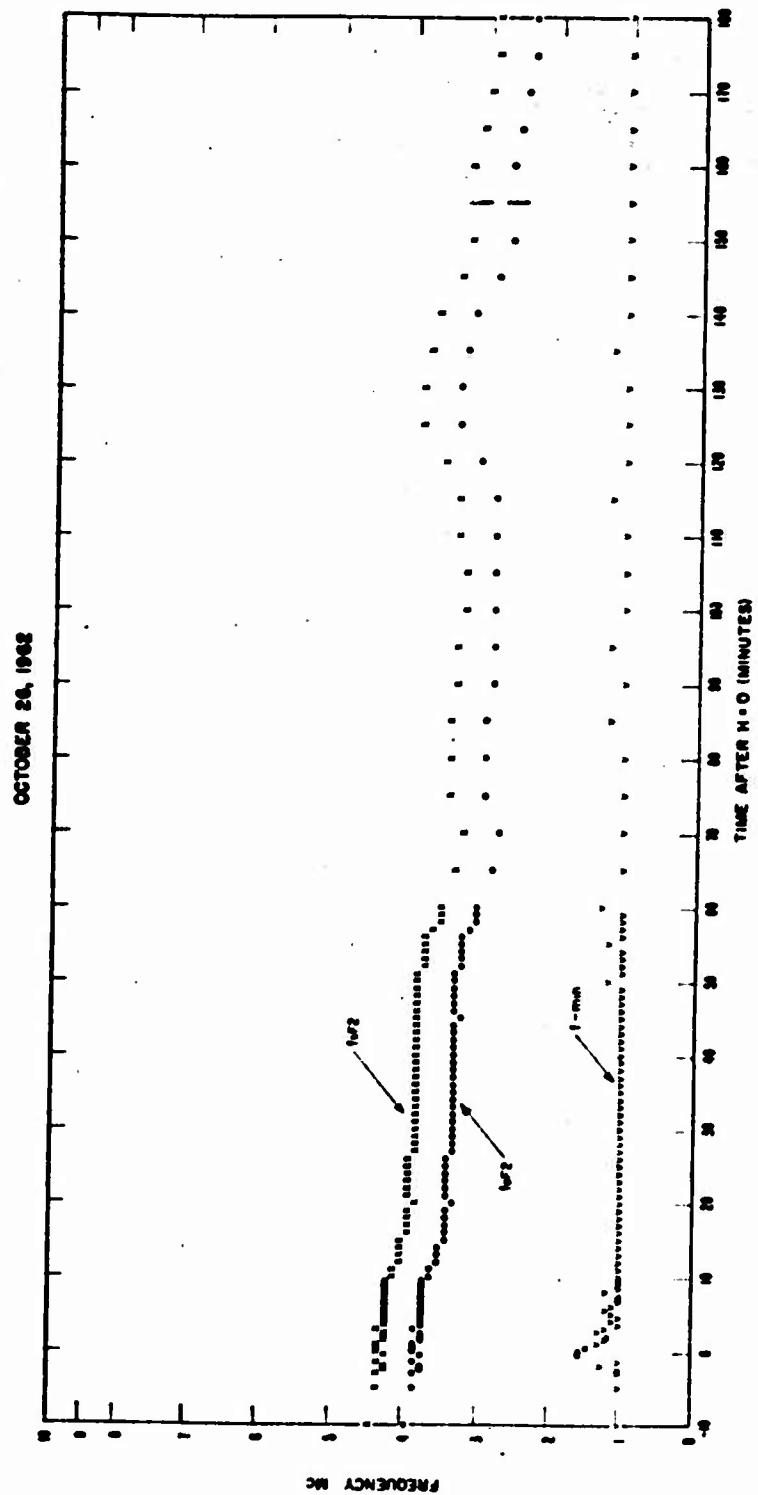
SECRET

Figure 51 Blue Gill, Midway, 3-hour frequency plot.

121
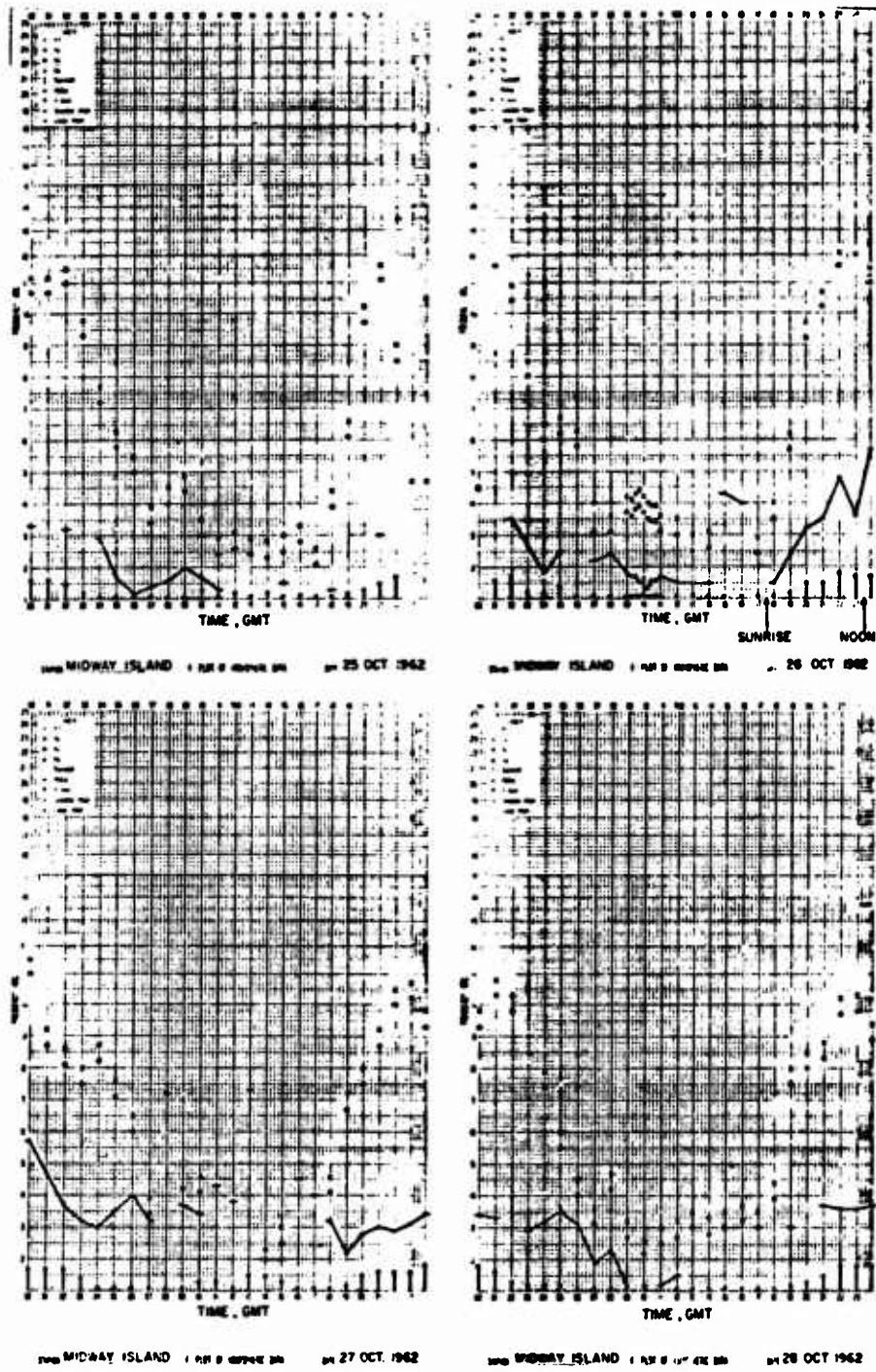
Figure 52 Blue Gill, Midway, f-plots.

122
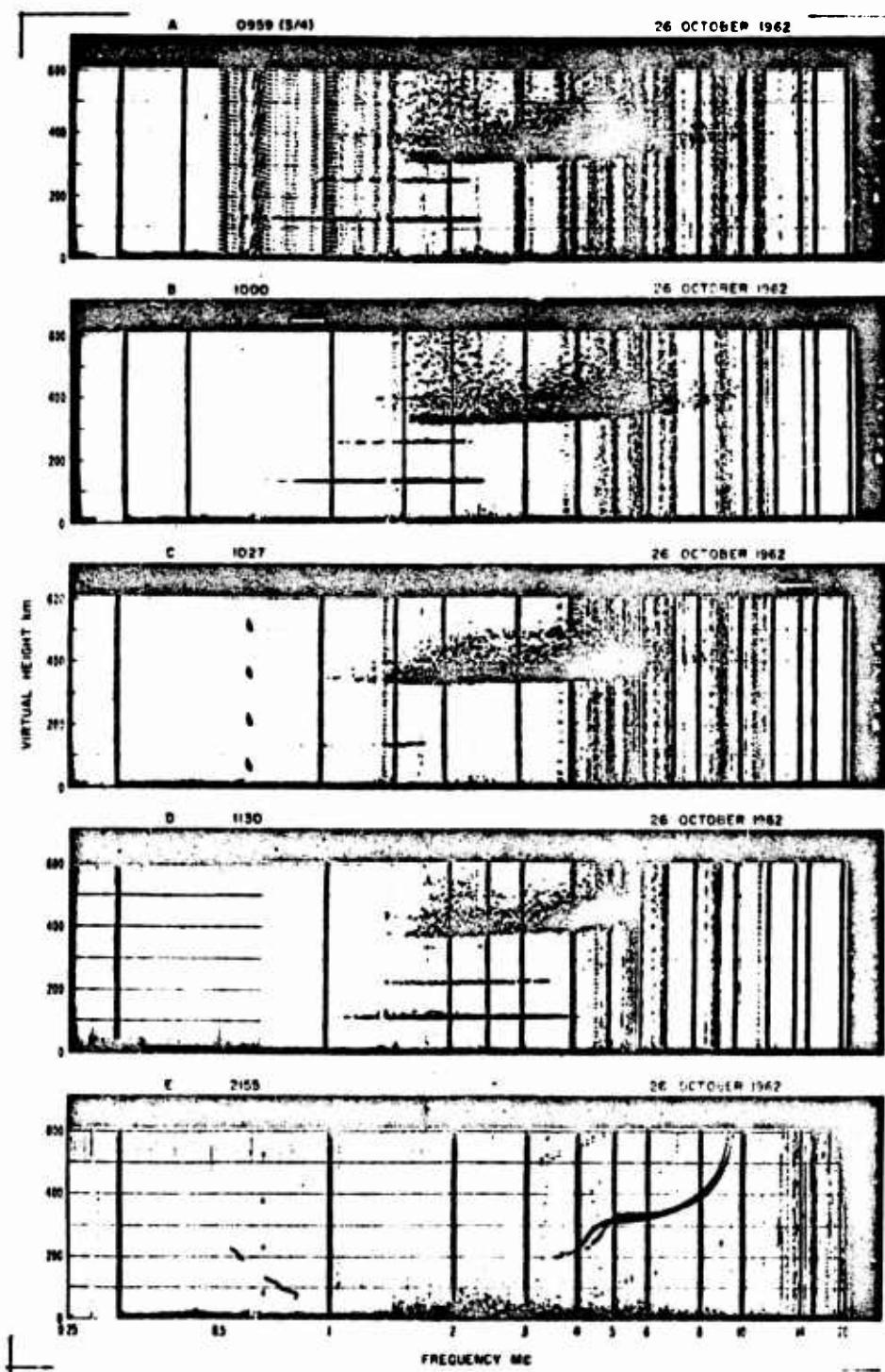
SECRET

Figure 53 Blue Gill, Canton, selected ionograms.

123

Figure 54 Blue Gill, Canton, 3-hour frequency plot.

124
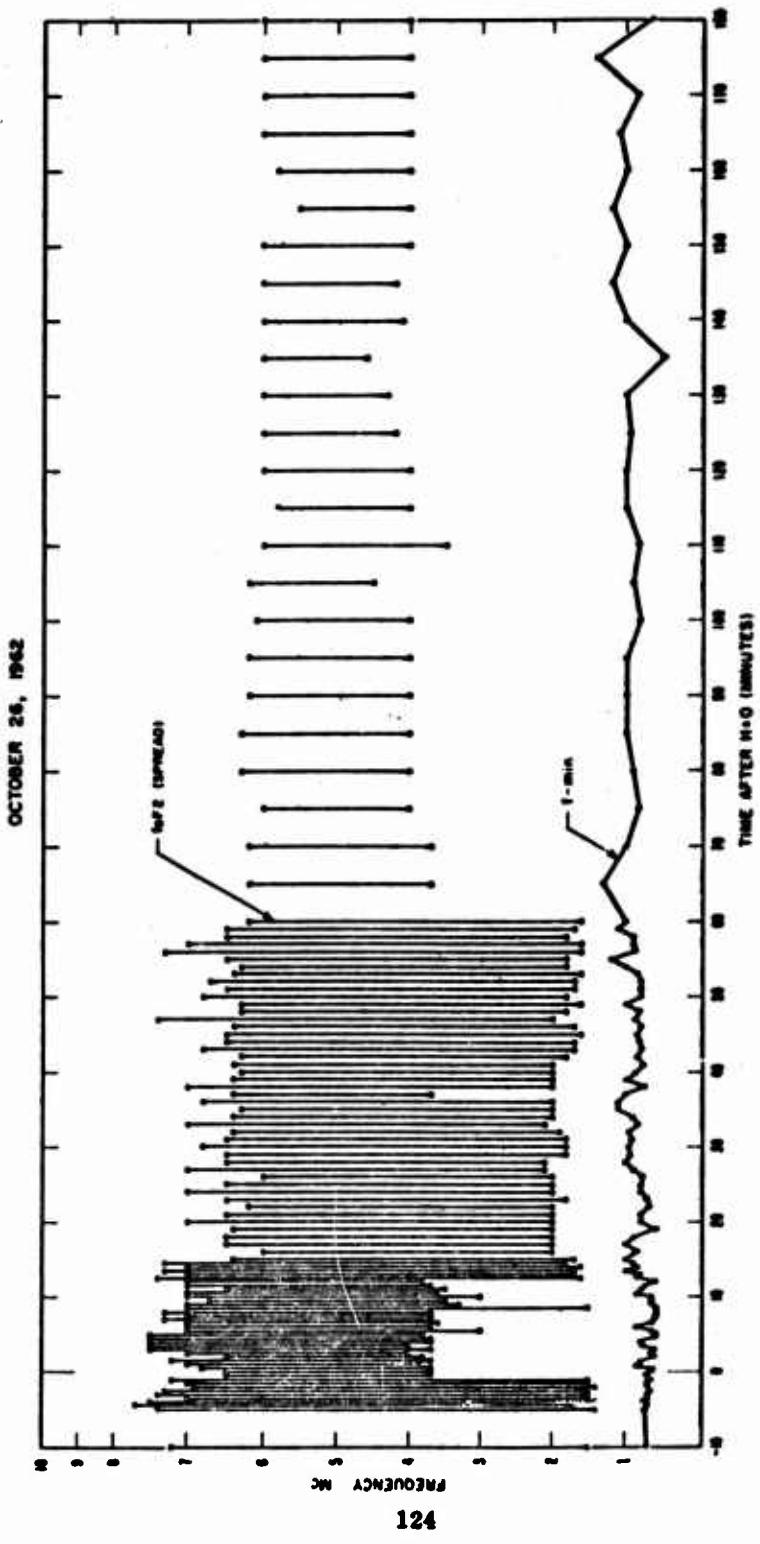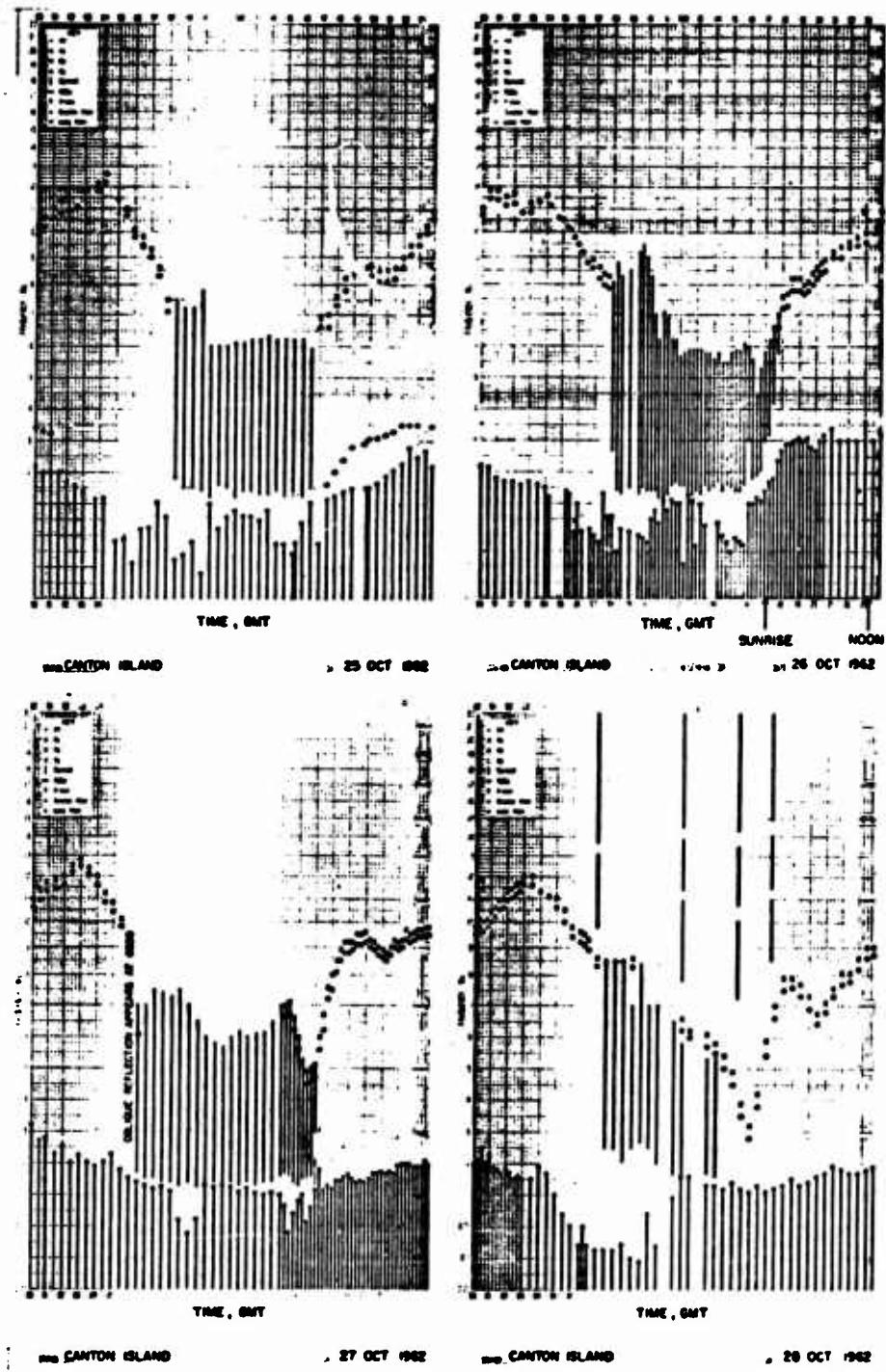
Figure 55 Blue Gill, Canton, f-plots.

125
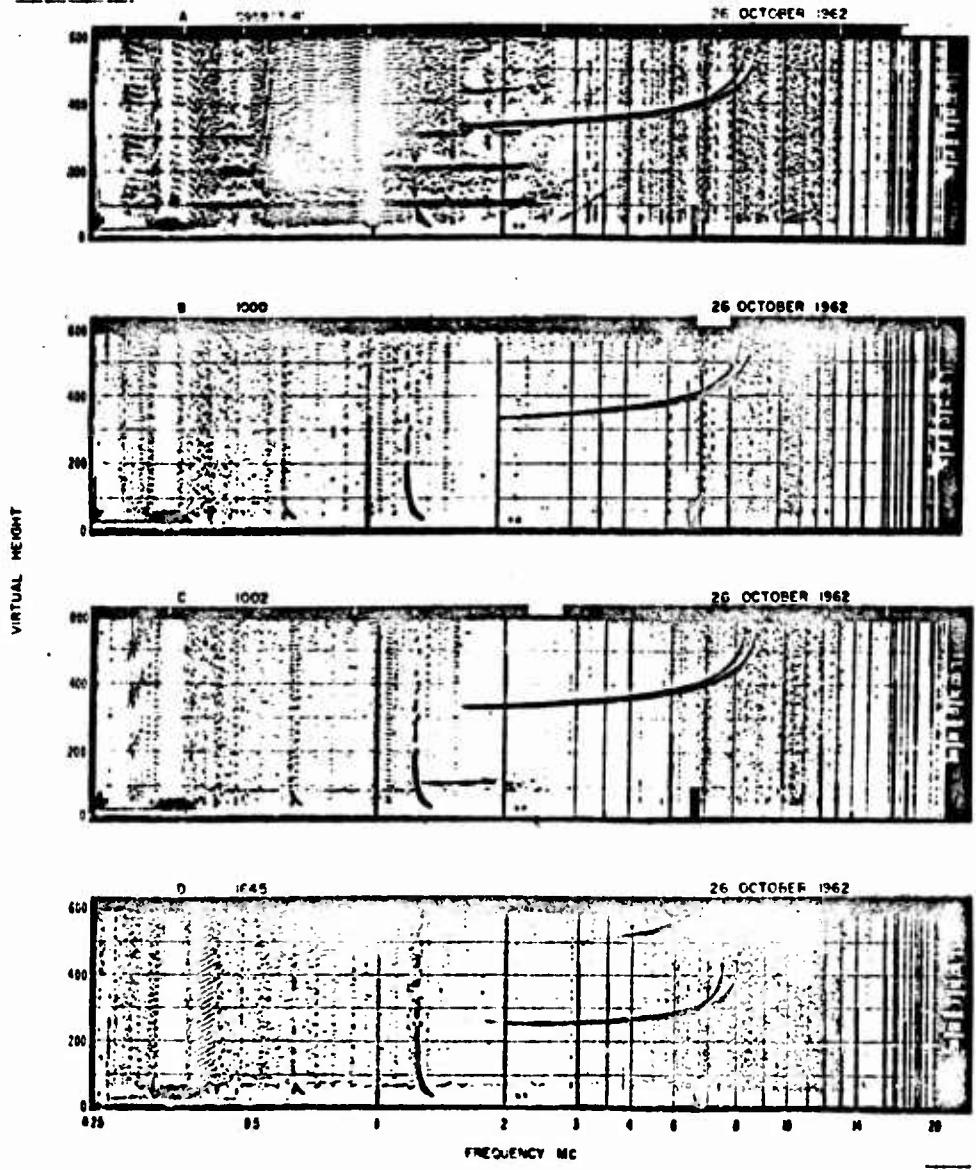
Figure 56   Blue Gill, Tutuila, selected ionograms.
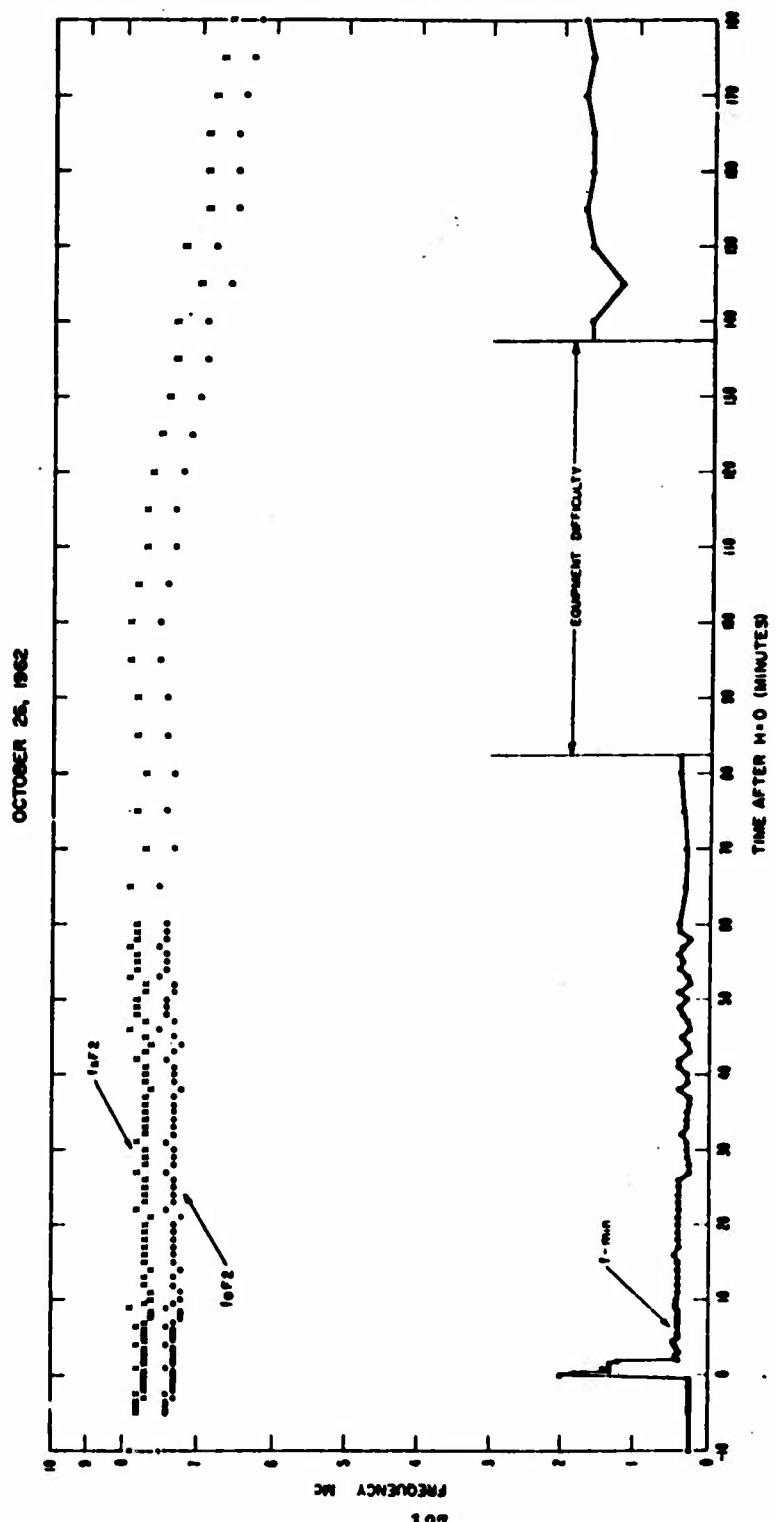
Figure 57 Blue Gill, Tutuila, 3-hour frequency plot.
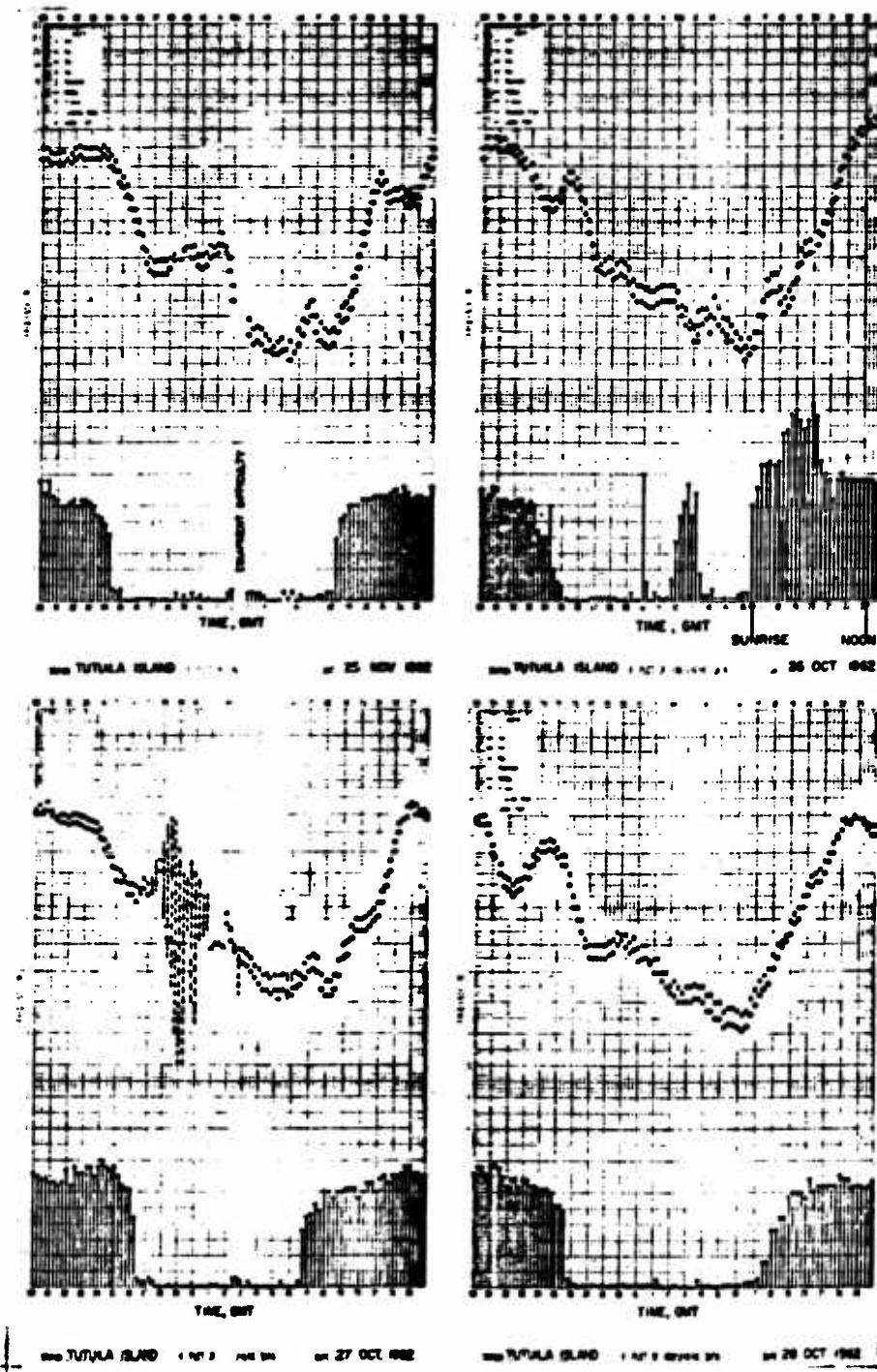
Figure 58 Blue Gill, Tutuila, f-plots.
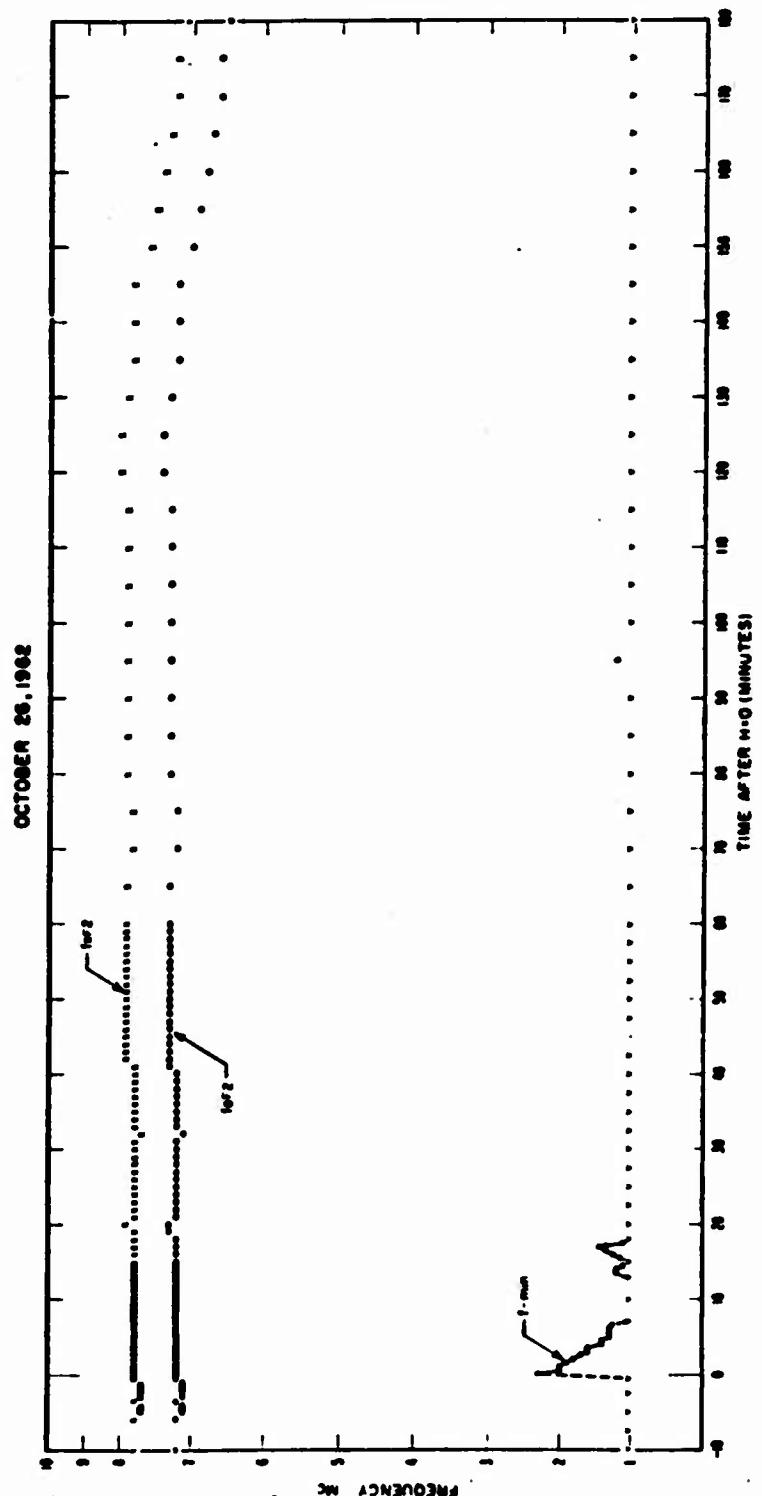
Figure 59 Blue Gill, Tonga, 3-hour frequency plot.
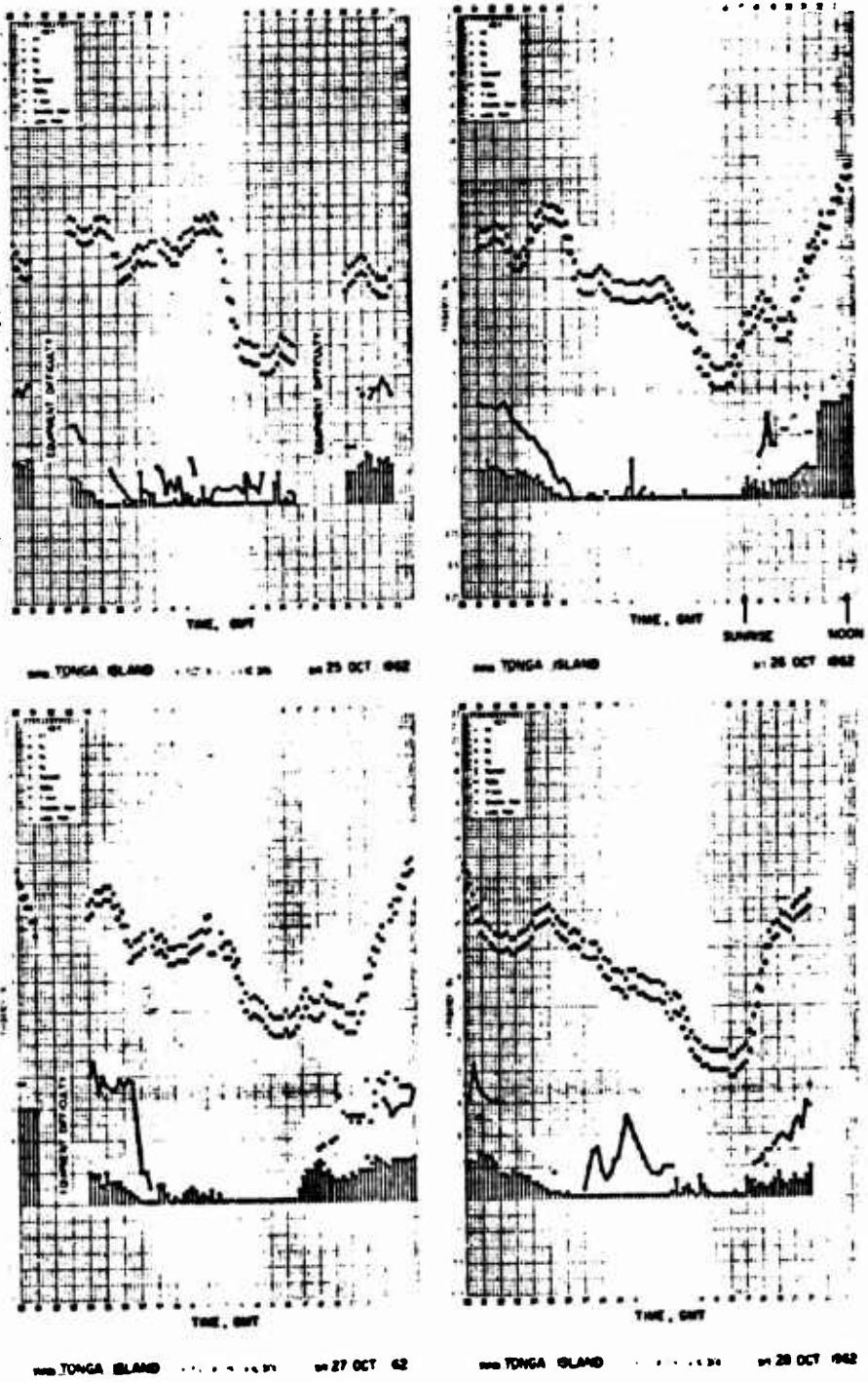
SECRET

Figure 60 Blue Gill, Tonga, f-plots.

130
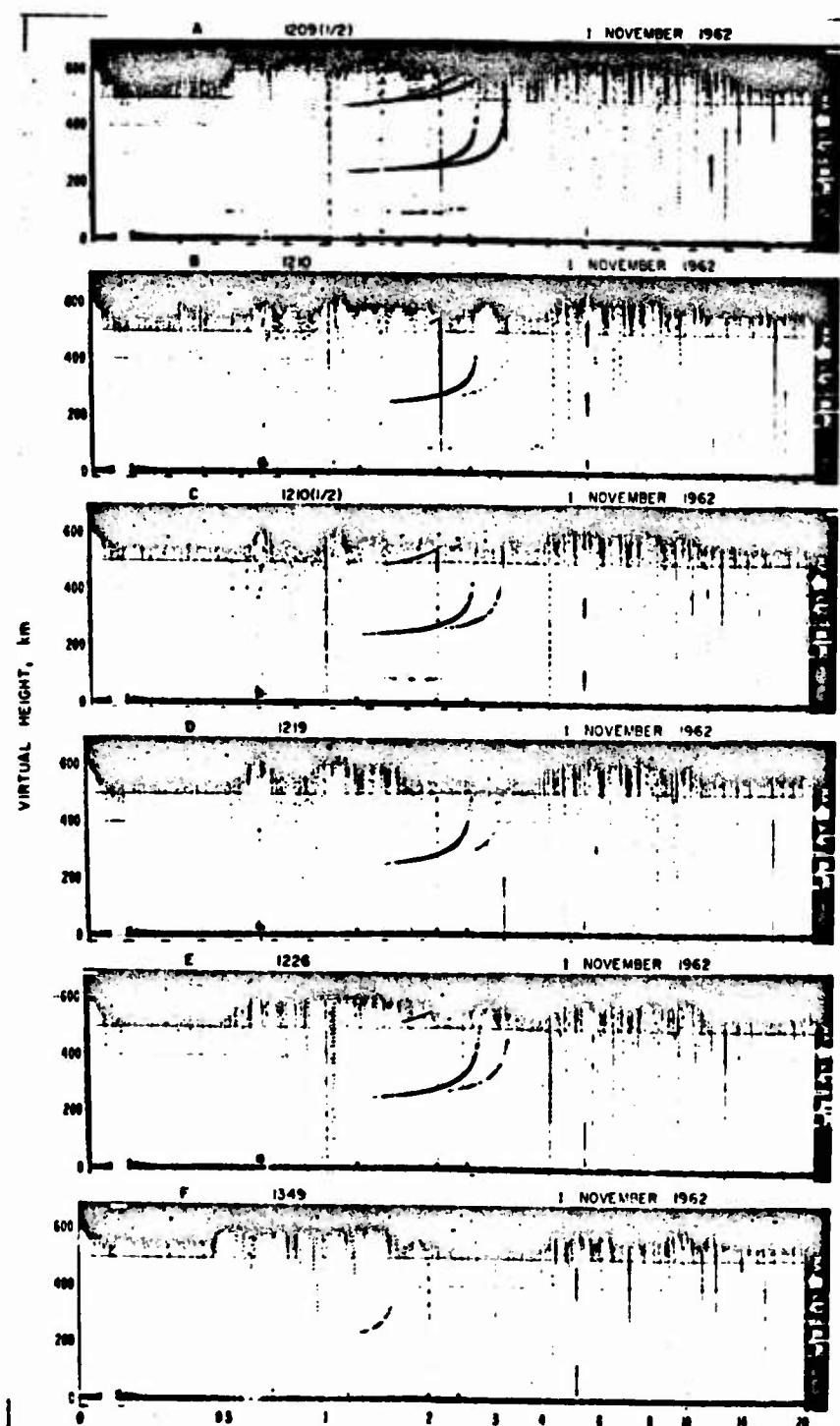
Figure 61 King Fish, Maui, selected ionograms.

131
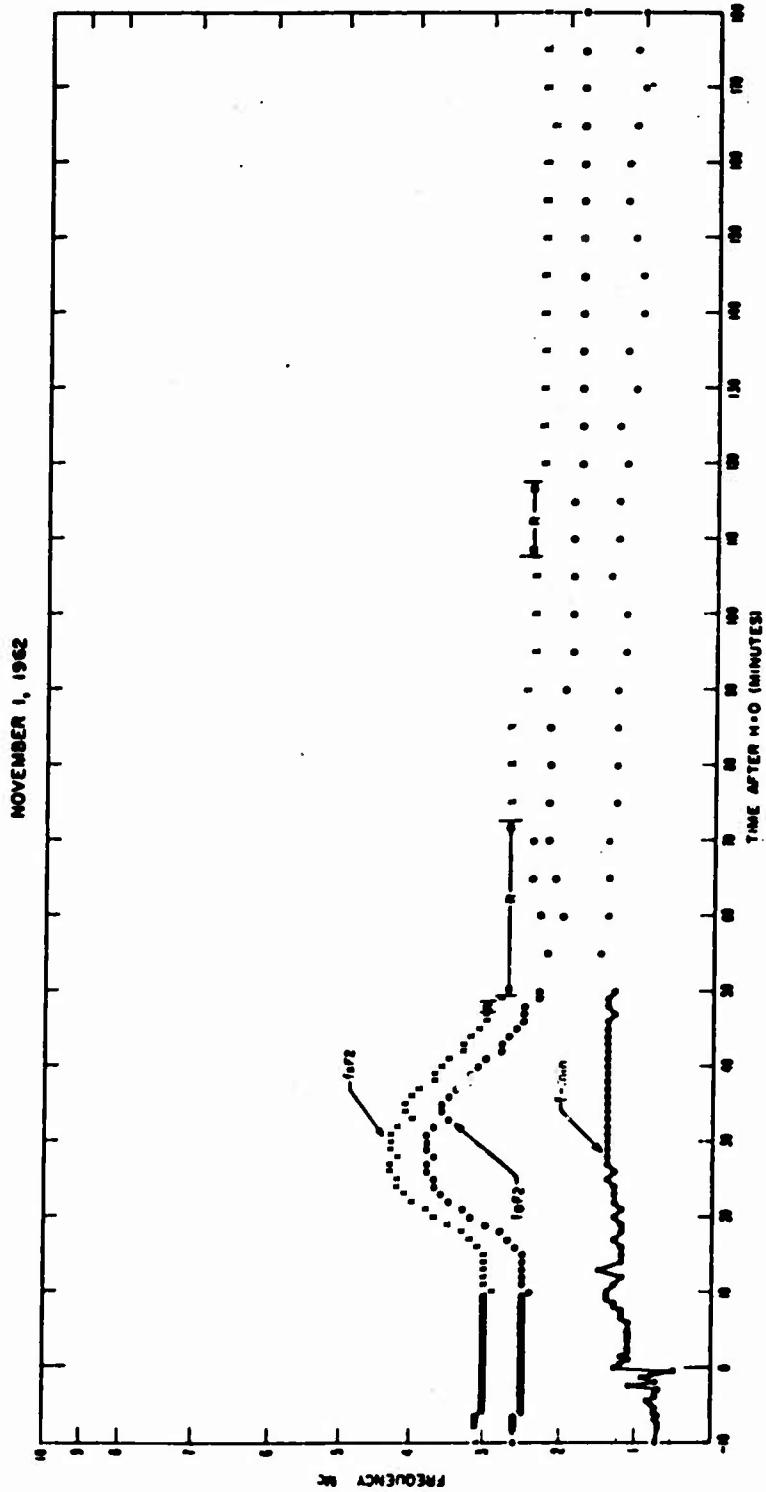
SECRET

Figure 62 King Fish, Maui, 3-hour frequency plot.

132
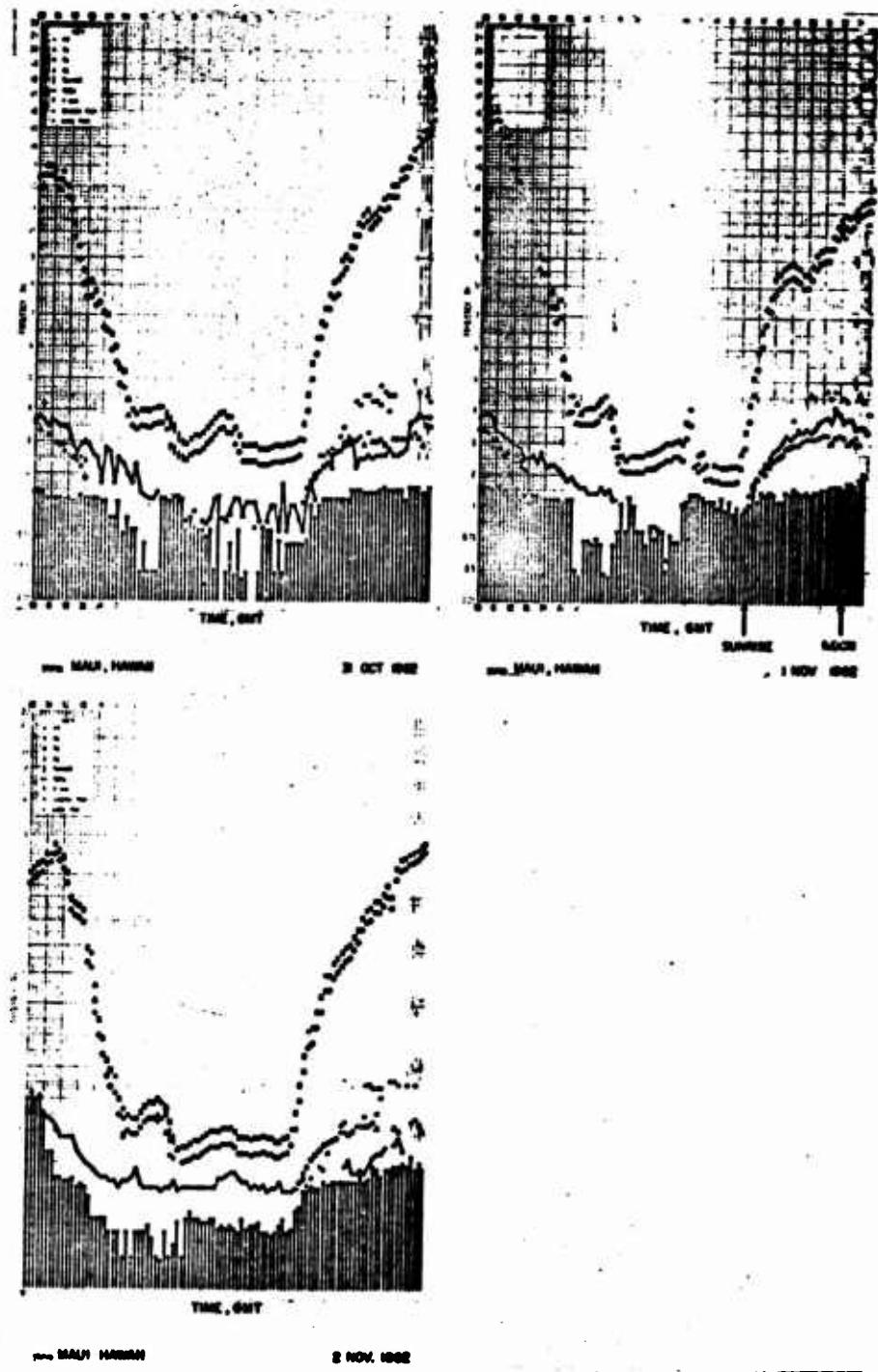
Figure 63 King Fish, Maui, f-plots.

133
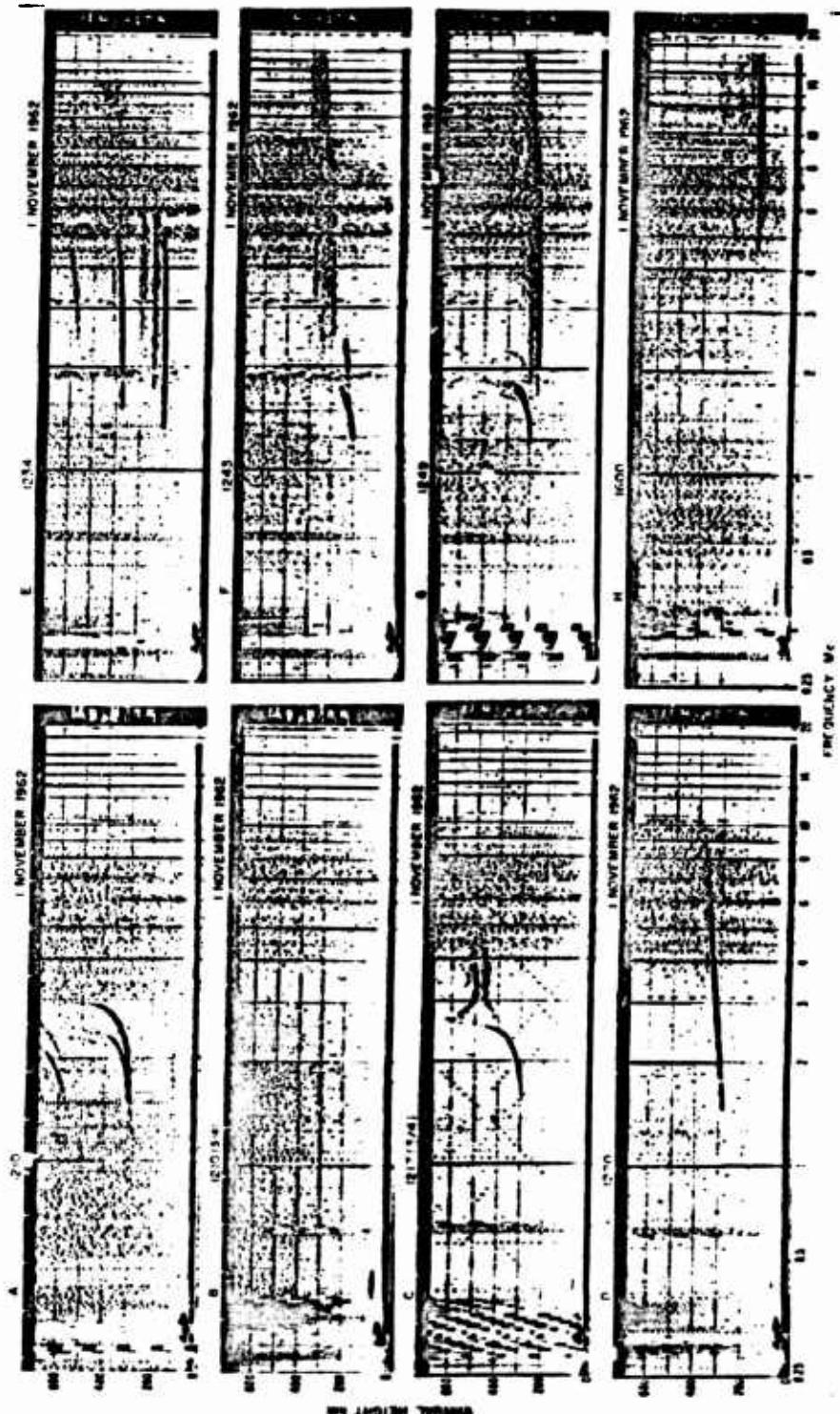
SECRET

Figure 64 King Fish, Tera, selected ionograms.
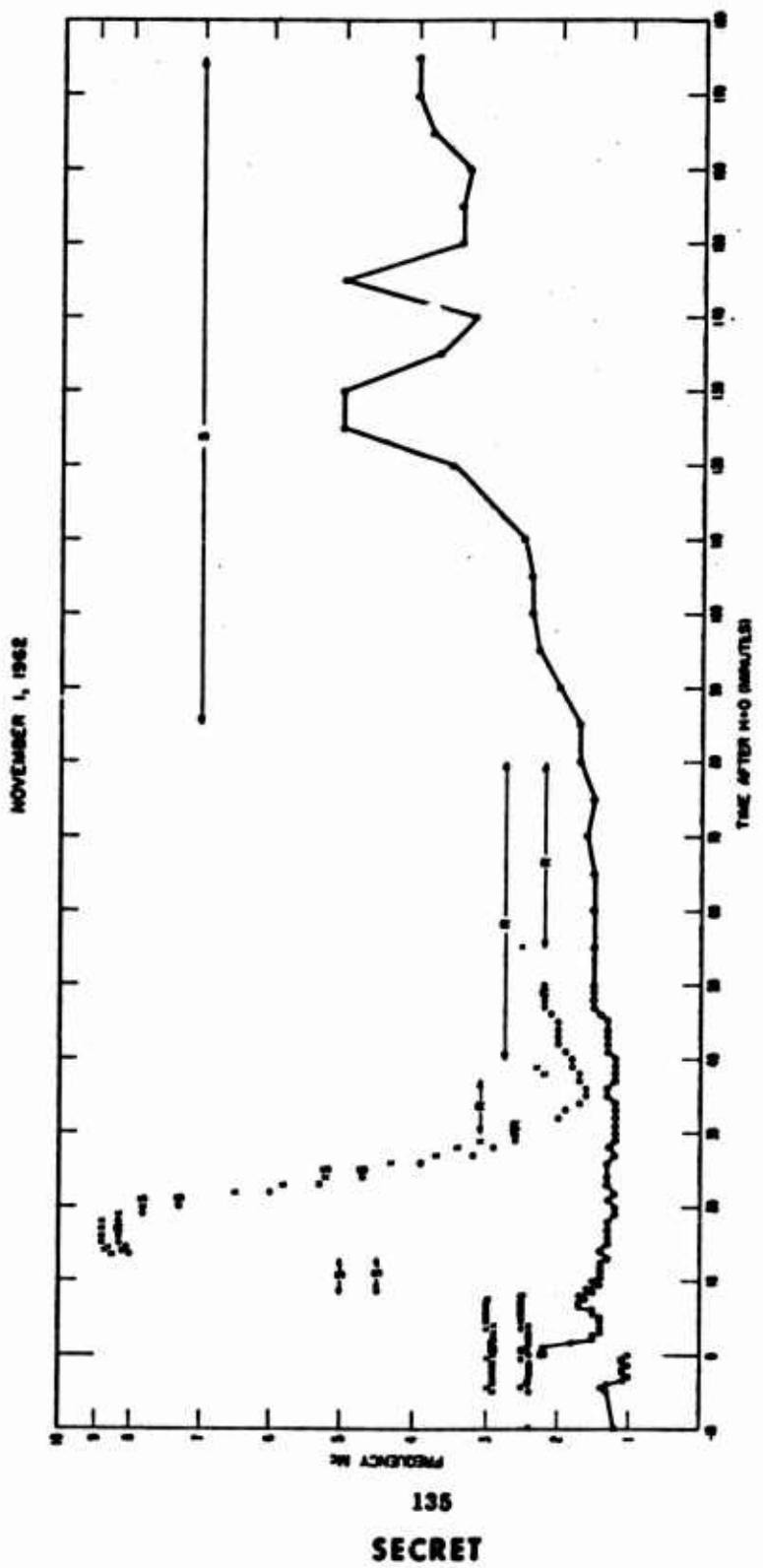
Figure 65 King Fish, Tern, 3-hour frequency plot.
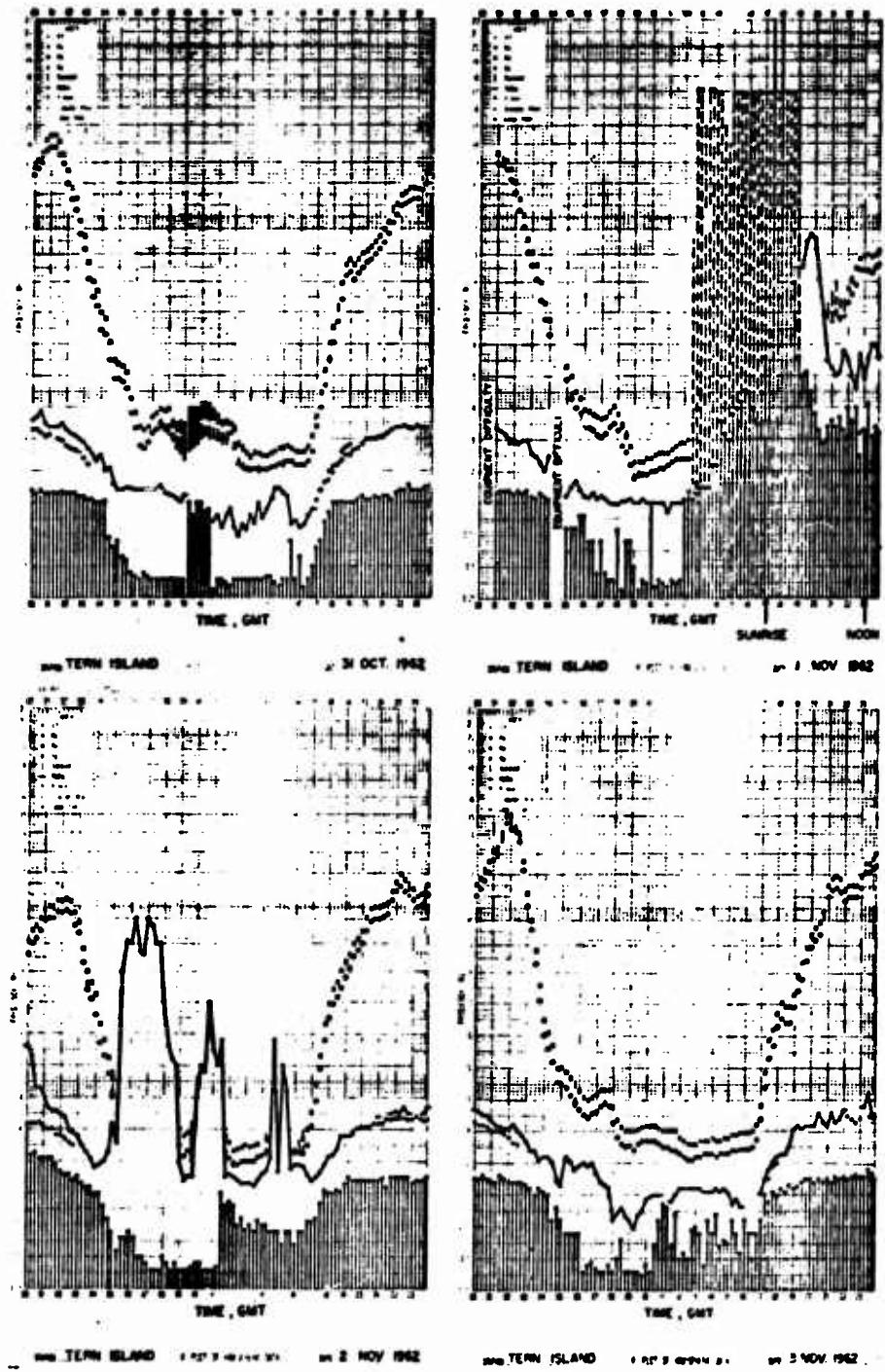
Figure 66 King Fish, Tern, f-plots.
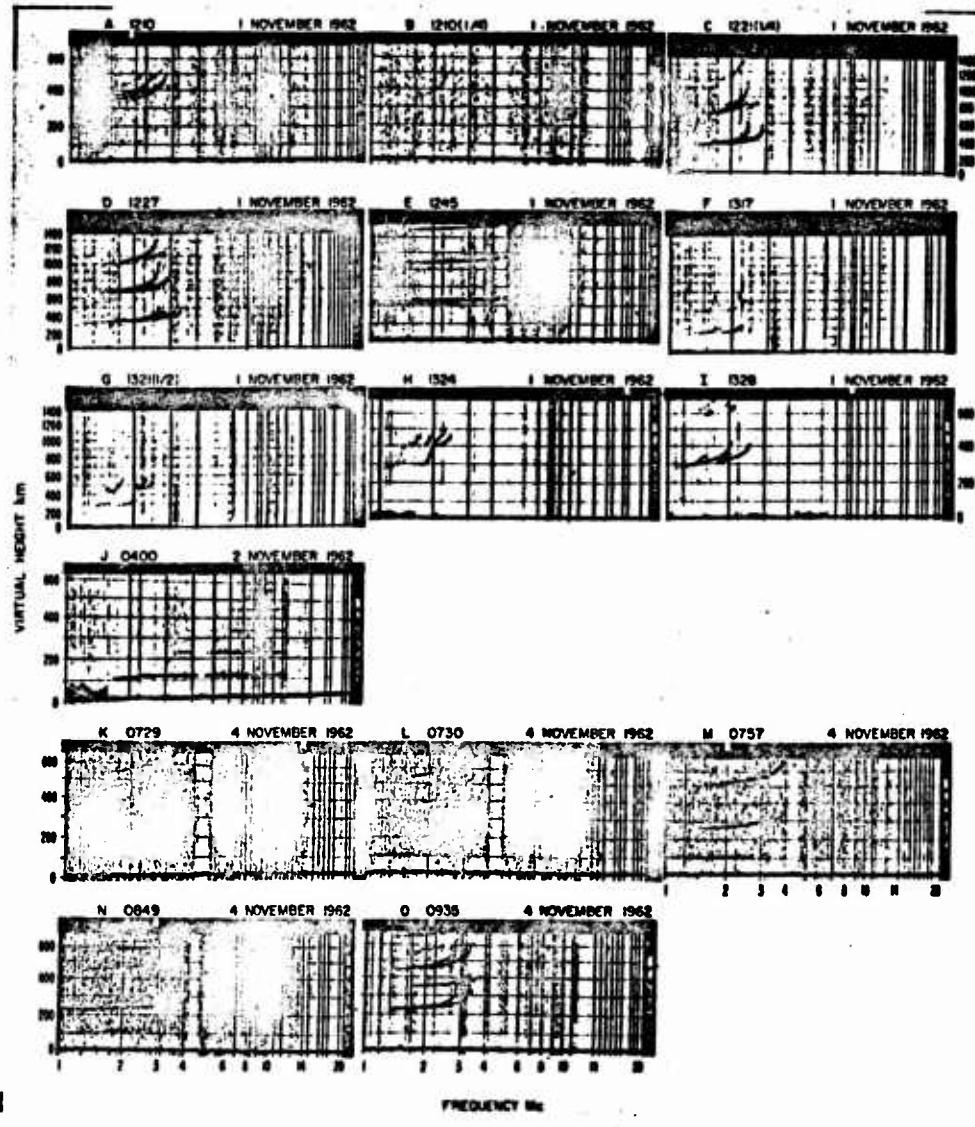
SECRET

Figure 67 King Fish, Tight Rope, Midway, selected ionograms.

NOVEMBER 1, 1962
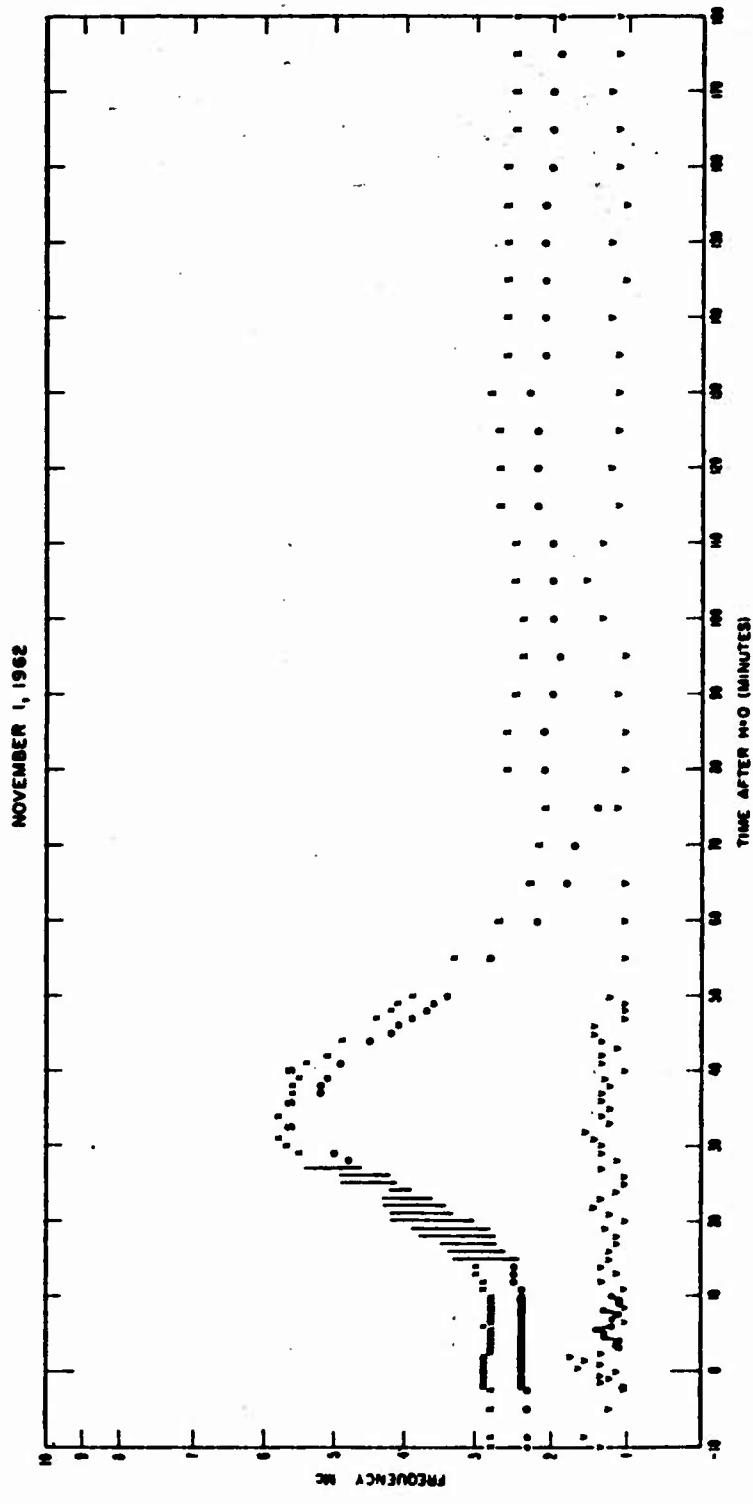
Figure 68 King Fish, Midway, 3-hour frequency plot.

138
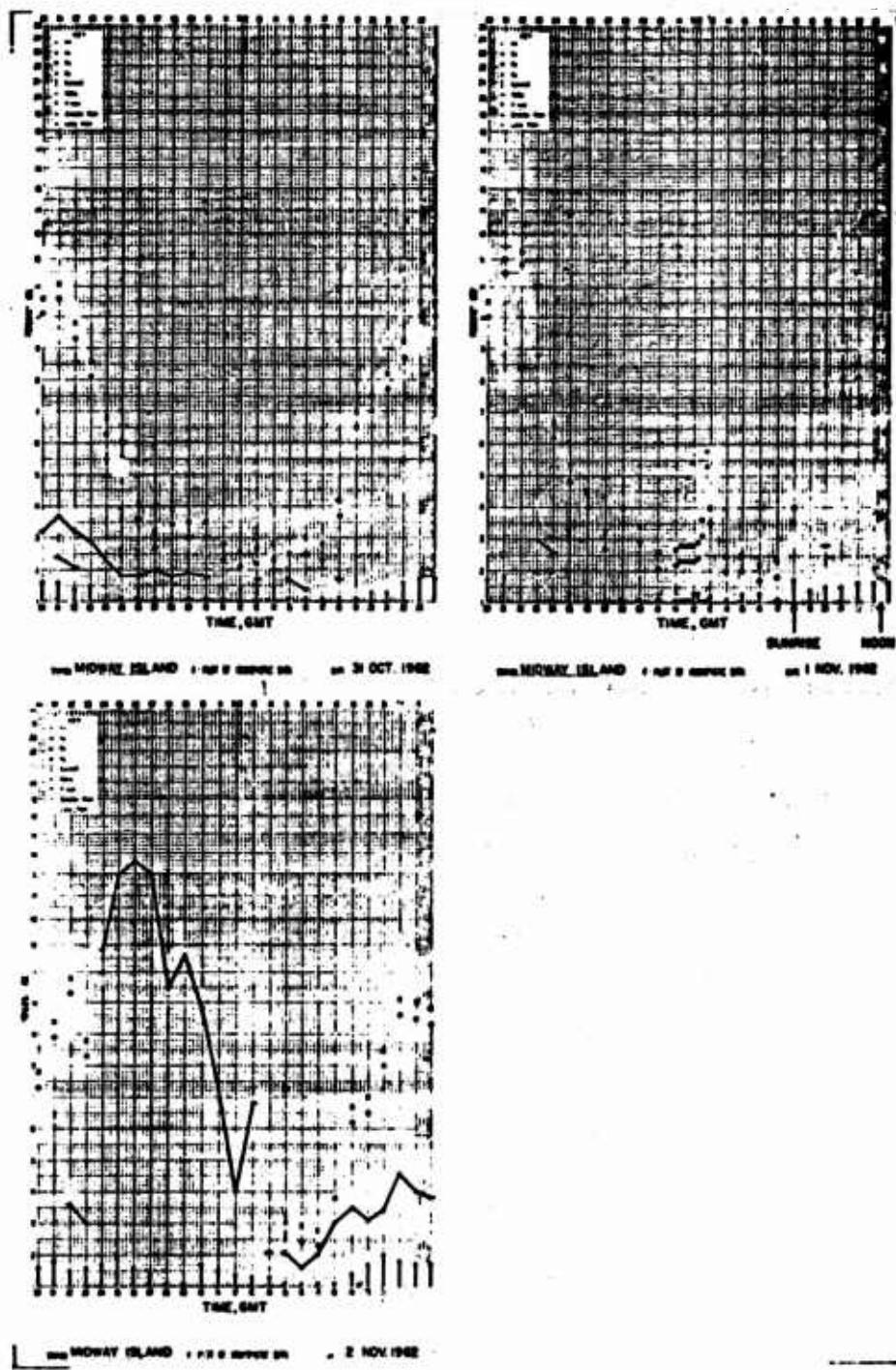
SECRET

Figure 69 King Fish, Midway, f-plots.

139
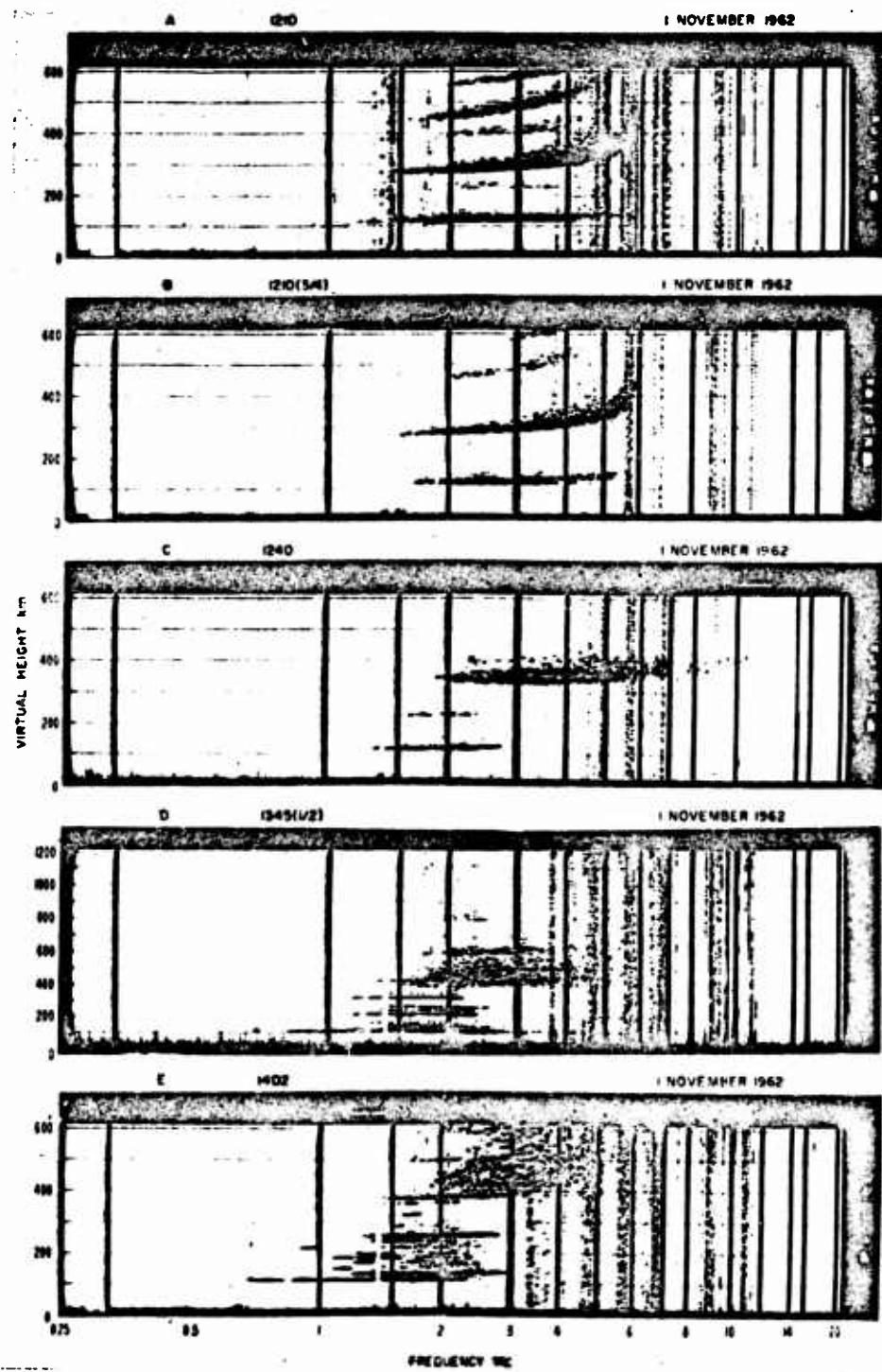
Figure 70 King Fish, Canton, selected ionograms.

140
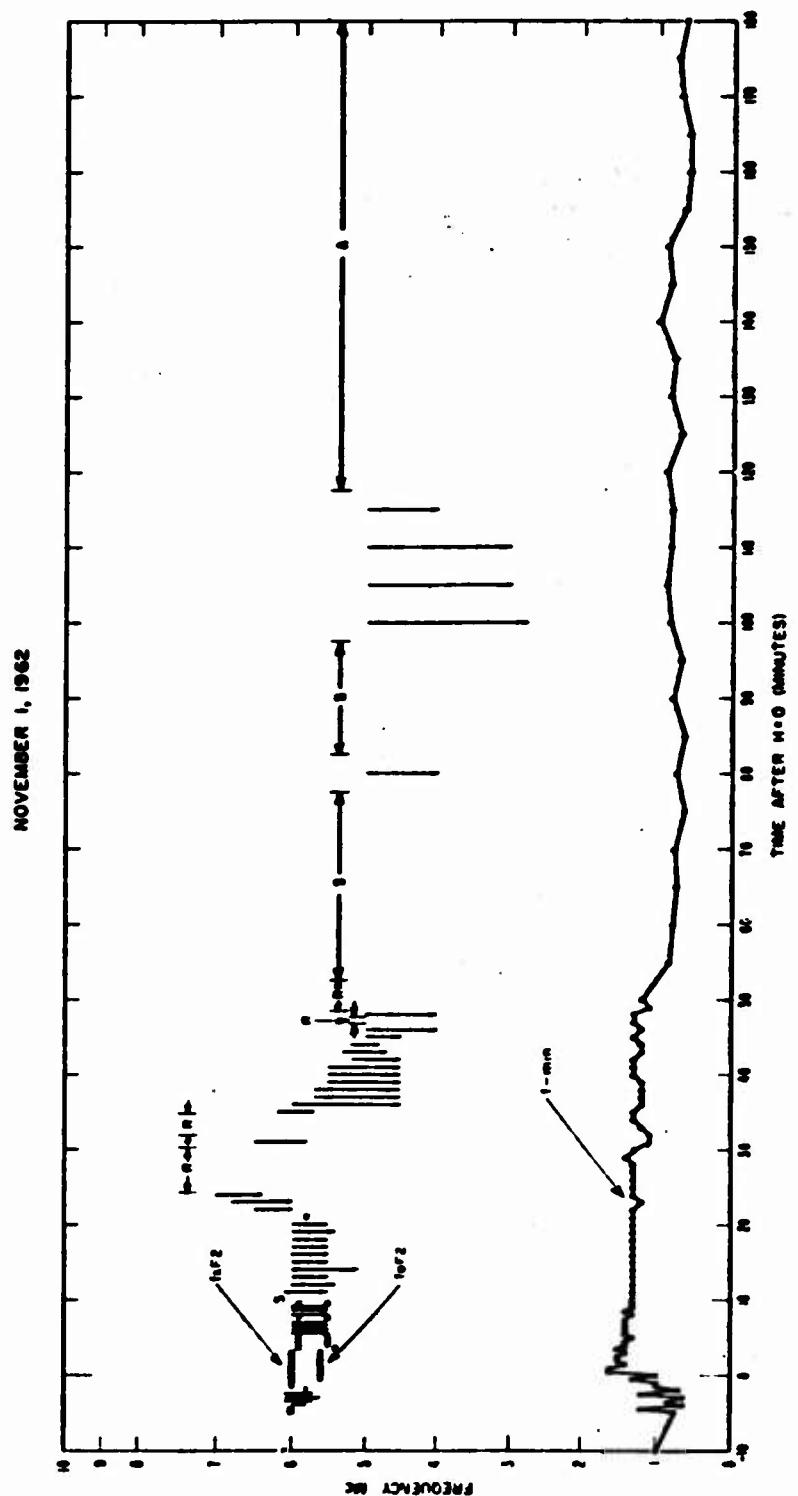
Figure 71 King Fish, Canton, 3-hour frequency plot.
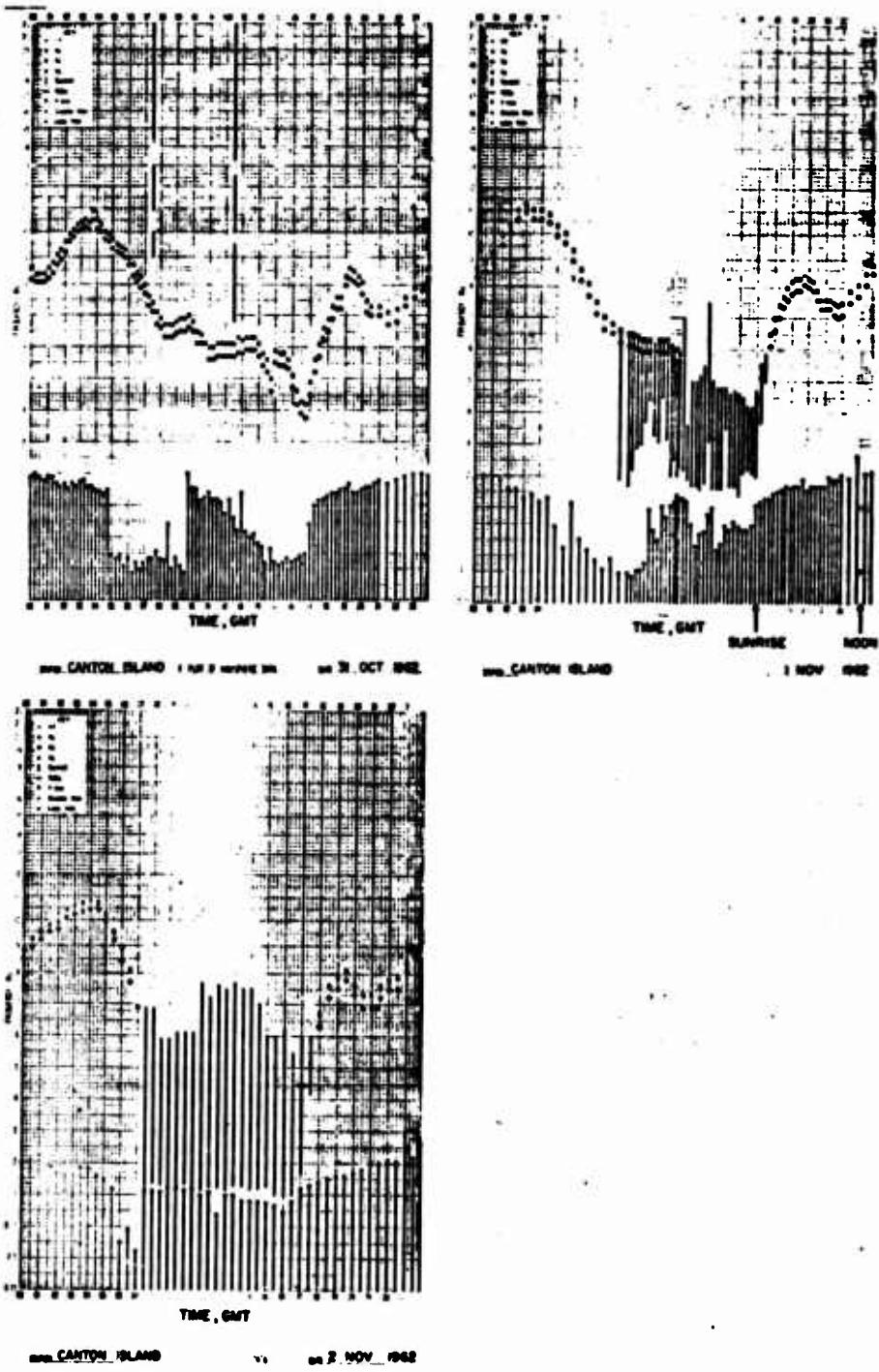
Figure 72 King Fish, Canton, f-plots.

142
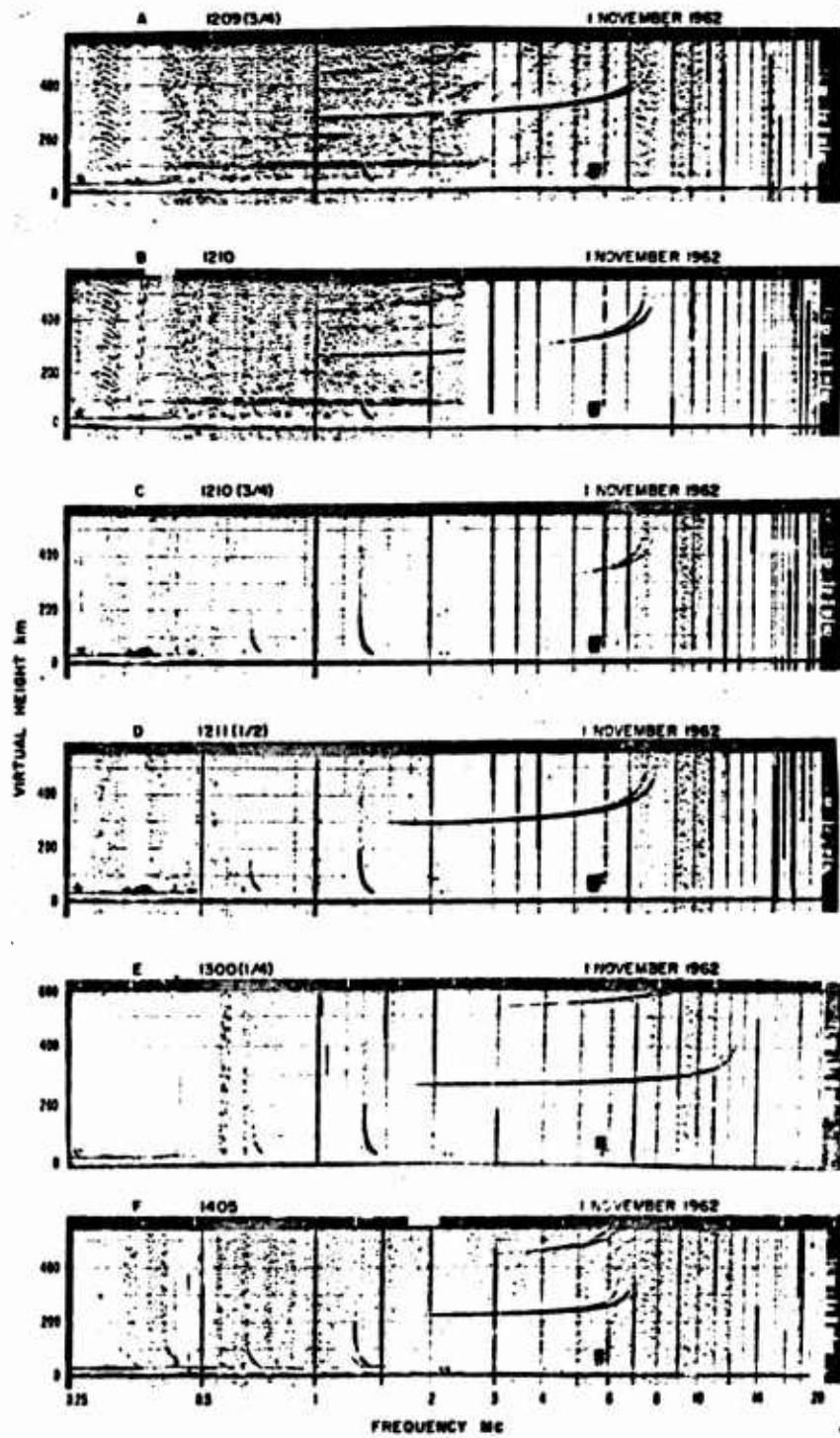
Figure 73 King Fish, Tutuila, selected ionograms.

143

SECRET
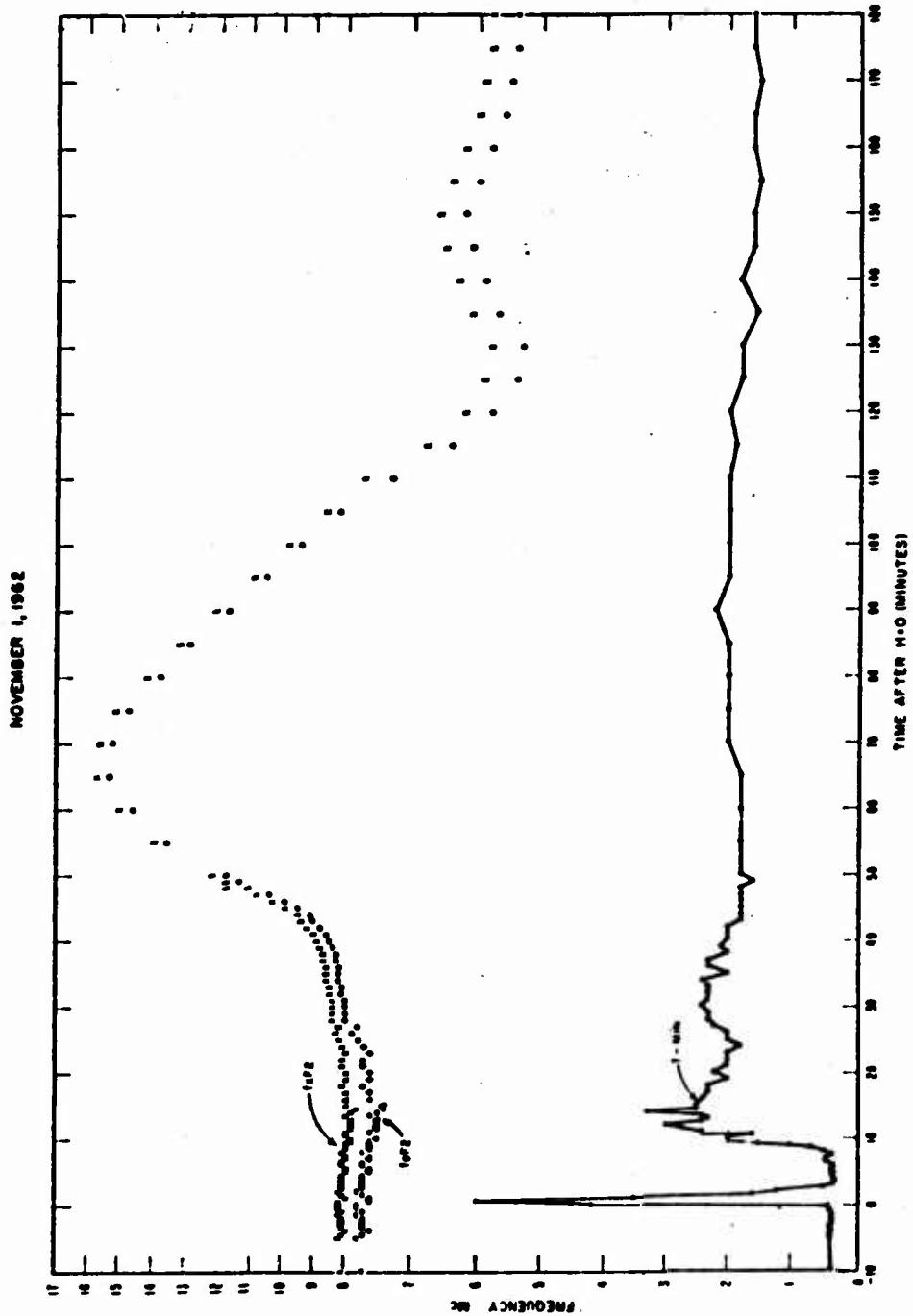
Figure 74 King Fish, Tutuila, 3-hour frequency plot.
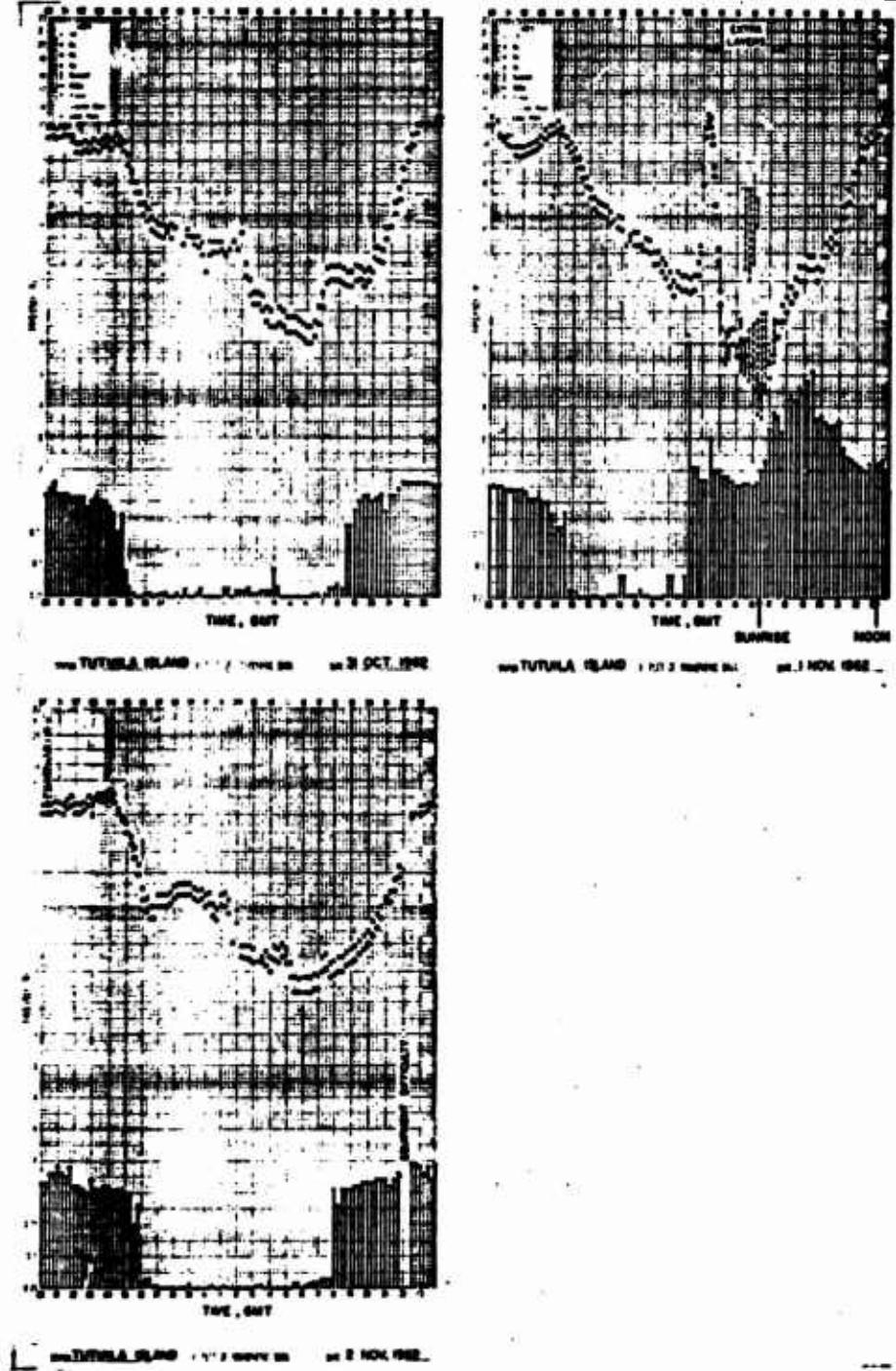
SECRET

Figure 75 King Fish, Tutuila, f-plots.

145
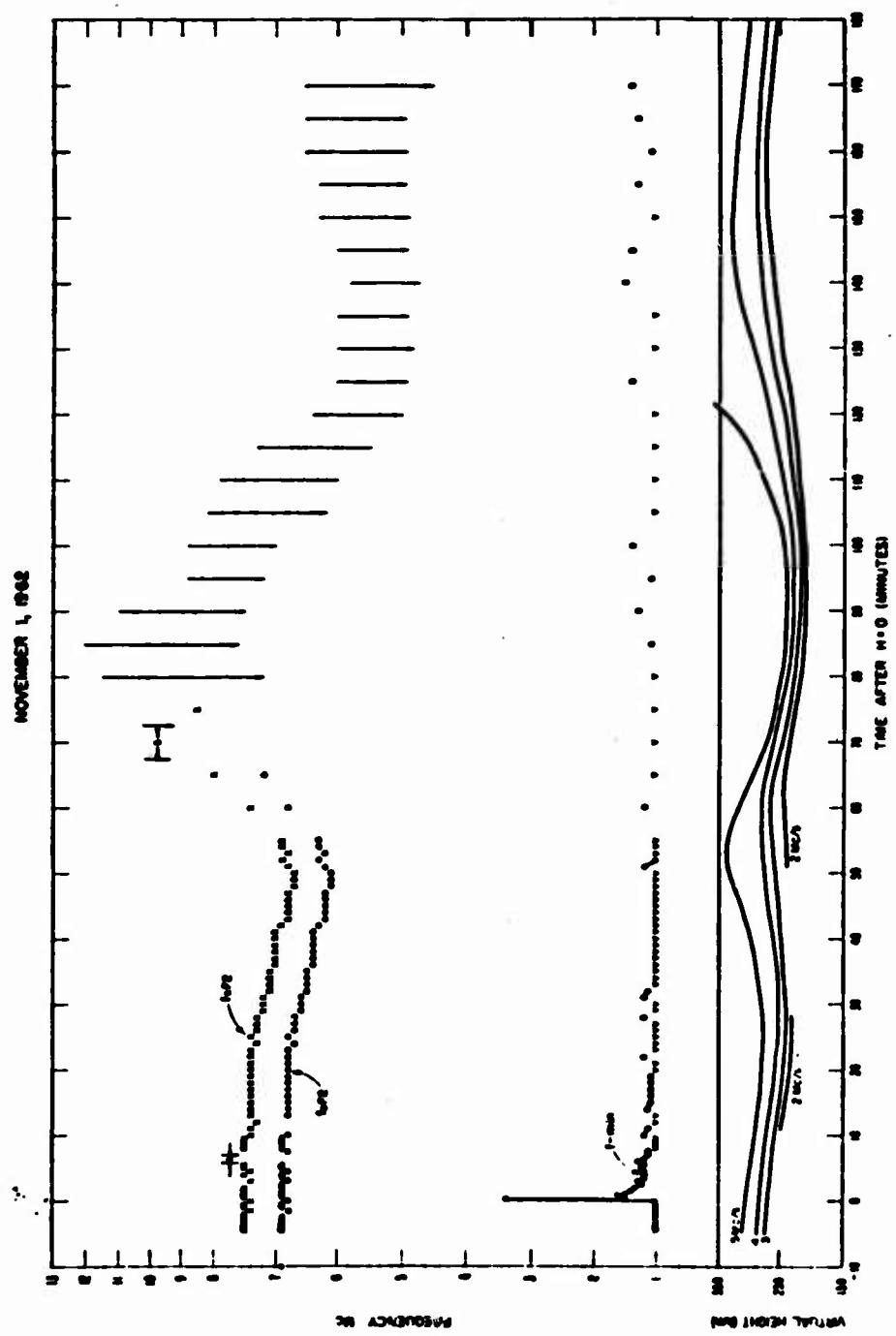
Figure 76 King Fish, Tonga, 3-hour frequency plot and F2 virtual heights.

146
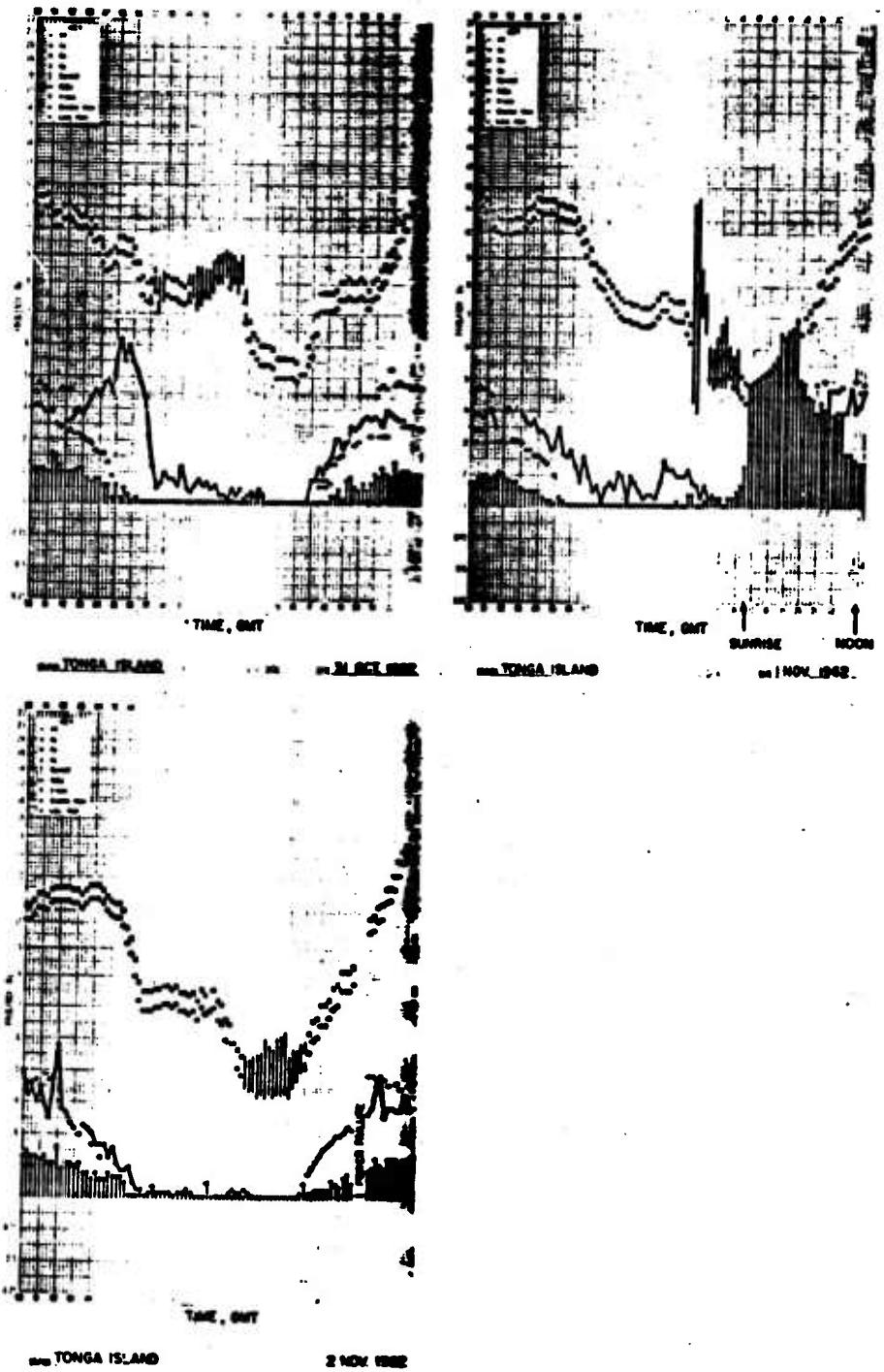
Figure 77 King Fish, Tonga, f-plots.
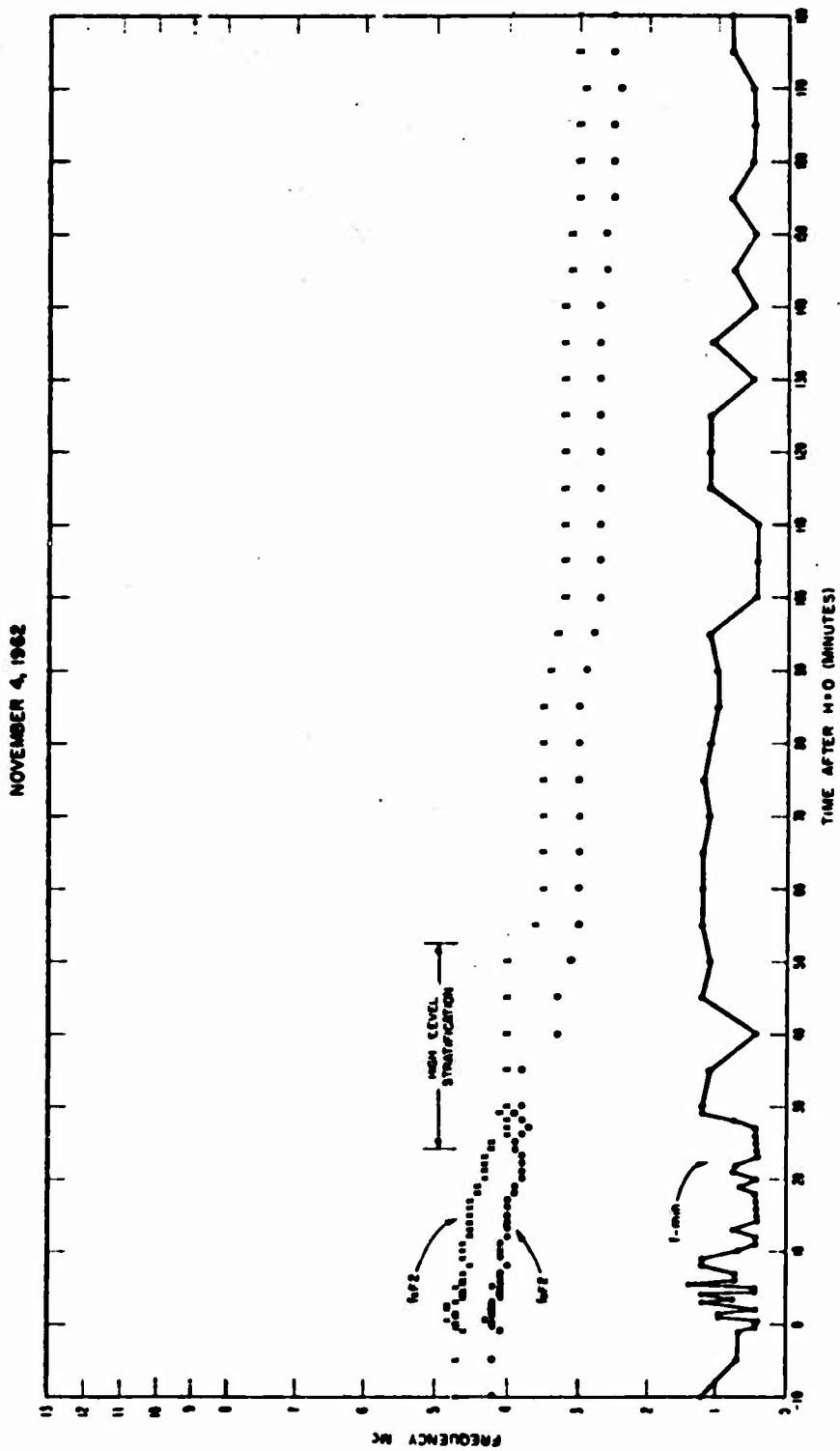
Figure 70 Tight Rope, Maui, 3-hour frequency plot.
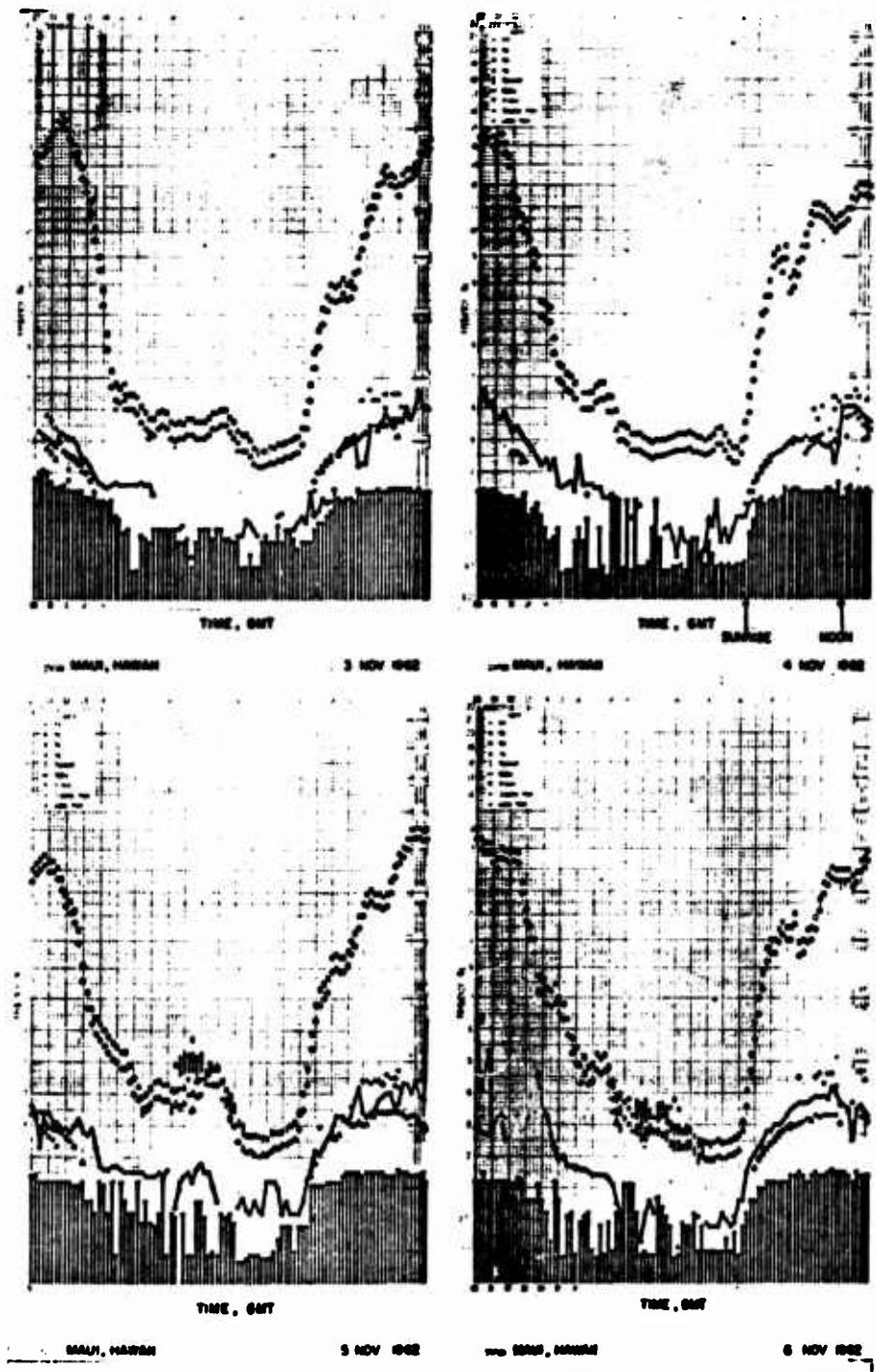
Figure 80 Tight Rope, Maxi, f-plots.

150
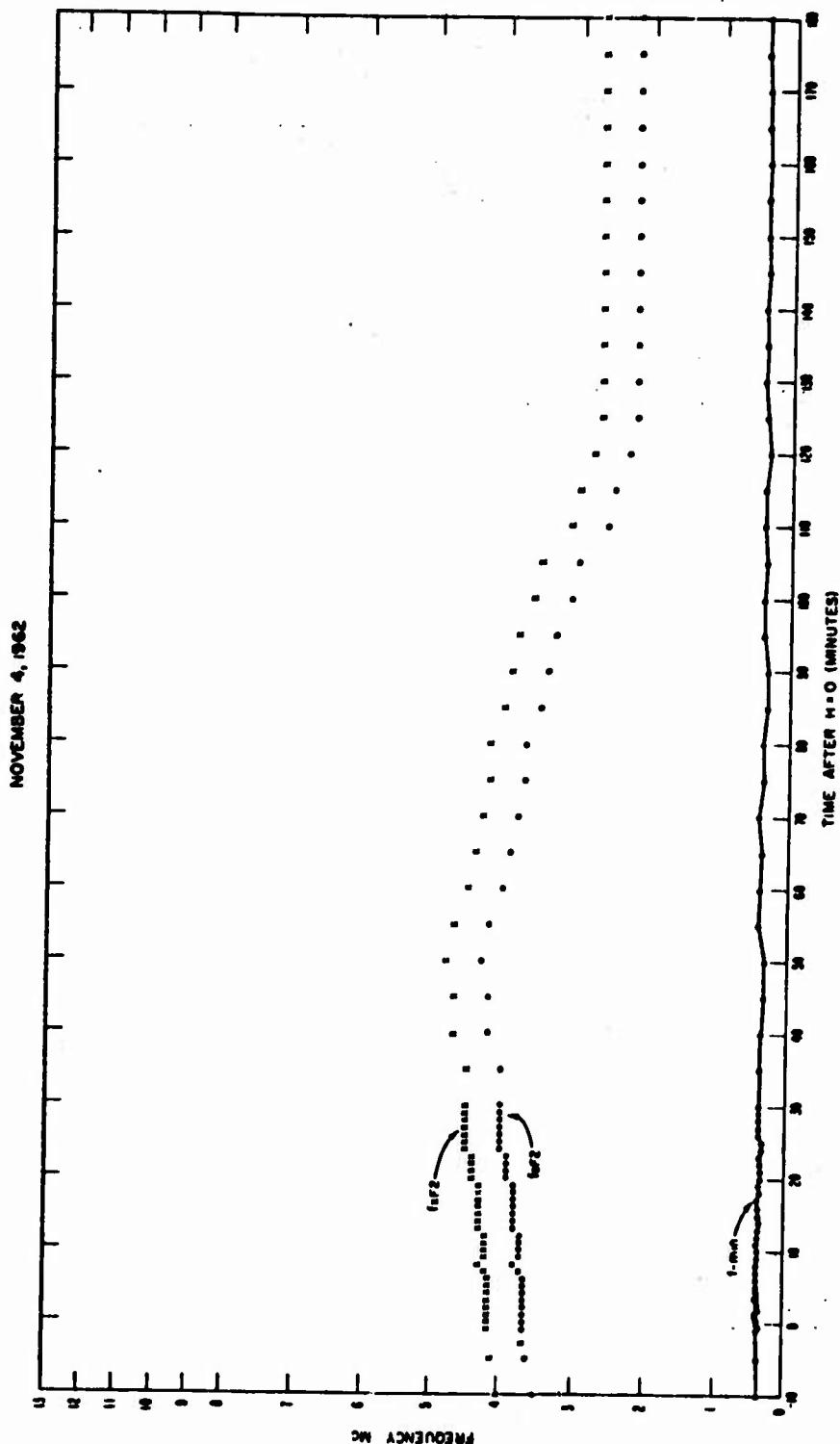
SECRET

Figure 81 Tight Rope, Tern, 3-hour frequency plot.
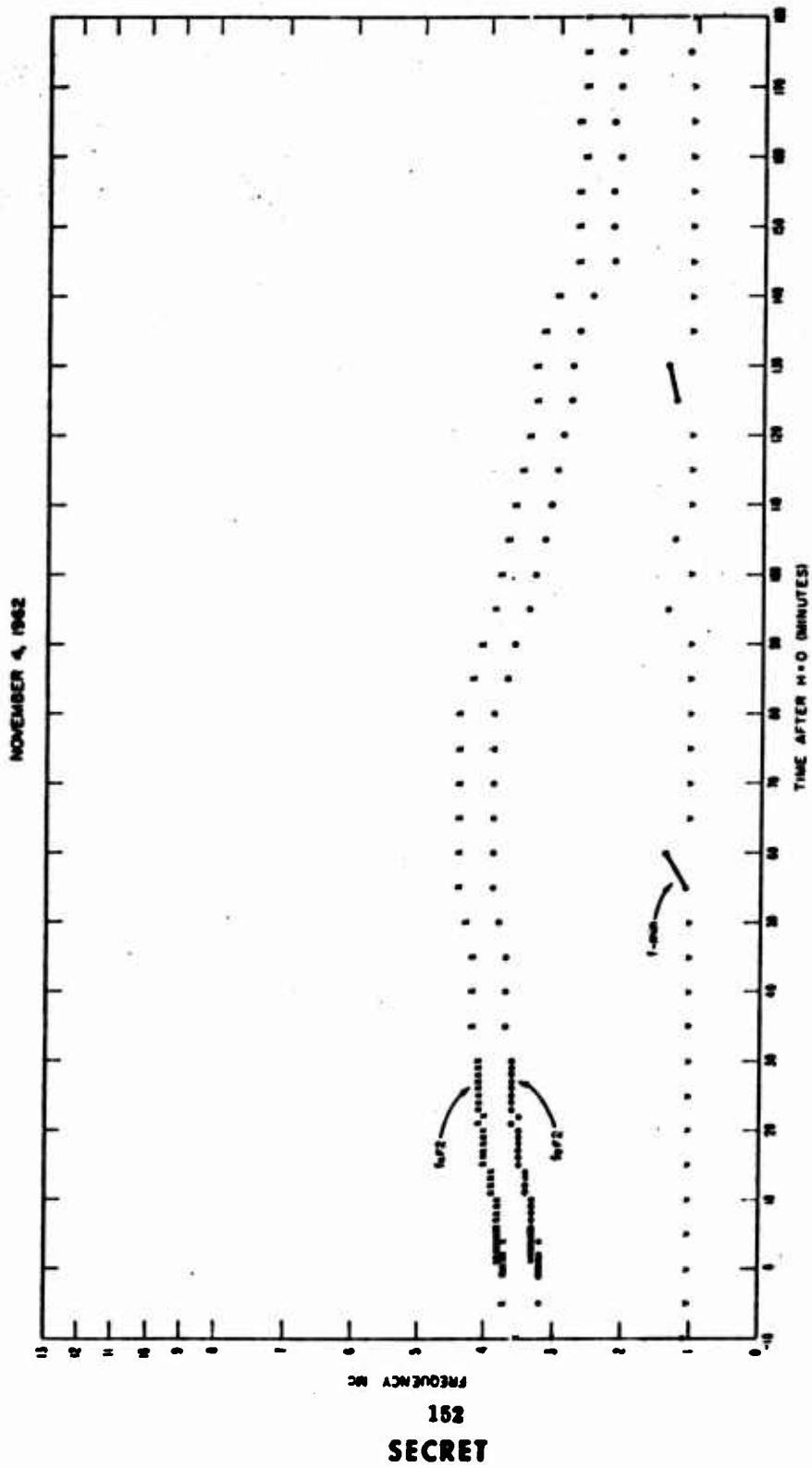
SECRET

Figure 82 Tight Rope, Midway, 3-hour frequency plot.
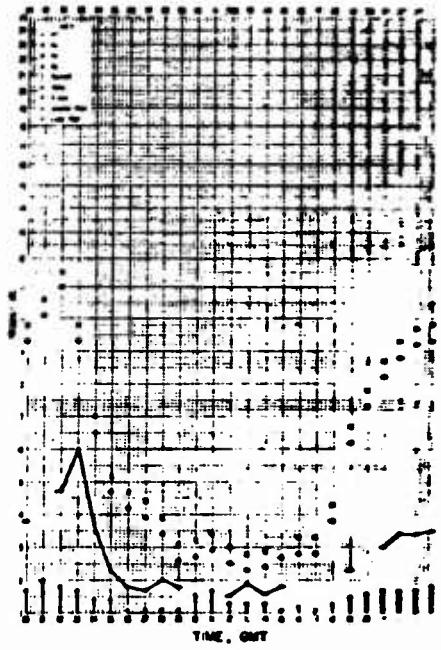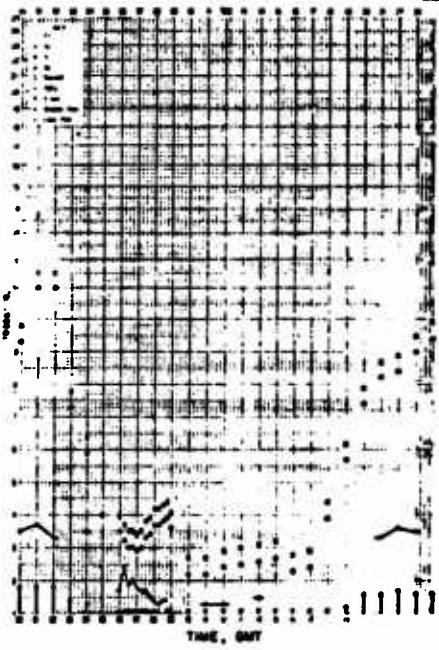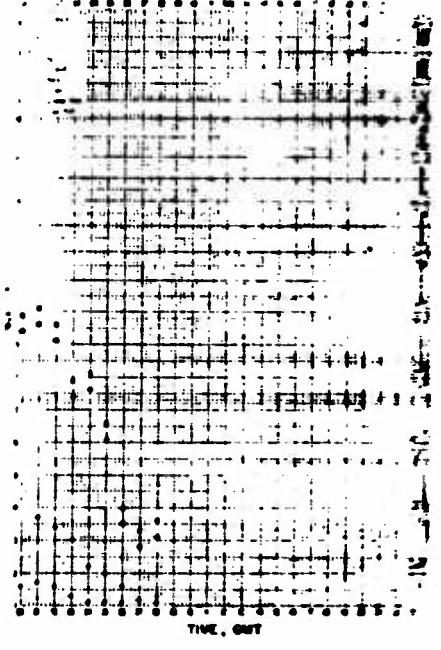
SECRET

Figure 83 Tight Reps, Midway, f-plots.

153
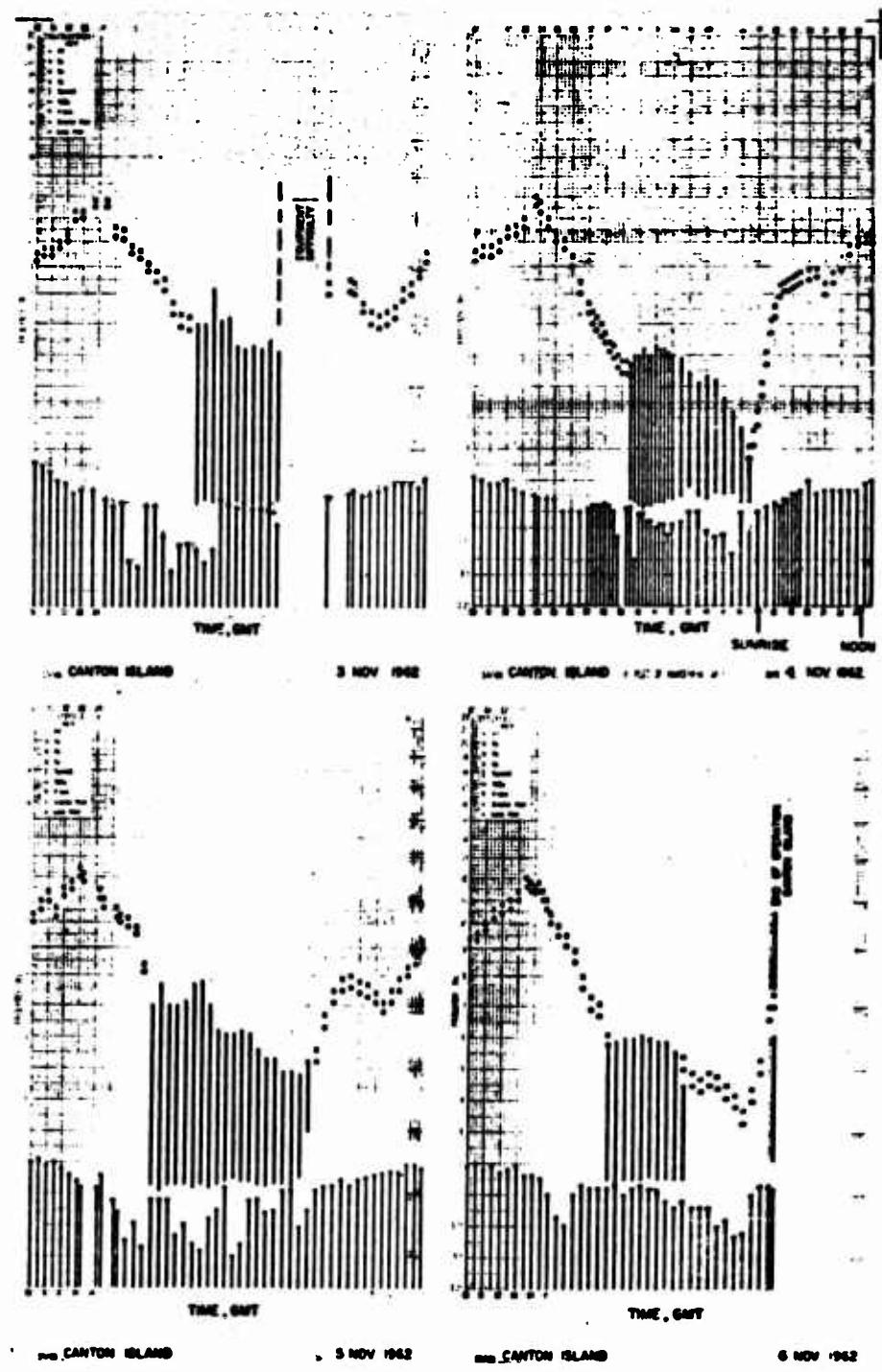
Figure 84 Tight Rope, Canton, f-plots.

154
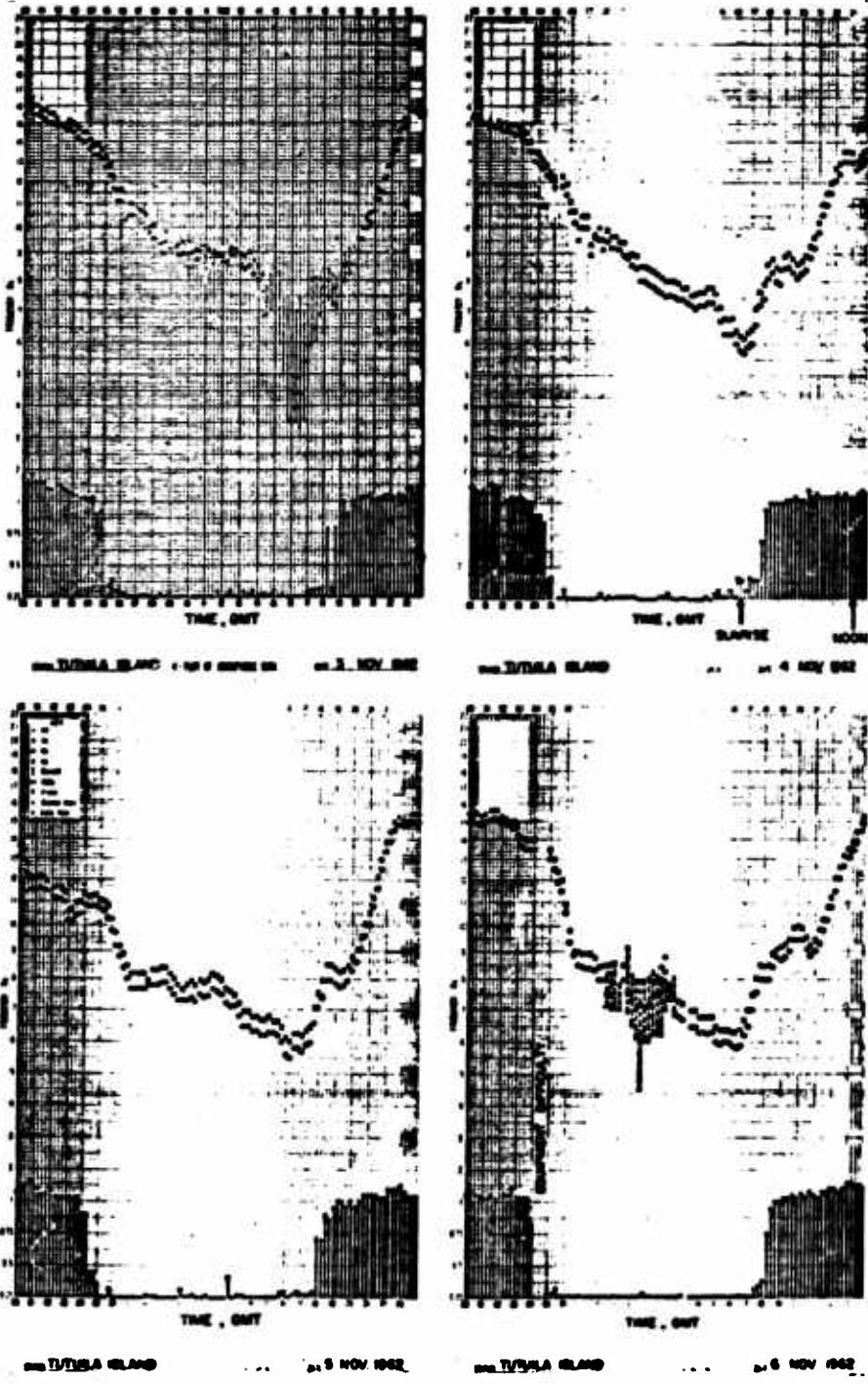
Figure 85 Tight Rope, Tutuila, f-plots.

155
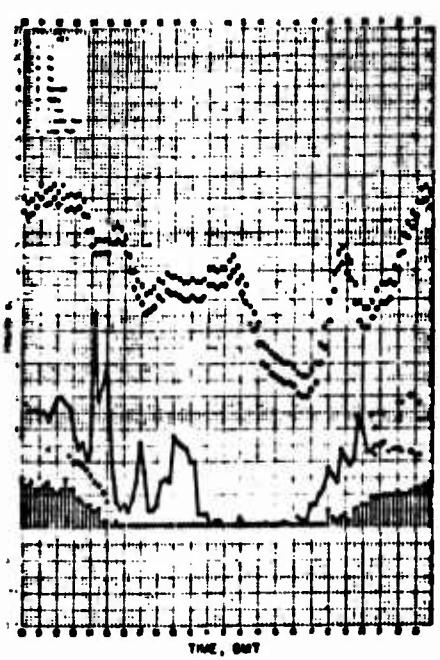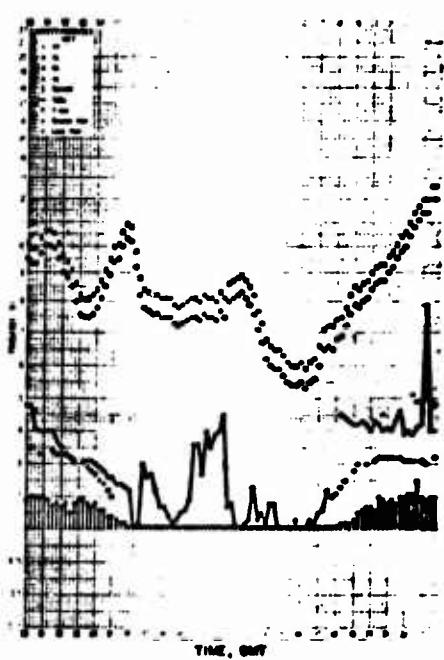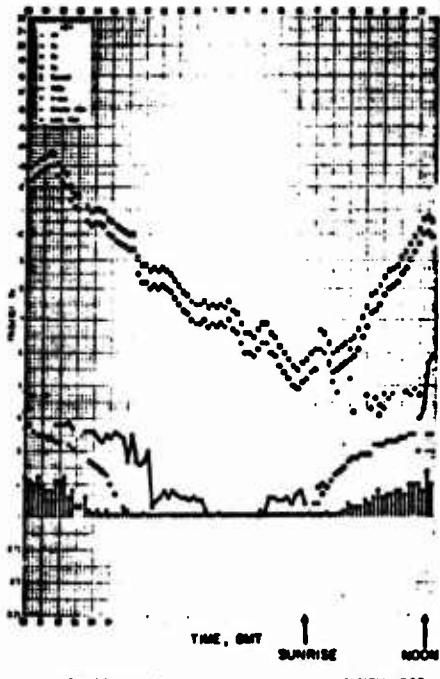
Figure 86 Tight Rope, Tonga, f-plots.

156
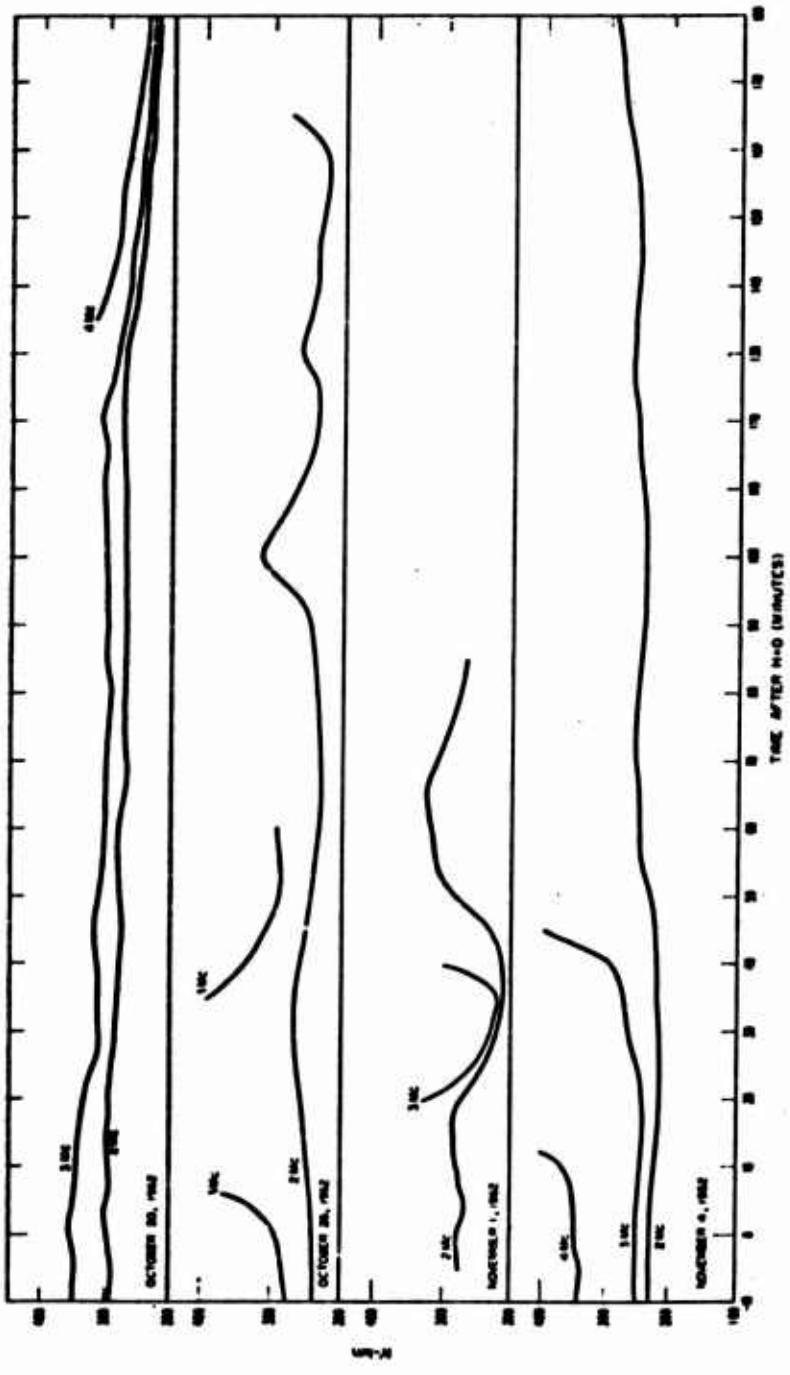
SECRET

Figure 87 Fall events, Maui, F2 virtual heights.

157

Figure 88 Full Growth, Turn, F2 virtual heights.
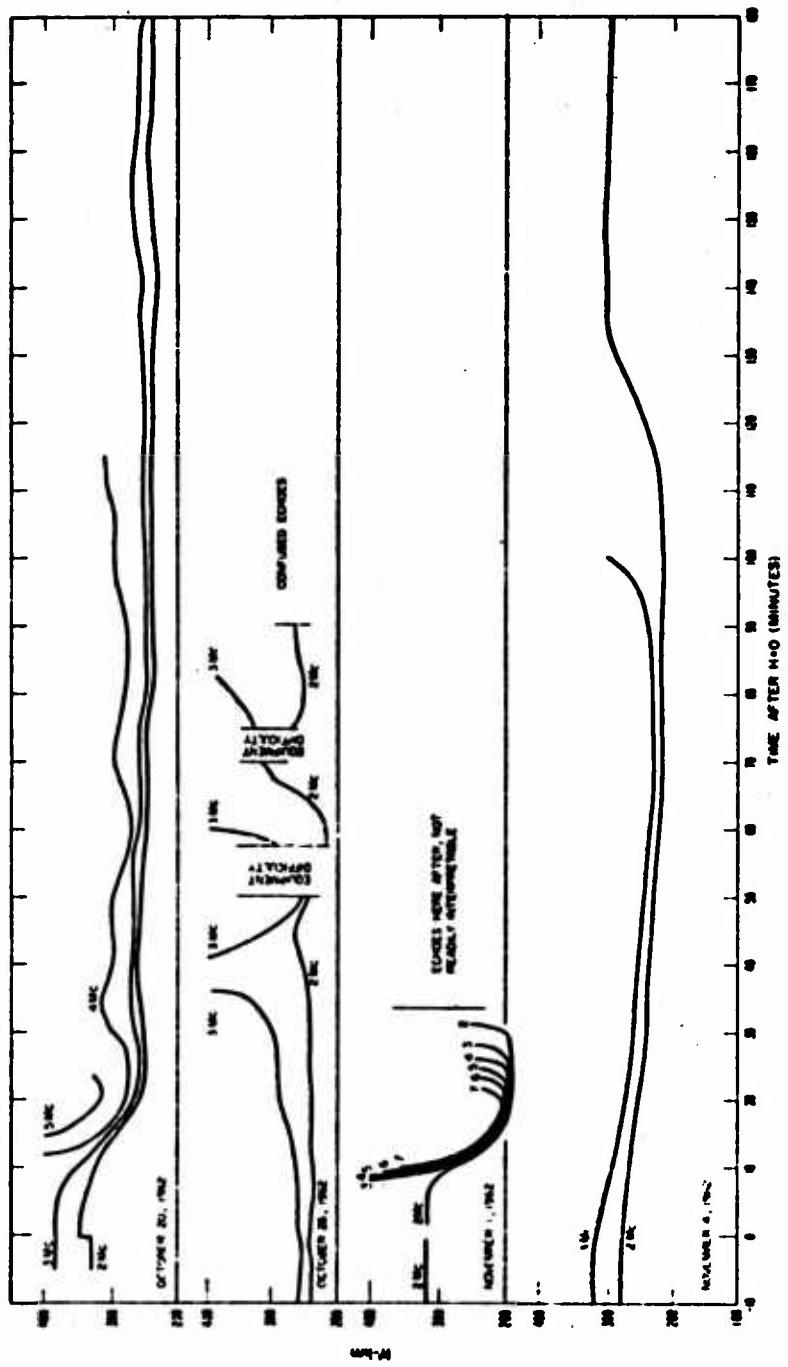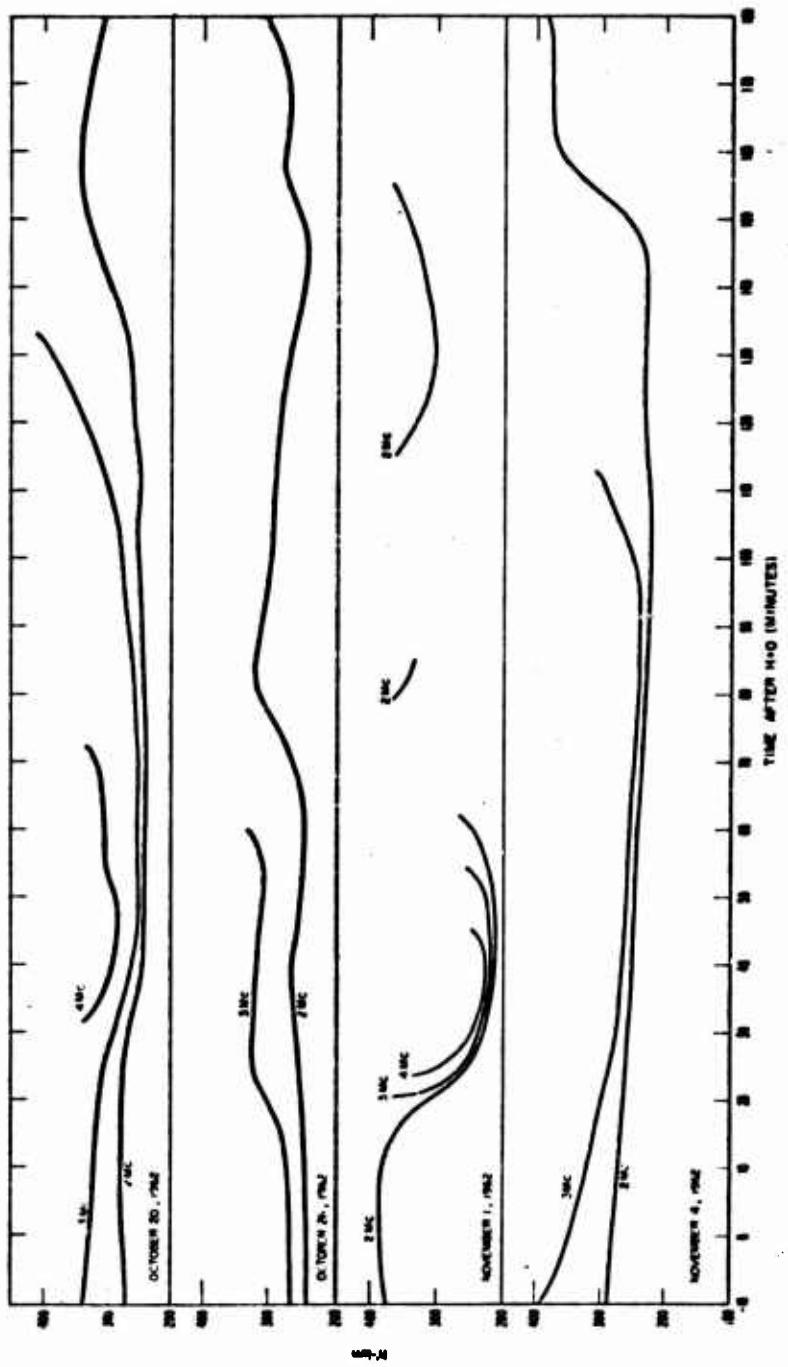
SECRET

Figure 89 Fall events, Midway, F2 virtual heights.

159
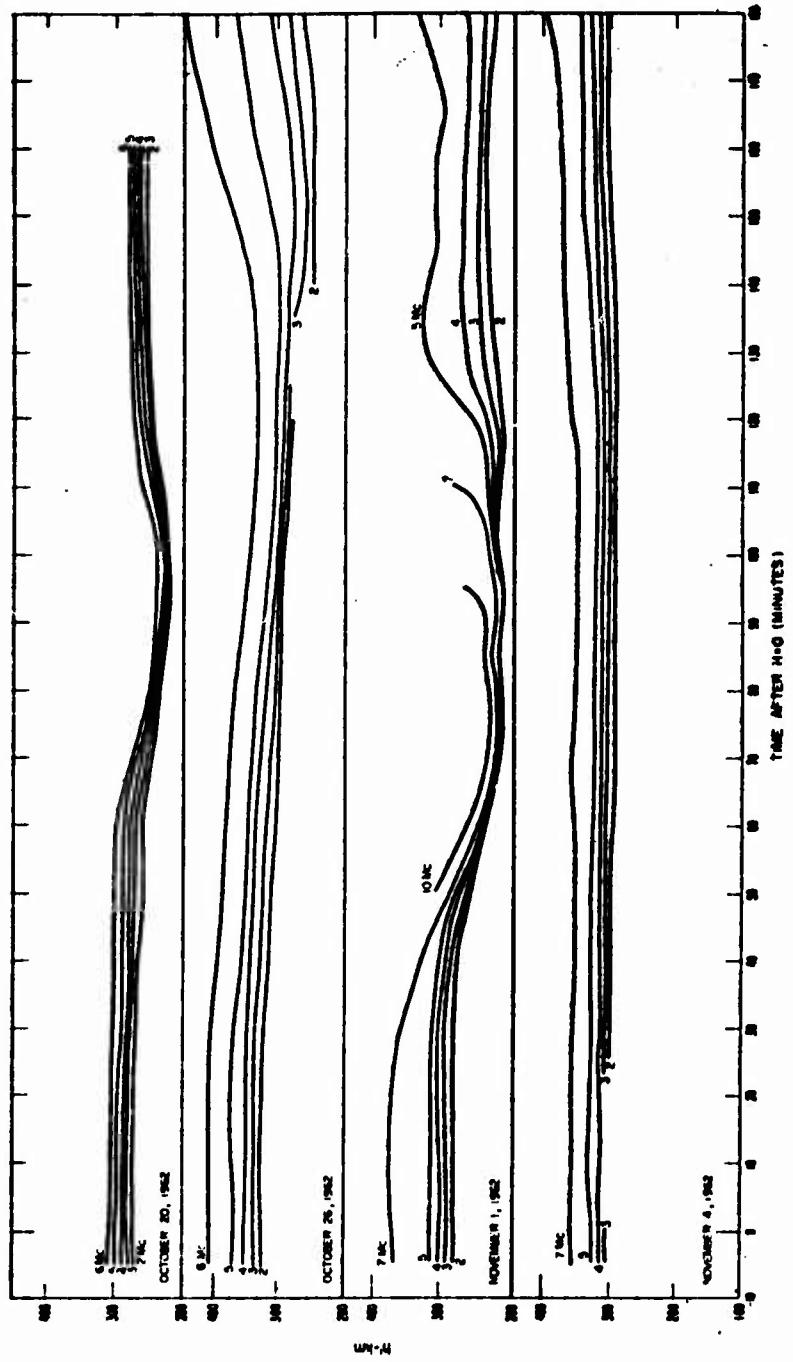
SECRET

Figure 90 Fall events, Tutuila, F2 virtual height.

160

REFERENCES

1. "Effects of High Altitude Nuclear Detonations on High Frequency Communications"; AFSWP–1104, August 1959; Armed Forces Special Weapons Project, Washington 25, D.C.; Secret.

2. W. Hausz, L. P. Malinowski, and S. R. Boyle; "Radar Blackout, Investigation of High-Altitude Nuclear Detonations on Propagation of Electromagnetic Waves"; RM 61 TMP154. AFCRL Contract AF 19(628)-207; General Electric Company, TEMPO, Santa Barbara, California; Secret Restricted Data.

3. DASA Data Center Bibliographies 62-3 and 62-4; DASA Data Center. General Electric Company, TEMPO, Santa Barbara, California; Secret Restricted Data.

4. R61TMP-51(1) and R61TMP-51(11) AFCRL-375; General Electric Company, TEMPO, Santa Barbara, California; Secret Restricted Data.

5. G.H. Munro; "Travelling Ionospheric Disturbances in the F-Region"; Aust. J. Phys. 11, 91-112 (1958).

6. C.O. Hines; "Internal Atmospheric Gravity Waves At Ionospheric Heights"; Canad. J. Phys. 38, 1441-1481 (1960).

7. C.H. Cummack and G.A.M. King; "Disturbance in the Ionospheric F-Region Following the Johnston Island Nuclear Explosion"; N. .J. Geol. Geophys. 2, 634-641 (1959).

DISTRIBUTION

Military Distribution Categories 23 and 68

ARMY ACTIVITIES

1 CHIEF OF R & D DA
2 AC OF S INTELLIGENCE DA
3 ASST.C OF S FORCE DEV. ATTN CRD-OPNS
4 CHIEF OF ENGINEERS DA
5- 7 ARMY MATERIAL COMMAND
8 CHIEF SIGNAL OFFICER DA
9 THE SURGEON GENERAL DA
10- 11 U S ARMY COMBAT DEVELOPMENTS COMMAND
12 U S ARMY CDC NUCLEAR GROUP
13 U S ARMY ARTILLERY BOARD
14 U S ARMY AIR DEFENSE BOARD
15 U S ARMY AVIATION BOARD
16 U S ARMY COMMAND AND GENERAL STAFF COLLEGE
17 U S ARMY AIR DEFENSE SCHOOL
18 U S ARMY CDC ARMOR AGENCY
19 U S ARMY CDC ARTILLERY AGENCY
20 U S ARMY CDC INFANTRY AGENCY
21 U S ARMY CDC CBR AGENCY
22 U S ARMY SIGNAL SCHOOL
23 ARMY MEDICAL RESEARCH LAB
24- 25 ENGINEER RESEARCH & DEV LAB
26 WATERWAYS EXPERIMENT STATION
27 ARMY RESEARCH OFFICE DURHAM
28 PICATINNY ARSENAL
29 DIAMOND ORDNANCE FUZE LABORATORY
30- 31 BALLISTIC RESEARCH LABORATORY
32- 34 REDSTONE SCIENTIFIC INFORMATION CENTER
35- 36 WHITE SANDS MISSILE RANGE
37 ARMY MATERIALS RESEARCH AGENCY
38 U S ARMY MOBILITY COMMAND
39 U S ARMY AMMUNITION COMMAND
40 U S ARMY MUNITIONS COMMAND
41 ELECTRONICS COMMAND
42 U S ARMY ELECTRONIC PROVING GROUND
43- 45 U S ARMY ELECTRONIC R & D LABORATORY
46- 47 U S ARMY CDC COMBAT SERVICE SUPPORT GROUP
48 THE RESEARCH & ANALYSIS CORP
49- 50 WHITE SANDS SIGNAL SUPPORT AGENCY
51- 52 U S ARMY NUCLEAR DEFENSE LABORATORY
53 U S ARMY CDC AIR DEFENSE AGENCY
54 UNITED STATES CONTINENTAL ARMY COMMAND
55 CHIEF OF R&D DEPARTMENT OF THE ARMY
56 U S ARMY CDC COMBINED ARMS GROUP
57 US ARMY ENGINEER R&D LABS SMOFR-ED
58- 60 US ARMY MATERIAL COMMAND, SANDIA
61- 62 US ARMY ENGR.RES. & ENGR.LABS.

NAVY ACTIVITIES

63- 64 CHIEF OF NAVAL OPERATIONS OP03EG
65 CHIEF OF NAVAL OPERATIONS OP-09B0
66 CHIEF OF NAVAL OPERATIONS OP-75
67 CHIEF OF NAVAL OPERATIONS OP-922B1
68 CHIEF OF NAVAL OPERATIONS OP-922B2
69 CHIEF OF NAVAL OPERATIONS OP-04
70 CHIEF OF NAVAL OPERATIONS OP-922F2
71- 72 CHIEF OF NAVAL OPERATIONS CODE 411
74- 75 CHIEF BUREAU OF NAVAL WEAPONS DLI-3
76 CHIEF BUREAU OF MEDICINE & SURGERY CODE 74
77 CHIEF BUREAU OF NAVAL WEAPONS SP-03
78 CHIEF BUREAU OF SHIPS CODE 423
79 CHIEF BUREAU OF YARDS & DOCKS CODE 74
80 DIR. US NAVAL RESEARCH LAB.
81- 82 U S NAVAL ORDNANCE LABORATORY
83 MATERIAL LABORATORY CODE 900

NAVY ACTIVITIES (continued)

84 NAVY ELECTRONICS LABORATORY
85 U S NAVAL RADIOLOGICAL DEFENSE LAB
86 U S NAVAL CIVIL ENGINEERING LABORATORY
87 U S NAVAL SCHOOLS COMMAND U S NAVAL STATION
88 U S NAVAL POSTGRADUATE SCHOOL
89 U S NAVAL DAMAGE CONTROL TNG CENTER ARC
90 AIR DEVELOPMENT SQUADRON 5 VX-5
91 U S NAVAL AIR DEVELOPMENT CENTER
92 U S NAVAL WEAPONS EVALUATION FACILITY
93 U S NAVAL MEDICAL RESEARCH INSTITUTE
94 DAVID W TAYLOR MODEL BASIN
95- 98 U S MARINE CORPS CODE A03H

AIR FORCE ACTIVITIES

99-101 HQ USAF AFTAC-TD
102 HQ USAF AFRNEA
103 HQ USAF AFRDQS
104 HQ USAF AFOCCRR
105 HQ USAF AFOCERA
106 HQ USAF AFGOA
107-111 HQ USAF AFCIN-3B1
112 AC OF S INTELLIGENCE HQ USAFE
113 RESEARCH & TECHNOLOGY DIV BOLLING AFB
114 BALLISTIC SYSTEMS DIVISION
115 HQ USAF AFMSPAA
116-117 SPACE SYSTEMS DIVISION SSTDS
118 TACTICAL AIR COMMAND
119 AIR DEFENSE COMMAND
120 AIR FORCE SYSTEMS COMMAND
121 AF COMMUNICATIONS SERVICE
122 RADC-RAALD,GRIFFISS AFB
123 PACIFIC AIR FORCES
124 SECOND AIR FORCE
125-126 AF CAMBRIDGE RESEARCH CENTER
127-131 AFWL WLL-3 KIRTLAND AFB
132-133 AIR UNIVERSITY LIBRARY
134 SCHOOL OF AVIATION MEDICINE
135-136 AERONAUTICAL SYSTEMS DIVISION
137-138 USAF PROJECT RAND
139 ELECTRONIC SYSTEMS DIV ESAT
140 AIR TECHNICAL INTELLIGENCE CENTER
141 HQ USAF AFRNO
142 HQ USAF AFRPDR

OTHER DEPARTMENT OF DEFENSE ACTIVITIES

143 DIRECTOR OF DEFENSE RESEARCH AND ENGINEERING
144 ASST TO THE SECRETARY OF DEFENSE ATOMIC ENERGY
145-146 ADVANCE RESEARCH PROJECT AGENCY
147 WEAPONS SYSTEM EVALUATION GROUP
148-151 DEFENSE ATOMIC SUPPORT AGENCY
152 FIELD COMMAND DASA
153 FIELD COMMAND DASA FCTG
154-155 FIELD COMMAND DASA FCWT
156-157 DEFENSE INTELLIGENCE AGENCY
158 DEFENSE COMMUNICATIONS AGENCY
159 JOINT TASK FORCE-8
160 COMMANDER-IN-CHIEF PACIFIC
161 COMMANDER-IN-CHIEF ATLANTIC FLEET
162 STRATEGIC AIR COMMAND
163 CINCMAR
164 DIR.DEFENSE INTELLIGENCE AGENCY
165-166 DEFENSE DOCUMENTATION CENTER

FOR CIVILIAN DISTR CAT. A 1

185 AEROSPACE CORPORATION ATTN MR.T.F.WYCKE
186 AEROJET GENERAL NUCLEONICS SAN RAMON CALIF
187 FORD MOTOR CO NEWPORT BEACH CALIF ATTN TECH LIBRARY
188 AEROSPACE CORP EL SEGUNDO CALIF
189 ALLIED RESEARCH ASSOC.INC CNCORD MASS
190 AMER.SCIENCE GENG CO CAMBRIDGE MASS
191 IIT RESEARCH INSTITUTE CHICAGO ILL.
192 AVCO CORP EVERETT MASS
193 AVCO CORP WILMINGTON MASS ATTN TECH.LIBRARY
194 AMI COLUMBUS OHIO ATTN DEFENDER INFO CENTER
195 BELL TEL LAB.WHIPPANY NEW JERSEY
196 BENDIX CORP DETROIT MICH
197 BOEING COMPANY SEATTLE WASHINGTON ATTN TECH LIBRARY
198 COLLINS RADIO CO.CEDAR RAPIDS IOWA
199 COLUMBIA UNIV ELEC RESEARCH LAB NEW YORK
200 CORNELL AERONAUTICAL LAB INC BUFFALO NY
201 DEFENSE RESEARCH CORP SANTA BARBARA ATTN WEITZ
202 DOUGLAS AIRCRAFT CORP SANTA MONICA CALIF
203 EDGERTON GERMESHAUSEN & GRIER INC BOSTON
204 E H PLESSET ASSOC INC LOS ANGELES ATTN TECH.LIBRARY
205 ELECTRO-OPTICAL SYSTEMS PASADENA CALIF
206 SPERRY RAND CORP LONG ISLAND N Y
207 GEN DYNAMICS ASTRO DIV SAN DIEGO ATTN MAPLIN
208 GEN DYNAMICS GEN ATOMIC DIV SAN DIEGO ATTN T J S
209 GEN DYNAMICS CORP FT WORTH TEXAS
210 GEN ELEC CO ADVANCED ELEC CENTER ITHACA N Y
211 GEO TECH MIL PLANNING OPER SANTA BARBARA ATTN BASA
212 SYLVANIA DIV ELEC DEF LAB MT VIEW CALIF
213 GEOPHYSICS CORP OF AMER MEDFORD MASS
214 H R B SINGER INC STATE COLLEGE PA
215 GEO.RE-ENTRY SYSTEMS DEPT ATTN TECH.INFO.CENTER
216 HUGHES AIRCRAFT CO CULVER CITY CALIF ATTN HANSCOME
217 INST FOR DEFENSE ANALYSIS WASHINGTON
218 INTER TEL & TELGR CORP NUTLEY N J
219 J HOPKINS UNIV APPL PHYSICS LAB SILVER SPRINGS
220 KAMAN NUCLEAR COLORADO SPRINGS ATTN SHELTON

221 LOCKHEED AIRCRAFT CORP PALO ALTO CALIF ATTN MEYROTT
222 MARTIN MARIETTA CO JEFFERSON COUNTY.COL.
223 MIT.LINCOLN LABORATORY ATTN TECH.LIBRARY
224 MITRE CORP BEDFORD MASS ATTN TECH LIBRARY
225 MT.AUBURN RESEARCH ASSOC.INC.
226 N AMERICAN AVIATION DOWNEY CALIF
227 NORTHROP AIRCRAFT INC HAWTHORNE CALIF
228 RCA DEFENSE ELEC PRODUCTS MOORESTOWN ATTN INFO. LIB
229 RCA DAVID SARNOFF RES CENTER PRINCETON NJ
230 THOMPSON RAMO-WOOLDRIDGE CALIF.ATTN TECH.LIBRARY
231 RAND CORP SANTA MONICA CALIF
232 RAYTHEON CO MISSILE & SPACE DIV BEDFORD MASS
233 REPUBLIC AVIATION MINEOLA N Y
234 SPACE GEN CORP EL MONTE CALIF
235 SPCE TECH LAB LOS ANGELES CALIF
236 STANFORD RESEARCH INST..ATTN TECH.LIBR.
237 STANFORD RESEARCH INST..ATTN COMMUNICATIONS
238 TECH OPER.INC BURLINGTON MASS ATTN CHAPUS
239 UNIV OF MICHIGAN ANN ARBOR MICH AT.N BAMIRAC LIBR
240 VITRO CORP OF AMERICA WEST ORANGE N J
241 WESTINGHOUSE RESEARCH LAB PITTSBURG. PA
242 WESTINGHOUSE ELEC.CORP. WASH.ATTN P.-TULA
243 NATIONAL BUREAU OF STANDARDS BOULDER LABS UTLAUT
244 GENERAL ELCTRIC CO DEF.ELEC.DIV.

ATOMIC ENERGY COMMISSION ACTIVITIES

245-247 AEC WASHINGTON TECH LIBRARY
248-249 LOS ALAMOS SCIENTIFIC LAB
250-254 SANDIA CORPORATION
255-264 LAWRENCE RADIATION LAB LIVERMORE
265 NEVADA OPERATIONS OFFICE.LAS VEGAS
266 DTIE OAK RIDGE.MASTER
267-290 DTIE OAK RIDGE SURPLUS